NUREG/CR-0237
TREE-NUREG-1166
for U.S. Nuclear Regulatory Commission

POOR ORIGINAL

LOFT STEADY STATE CRITICAL HEAT FLUX TESTS (6.9 to 13.8 MPa)

RICHARD C. GOTTULA

June 1978

EG&G Idaho, Inc.

IDAHO NATIONAL ENGINEERING LABORATORY

DEPARTMENT OF ENERGY

IDAHO OPERATIONS OFFICE UNDER CONTRACT EY-76-C-07-1570

8002 260874

Available from
National Technical Information Service
Springfield, Virginia 22161
Price Codes:
Microfiche $3.00
Printed copy A06

The price of this document for requesters outside of the North American continent can be obtained from the National Technical Information Service.

NUREG/CR-0237
TREE-NUREG-1166

LOFT STEADY STATE CRITICAL HEAT FLUX TESTS
(6.9 TO 13.8 MPa)

Approved:

L. P. Leach, Manager
LOFT Experimental Program Division

for N. C. Kaufman, Director
LOFT

NUREG/CR-0237
TREE-NUREG-1166

Distributed Under Category:
R2
Water Reactor Safety Research
Systems Engineering

LOFT STEADY STATE CRITICAL HEAT FLUX TESTS
(6.9 TO 13.8 MPa)

by

Richard C. Gottula

EG&G Idaho, Inc.

June 1978

PREPARED FOR THE
U.S. NUCLEAR REGULATORY COMMISSION
AND
DEPARTMENT OF ENERGY
IDAHO OPERATIONS OFFICE
UNDER CONTRACT NO. EY-76-C-07-1570

ACKNOWLEDGMENTS

EG&G Idaho, Inc. wishes to express appreciation to the staff of the Heat Transfer Research Facility of Columbia University for their many contributions in the fabrication of the test bundles and performance of the tests for this experimental program.

The author expresses appreciation to S. A. Eide for his work in performing the subchannel analysis of the critical heat flux data and to G. L. Ondricek for his work in preparing the figures for this report and the tables in the Appendix.

The assistance of S. J. Bengston, D. J. Carroll, and S. D. Matthews in developing the LOFT-2 critical heat flux correlation is acknowledged.

ABSTRACT

Steady state critical heat flux (CHF) tests have been performed on electrically heated rod bundles simulating the central region of the Loss-of-Fluid Test (LOFT) nuclear reactor core. Previously reported steady state CHF tests have shown that cladding surface thermocouples on LOFT fuel rods reduce the critical heat flux over the pressure range of 13.8 to 16.5 MPa. Additional steady state CHF tests, reported herein, have been performed to determine the effects of rod external thermocouples on CHF over the ranges of pressure (about 11 MPa) and quality (30 to 40 percent) where CHF is predicted to occur in LOFT during blowdown operation and to determine if sufficient data could be obtained to develop a CHF correlation to predict critical heat fluxes in the LOFT core for blowdown operation.

These low pressure tests were conducted on similar electrically heated 25-rod bundles, which simulate the central region of the LOFT core, both with and without rod external thermocouple simulators. The test data indicated that rod external thermocouples do not significantly affect the magnitude of CHF in the pressure and quality range where CHF is predicted to occur in LOFT during blowdown operation. Therefore, based on these results cladding surface thermocouples are not expected to have a significant effect on transient critical heat flux or time-to-CHF for the nuclear rods in the LOFT core under blowdown conditions. These conclusions are consistant with previously reported transient (blowdown) CHF tests which have shown the same results.

From these initial tests, an insufficient data base was obtained over the pressure range of 6.9 to 13.8 MPa to develop a new correlation that could potentially be used to predict critical heat fluxes for LOFT under blowdown conditions. This resulted from experimental facility limitations on fluid quality during these tests.

SUMMARY

A steady state experimental program was performed to investigate the behavior of critical heat flux (CHF) in electrically heated rod bundles simulating a portion of the central assembly of the Loss-of-Fluid Test (LOFT) nuclear Core-1. The effects on CHF due to cladding surface thermocouples attached to some of the LOFT fuel rods were investigated over the pressure range where CHF is expected to occur during a loss-of-coolant-experiment in the LOFT facility. Twenty five-rod bundles, both with and without simulated cladding surface thermocouples, were tested.

The ranges of the experimental parameters investigated were:

pressure:	6.9 to 13.8 MPa
mass velocity:	680 to 3400 $Kg/s\text{-}m^2$
local quality at CHF:	-0.25 to 0.60

One-hundred-fifty-seven data points were obtained with the rod bundles having rod external thermocouple simulators. These data were compared with 53 data points obtained with the rod bundles without external thermocouple simulators. The comparison showed that the critical heat fluxes in the rod bundles with external thermocouple simulators were an average of 13 percent lower at 13.8 MPa, an average of 2.5 percent higher at 10.3 MPa, and an average of 7 percent higher at 6.9 MPa than the critical heat fluxes in the rod bundles without external thermocouple simulators. In the regions of pressure and quality where CHF is predicted to occur in the LOFT core during blowdown operation (about 11 MPa and 30 to 40 percent quality), the magnitudes of CHF between the bundles tested were about the same. Thus, cladding surface thermocouples are

not expected to have a significant effect on transient CHF or time-to-CHF for the nuclear rods in the LOFT core under blowdown conditions.

A new CHF correlation (designated LOFT-2) was developed, based on the 157 data points from the bundles with rod external thermocouple simulators, to allow a comparison of the data between the bundles with and without rod external thermocouple simulators. However, since a complete data base could not be obtained over the intended range of mass velocities and qualities, the correlation is not adequate to predict CHF for LOFT under blowdown conditions.

The data were compared to predictions based on steady state CHF correlations such as B&W-2, GE and Barnett which are currently used in codes such as RELAP and FRAP-T to predict CHF for LOFT blowdowns. The B&W-2 correlation poorly predicts the magnitude and trend of the data. Most of the data fall outside the applicable range of the B&W-2 correlation. The Barnett correlation severely underpredicts all of the data at mass velocities less than 1360 kg/s-m^2 and qualities greater than +0.05. The GE correlation provided a good prediction of the data except at mass velocities less than 1360 kg/s-m^2 and qualities higher than +0.2. In these ranges the GE correlation tends to underpredict almost all of the data.

CONTENTS

FIGURES

TABLES

I. INTRODUCTION

The Loss-of-Fluid Test (LOFT) facility is an integral nuclear reactor test facility which has been designed to simulate, as nearly as possible all of the important effects that are anticipated to occur during a loss-of-coolant accident (LOCA) in a large pressurized water reactor (LPWR) type nuclear steam supply system. LOFT utilizes special experimental instrumentation which has been located to measure the significant interacting nuclear and thermal-hydraulic processes required to assess LOCA and emergency core coolant system (ECCS) performance. The in-core experimental instrumentation includes thermocouples attached to the outside surfaces of the fuel rod cladding. (See Reference 1, Section 2.1.1.2 for details of the thermocouples and attachment.)

An extensive critical heat flux test program has been conducted on electrically heated rod bundles simulating the central region of the LOFT nuclear reactor core. The evaluation and results of initial test data over the pressure range of 13.8 to 16.5 MPa have been previously reported in Reference 2. The results of that data indicate that cladding surface thermocouples reduce the CHF an average of 18 percent over that pressure range.

The purpose of this test program was to determine the effect on CHF due to thermocouples mounted on the cladding surface of some of the LOFT fuel rods over the pressure range of 6.9 to 13.8 MPa in order to:

(1) determine if rod external thermocouples significantly affect the critical heat flux in the LOFT core for steady state operating conditions in the pressure range where CHF occurs

during blowdown operation and

(2) obtain a data base to develop a CHF correlation to predict critical heat fluxes in the LOFT core for blowdown operation, and to provide data to compare to current steady state CHF correlations used in codes such as RELAP and FRAP-T to predict transient CHF in LOFT under blowdown conditions.

The experimental parameters investigated were:

(1) Pressures from 6.9 to 13.8 MPa

(2) Inlet mass velocities from 680 to 3400 kg/s-m^2

(3) Local quality at CHF from -0.25 to +0.60.

Four 25-rod bundles simulating a portion of the Core-1 central (Type A) fuel assembly[1] in the LOFT reactor were used in the test program. One-hundred-fifty-seven data points were obtained with the rod bundles with rod external thermocouple simulators. These data were compared with 53 data points obtained with the rod bundles without rod external thermocouple simulators.

This report contains: a description of the CHF test program, test bundles, and test procedure (Section II); a description of the analysis of the data (Section III); a comparison of the data with existing CHF correlations; and a comparison of the data between the rod bundles with and without simulated rod external thermocouples (Section IV); conclusions regarding the effect of thermocouples on CHF conditions in LOFT and adequacy of current models (Section V), and additional tests necessary to obtain the data for developing a CHF correlation applicable for LOFT conditions (Section VI).

II. EXPERIMENT DESCRIPTION

1. SCOPE OF TESTS

CHF data were obtained at the following test conditions:

(1) Pressure: 6.9, 10.3 and 13.8 MPa

(2) Mass Velocity: 680 to 3400 $kg/s\text{-}m^2$

(3) Local Quality at CHF: -0.25 to +0.60.

2. TEST BUNDLE DESCRIPTION

Two electrically heated test section configurations were selected for the test program. These were:

(1) A 25-rod bundle in a 5x5 square array with a 1.68 m heated length. This bundle simulated the portion of the Loss-of-Fluid Test (LOFT) reactor central (Type A) fuel assembly as shown in Figure 1[1]. This asymmetric configuration was chosen to include the effect of rod external thermocouples and rod cluster control (RCC) guide tubes on critical heat flux.

(2) A 25-rod bundle identical to that described above except that it did not incorporate rod external thermocouple simulators.

Two rod bundles with external thermocouple simulators were built and tested, one by Exxon Nuclear Company (designated EXX2 and ANC1) and one by Aerojet Nuclear Company (designated ANC2)[a]. Also, two rod bundles without external thermocouple simulators were built (designated ANC3 and ANC4) and tested.

[a]As of October 1, 1976, contract being performed by EG&G Idaho, Inc.

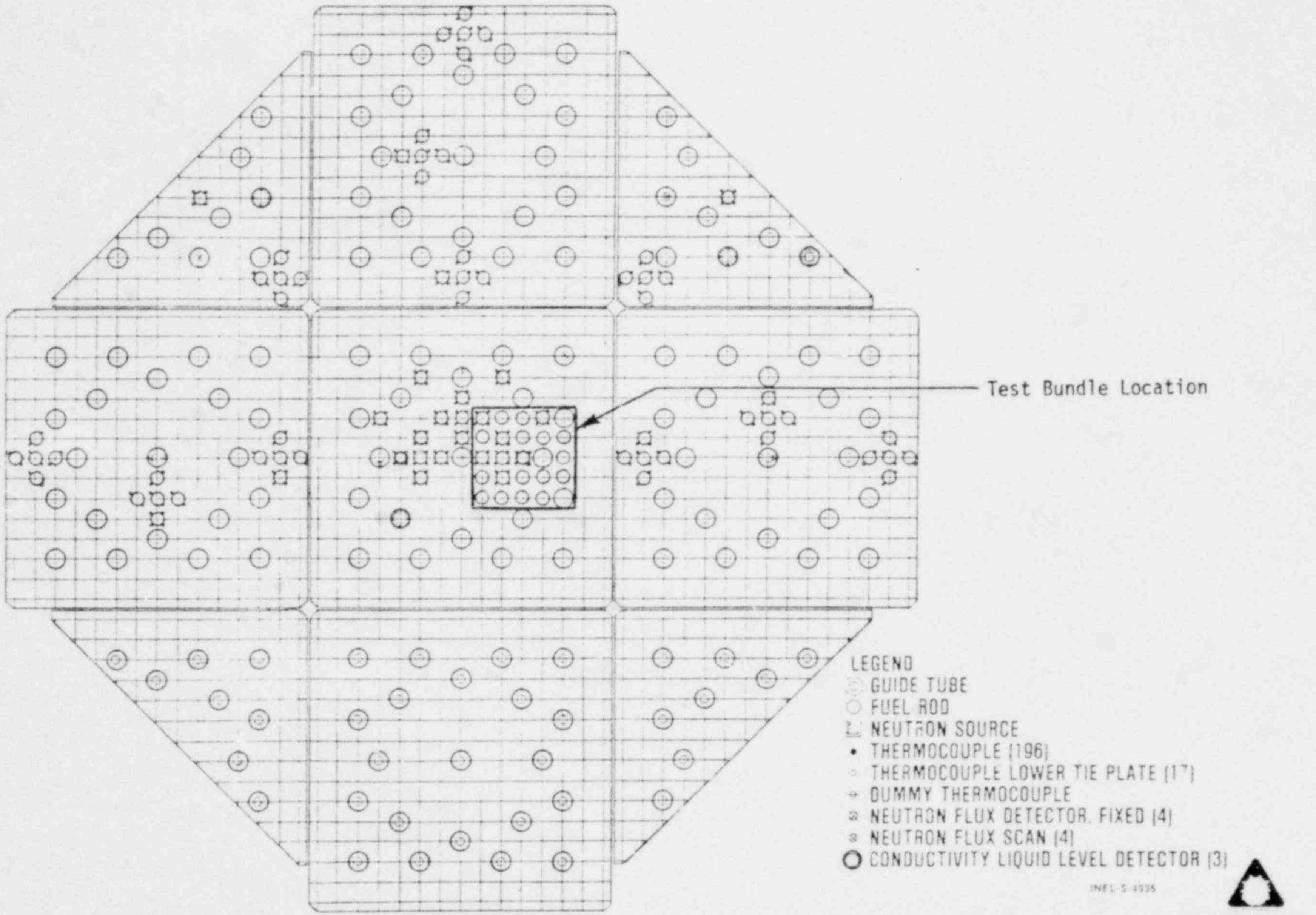

Figure 1 Segmer. of LOFT core simulated by 25-rod test bundles

2.1 Exxon Rod Bundle Description (bundle with external thermocouple simulators)

This 25-rod bundle (designated EXX2 or ANC1) was selected to investigate the combined effect on CHF of rod external thermocouples, guide tubes, and grid spacers. Its characteristics are described in Table I and a diagram is shown in Figure 2.

2.1.1 Heater Rod Description.

The heat generated in the LOFT fuel rods was simulated by passing direct electrical current through rods made of Type 347 stainless steel tubing. Three tube wall thicknesses of 0.287, 0.300, and 0.318 mm were chosen to simulate the radial power profile in the section of the LOFT core modeled by the test section. The normalized power factors of each rod are shown in Figure 2. The tubing outer diameter was 10.7 mm, the same as the fuel rods being simulated. Each rod was filled with ceramic cylinders to prevent collapse under external pressure. The 80-mm long cylinders were machined from 98% dense Al_2O_3 ceramic to fit inside the tubes. The inside of the heated tube was at atmospheric pressure during testing.

Each rod was composed of top and bottom electrodes and a heated section as shown in Figure 3. The heated section was 1.68-m long, the same as the LOFT fuel rods. The top electrode was made of solid nickel with the same OD as the heated section. The top end of the nickel end piece was ground with a self-locking taper which fitted a matching conical hole in the top grid plate. The bottom electrode was joined to copper tubing external to the pressure seal. A 6.4-mm hole through the bottom electrode and ceramic cylinder allowed access for thermocouple instrumentation.

TABLE I

ROD BUNDLE CHARACTERISTICS

Number of rods	25
Number of unheated rods	3
Array	5 x 5
Heated length	1.68 m
Pitch	14.3 mm
Heated Rod OD	10.7 mm
Unheated Rod OD	13.9 mm
Axial heat flux distribution	uniform
Radial heat flux distribution	nonuniform
Number of grid spacers (LOFT-type, no mixing vanes)	5
Grid spacing	0.42 m
Number of simulated external thermocouples on rods with thermocouple simulators	[illegible]
Simulated thermocouple OD	1.17 mm
Square flow channel dimension	73.8 mm

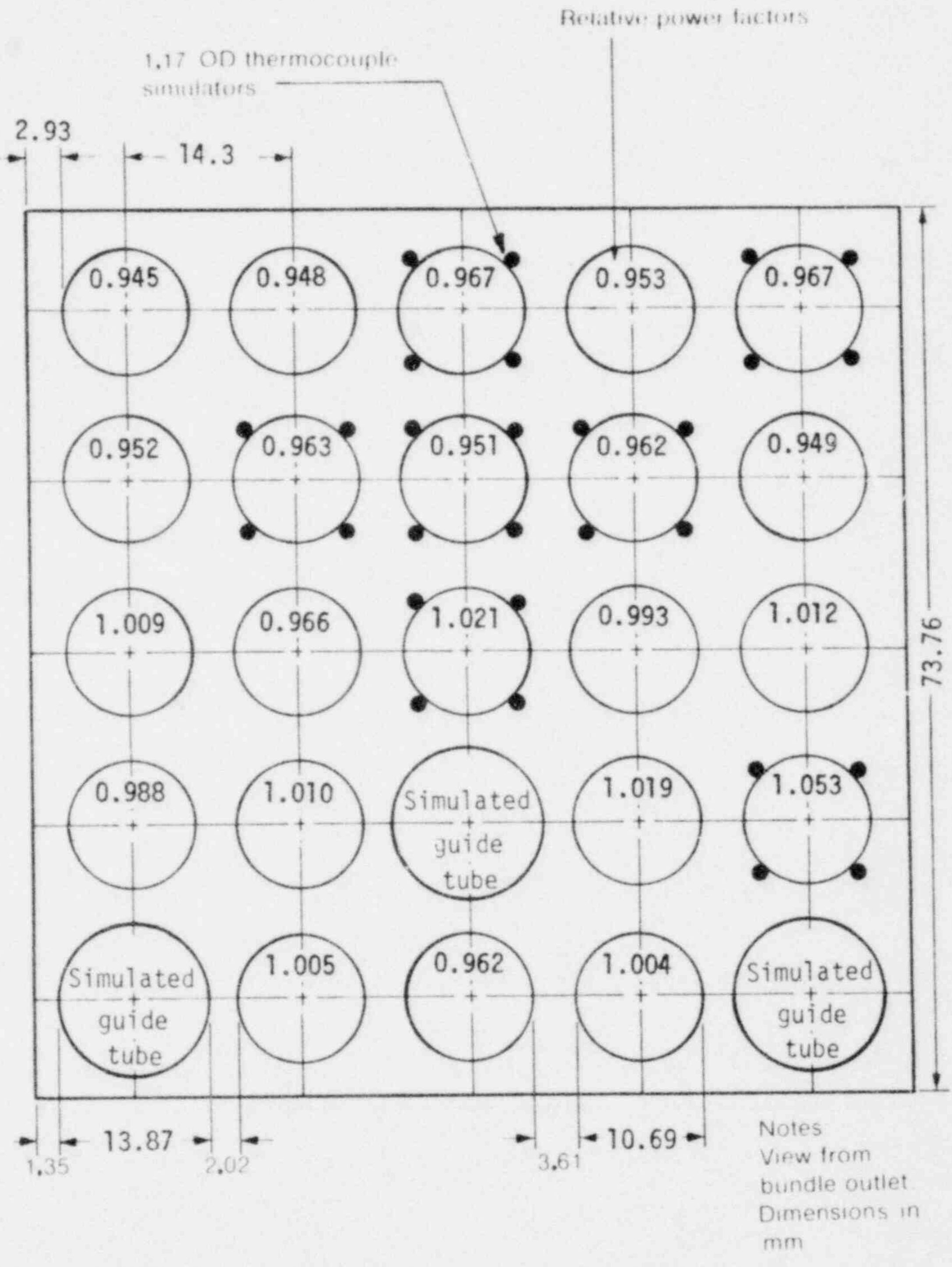

Fig. 2 Configuration of rod bundle with external thermocouple simulators (ANC1 & EXX2).

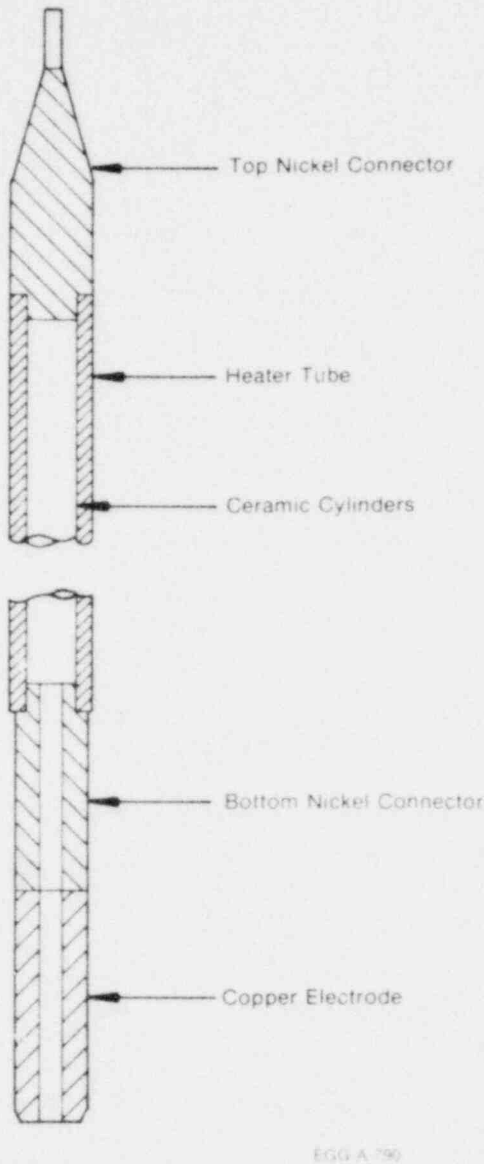

Figure 3 Heater rod assembly.

2.1.2 Simulated External Thermocouples. Seven of the rods in the test bundle incorporated external thermocouple simulators. Each rod had four simulators. The simulated thermocouples were fabricated from 1.17-mm OD Inconel tubing having a wall thickness of 0.05 mm. This tubing was filled with ceramic spaghetti to prevent collapse under pressure. The simulated thermocouples were laser welded axially along the rod in a manner similar to that of the actual thermocouples on the LOFT fuel rods[1]. The thermocouple simulators extended nearly the full length on each rod with a simulated thermocouple junction at the same axial level as the actual thermocouple junctions on the LOFT fuel rods. A typical thermocouple attachment and simulated junction are shown in Figure 4.

2.1.3 Simulated Guide Tubes. The test bundle incorporated three unheated rods which simulated RCC guide tubes in the LOFT reactor. These tubes were made of a stainless steel rod with 98% dense Al_2O_3 ceramic sleeves, 80-mm long with an OD of 13.9 mm, the same as the LOFT RCC guide tubes[1].

2.1.4 Grid Spacers. The test bundle incorporated five grid spacers (see Figure 5) similar to the LOFT fuel grid spacers[1]. These spacers did not have mixing vanes, the same as LOFT grid spacers. The spacers had an axial spacing of 0.42 m, the same as in the LOFT core. However, each grid spacer in the test section was located approximately 180 mm upstream of the corresponding LOFT spacer location. This placed the upstream side of the last grid spacer about 150 mm from the end of the heated length (see Figure 6). With this location, CHF occurred both

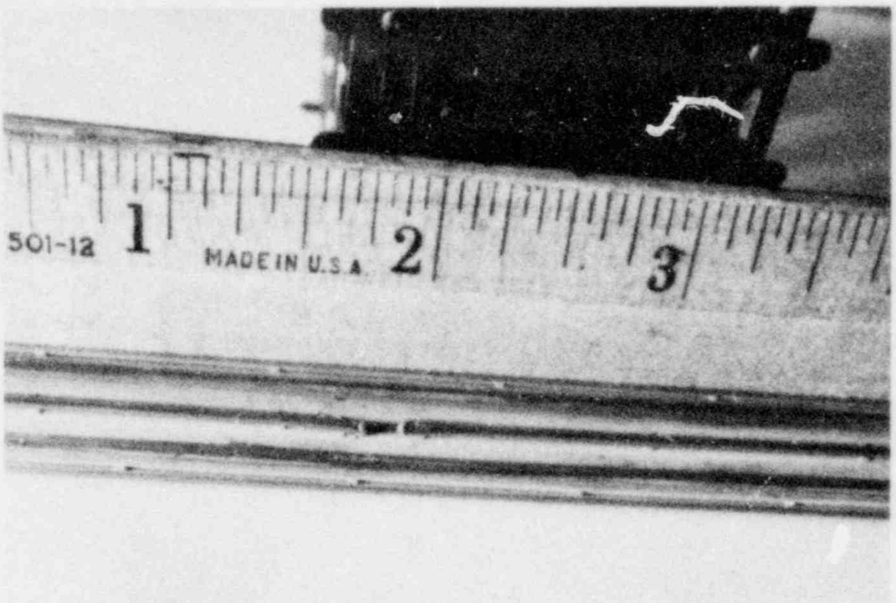

Figure 4 Photograph of a rod with thermocouple attached.

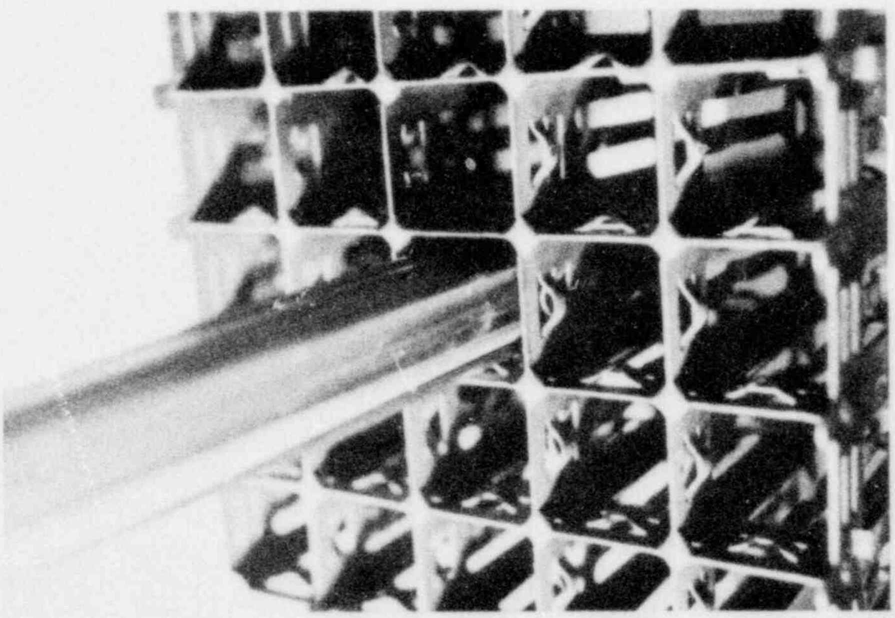

Figure 5 Photograph of grid spacer

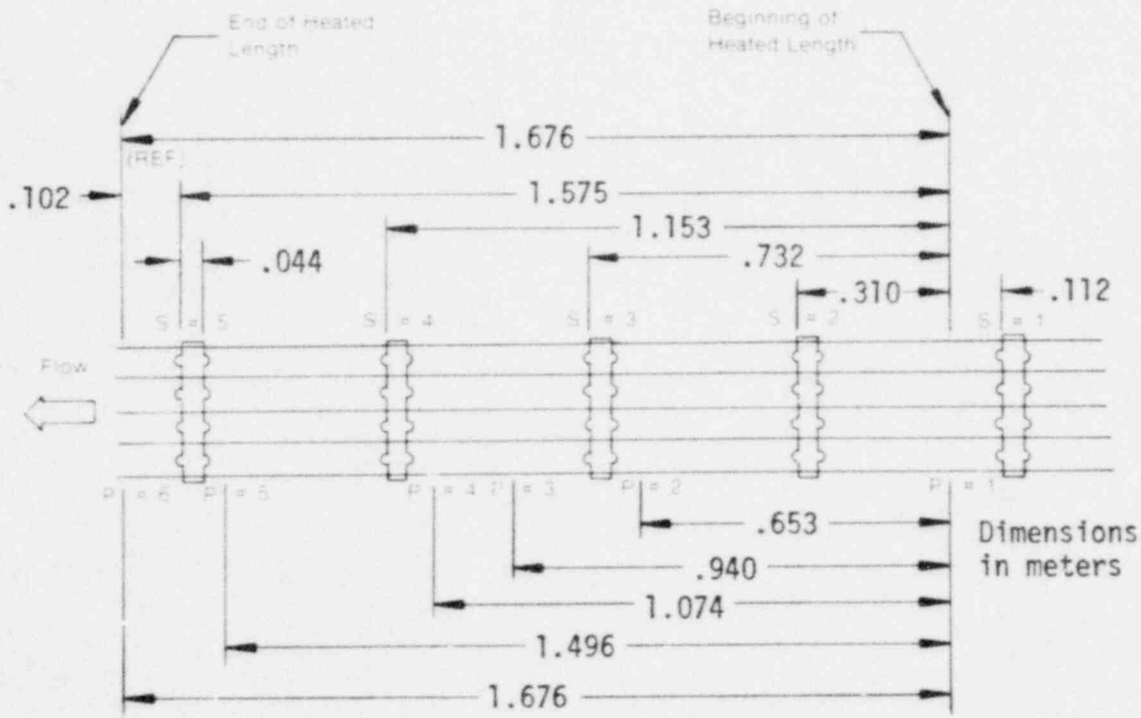

Figure 6 LOFT CHG test axial locatio of grid spacers and pressure taps.

upstream and downstream of the last spacer, thereby resulting in a mixture of CHF data strongly influenced by a grid spacer (CHF data from downstream of the last spacer) and weakly influenced by a grid spacer (immediately upstream of the last spacer).

Another reason for moving the spacers upstream 180 mm was to facilitate the measurement of the subchannel coolant temperatures at the test section outlet [see subsection 2.1.5 (3)]. The rake of thermocouples could not be installed at the end of the heated length without changing the location of the last grid spacer.

2.1.5 Test Section Instrumentation.

(1) CHF Detection Thermocouples. The heated rods contained internally mounted iron-constantan thermocouples employed as CHF detectors. These thermocouples were located 13 mm upstream from the end of the heated length and 13 mm upstream of the last grid spacer. These thermocouples were brazed to copper washers to improve the detection of temperature changes on the rod surface. This thermocouple installation is shown in Figure 7. The thermocouple leads were brought out of the bottom rod electrode.

(2) Pressure Transducers. The pressure drops across the heated length of the test section and across the grid spacers were measured. The pressure drops were visually read with mercury manometers and also measured with Barton differential pressure cells which were recorded by the data acquisition system. Pressure tap locations are shown in Figure 6.

(3) Subchannel Coolant Temperatures. Test section outlet subchannel coolant temperatures were measured with a rake of iron-constantan

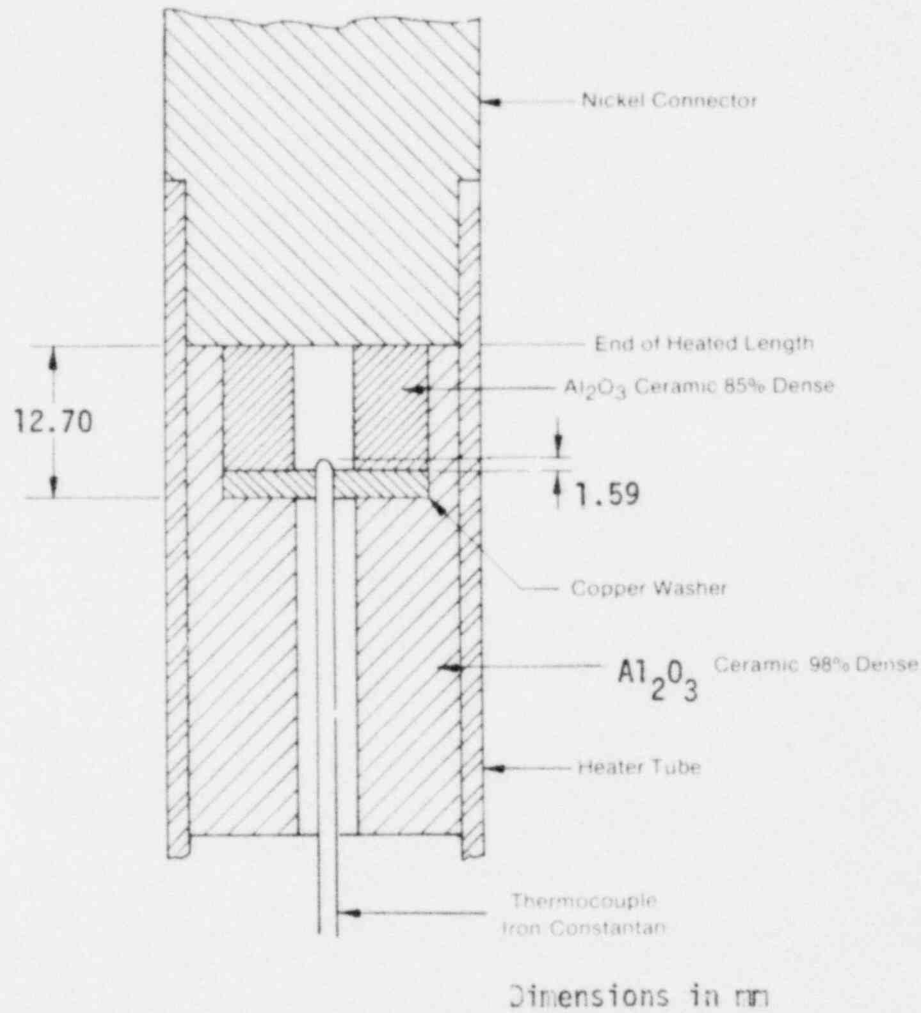

Figure 7 Single thermocouple instrumentation

thermocouples located 6.4-mm axially downstream from the end of the heated length. These thermocouples were centered within the subchannels.

2.1.6 Flow Housing. The flow housing consisted of four major components: the grid plate, the top adapter, the shroud box, and the bottom adapter.

The grid plate was machined from a nickel plate. It served as a top electrical connection, transferring the current from the rods to a large nickel disc, which in turn led the current out through the insulated pressure seals and to the copper bus. The grid plate was accurately machined to maintain the tops of the rods in proper geometry.

The top adapter located the shroud box with reference to the heated rod geometry and provided a transition from the geometry of the rod bundle channel to an open arrangement for the coolant discharge.

The shroud box was made of four rectangular pieces of stainless steel, machined and fitted to hold the ceramic liner which actually forms the flow channel. The ceramic shroud liner was made of 98% dense Al_2O_3 in 0.5 m long sections, and ground to the desired dimensions within a tolerance of $\pm$0.08 mm. Holes for pressure tap locations were drilled at selected points along the axial length of the flow channel. The inner dimensions of the installed shroud liner were 73.8 mm square and were sized to allow the enthalpy rise in the peripheral subchannels of the test section to simulate that in adjacent subchannels in the LOFT core.

The bottom adapter located the inlet end of the flow channel with respect to the heated rods, and provided a region for coolant entry into the channel.

2.1.7 "O" Ring Seals. Each rod passed from inside the loop pressure vessel out to the atmosphere through a series of "O" ring seals. This arrangement permitted independent axial movement of each rod.

2.1.8 Electrical Connections. The top electrical connection was made through the grid plate as described earlier. The bottom electrical connections were made by clamping a copper connector to each rod. The connectors were fitted with flexible leads which were connected to an octagonal bus arrangement surrounding the copper electrodes.

2.2 ANC Rod Bundle Description (bundle with external thermocouple simulators)

This 25-rod bundle (designated ANC2) was designed to duplicate the Exxon bundle with external thermocouple simulators. The characteristics of this bundle are the same as those listed in Table I; however, some minor differences existed in the fabrication and instrumentation of this bundle.

The heater rods for this bundle were made of Type 347 stainless steel tubing with wall thicknesses of 0.43, 0.46, and 0.48 mm. The wall thicknesses of these rods were increased to add integrity to the bundle and also to reduce the voltage drop across the grid spacers, thereby reducing the electrical arcing between the grid spacer dimples and the rods and increasing the life of the bundle. Also, the grid spacer dimples and spring tabs were plasma sprayed with a thin coating of Al_2O_3 to reduce arcing between the grid spacers and the rods.

The center rod in this bundle was changed to a high powered rod as compared to a medium powered rod in the Exxon bundle. This was done in an attempt to force CHF to occur in the center of the bundle away from the unheated walls of the test section. The normalized rod power factors for this bundle are shown in Figure 8.

The CHF detecting thermocouples in this bundle were located 13-mm upstream from the end of the heated length and 6.4-mm upstream of the last grid spacer. Four of the rods had several Chromel-Alumel thermocouples located azimuthally around the rod at the axial level just upstream of the last grid spacer as shown in Figure 9. The purpose of this additional instrumentation was to attempt to pinpoint the location of CHF initiation to help determine whether or not the external thermocouples have an effect on CHF. The installation of these thermocouples is shown in Figure 10.

2.3 ANC Rod Bundle Description (bundles without external thermocouple simulators)

These 25-rod bundles (designated ANC3 and ANC4) were designed to duplicate the ANC2 rod bundle except that they did not incorporate external thermocouple simulators. The characteristics of these bundles were the same as those listed in Table I except for the thermocouple simulators. The fabrication of the ANC3 bundle was the same as for the ANC2 bundle. The normalized rod power factors for this bundle are shown in Figure 11.

The ANC3 bundle was instrumented with azimuthal thermocouples just upstream of the last grid spacer as shown in Figure 12.

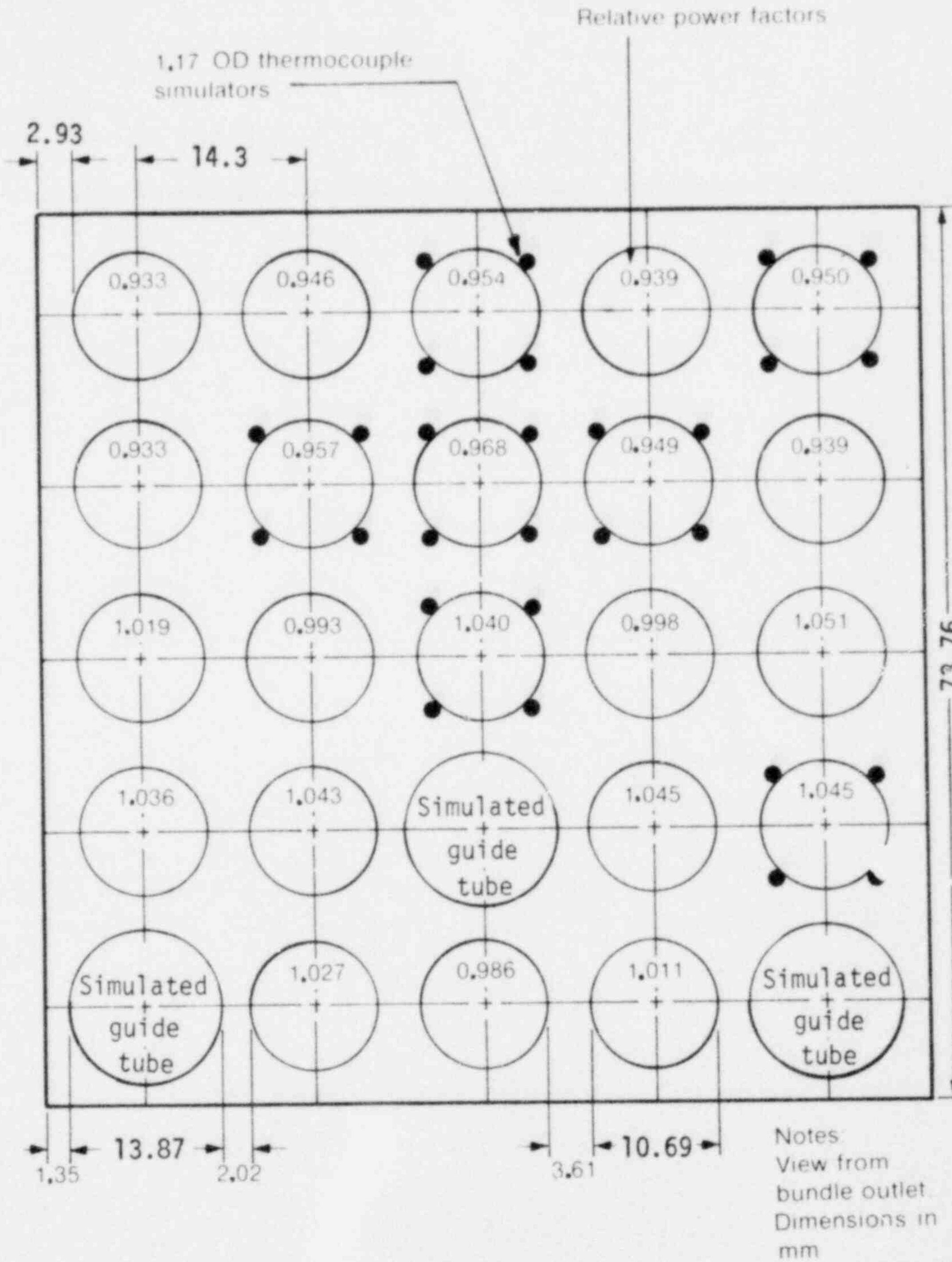

Figure 8 Configuration of rod bundle with external thermocouple simulators (ANC2).

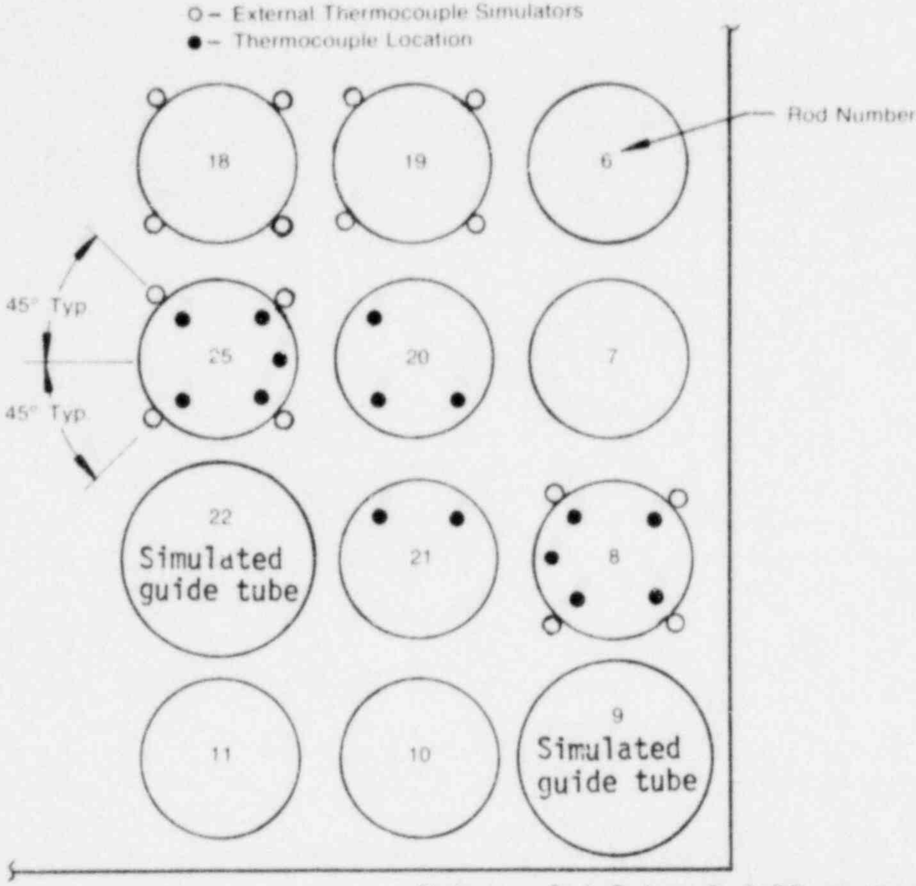

Notes: Axial Level 6.35 mm Upstream of Last Grid Spacer (0.152 m from end of heated length.) View from Bundle Outlet

Figure 9 Azimuthal location of CHF detecting thermocouples in ANC2 test bundle.

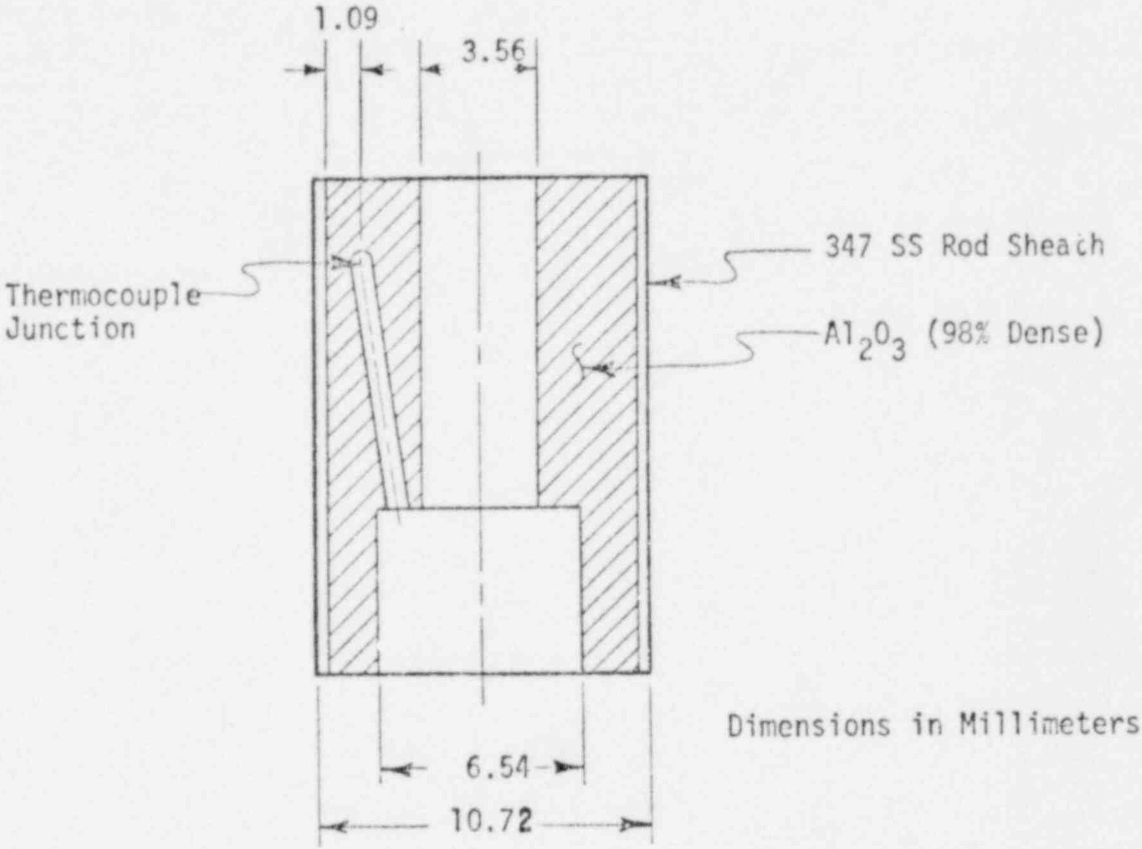

Figure 10 Installation of azimuthal CHF detecting thermocouples.

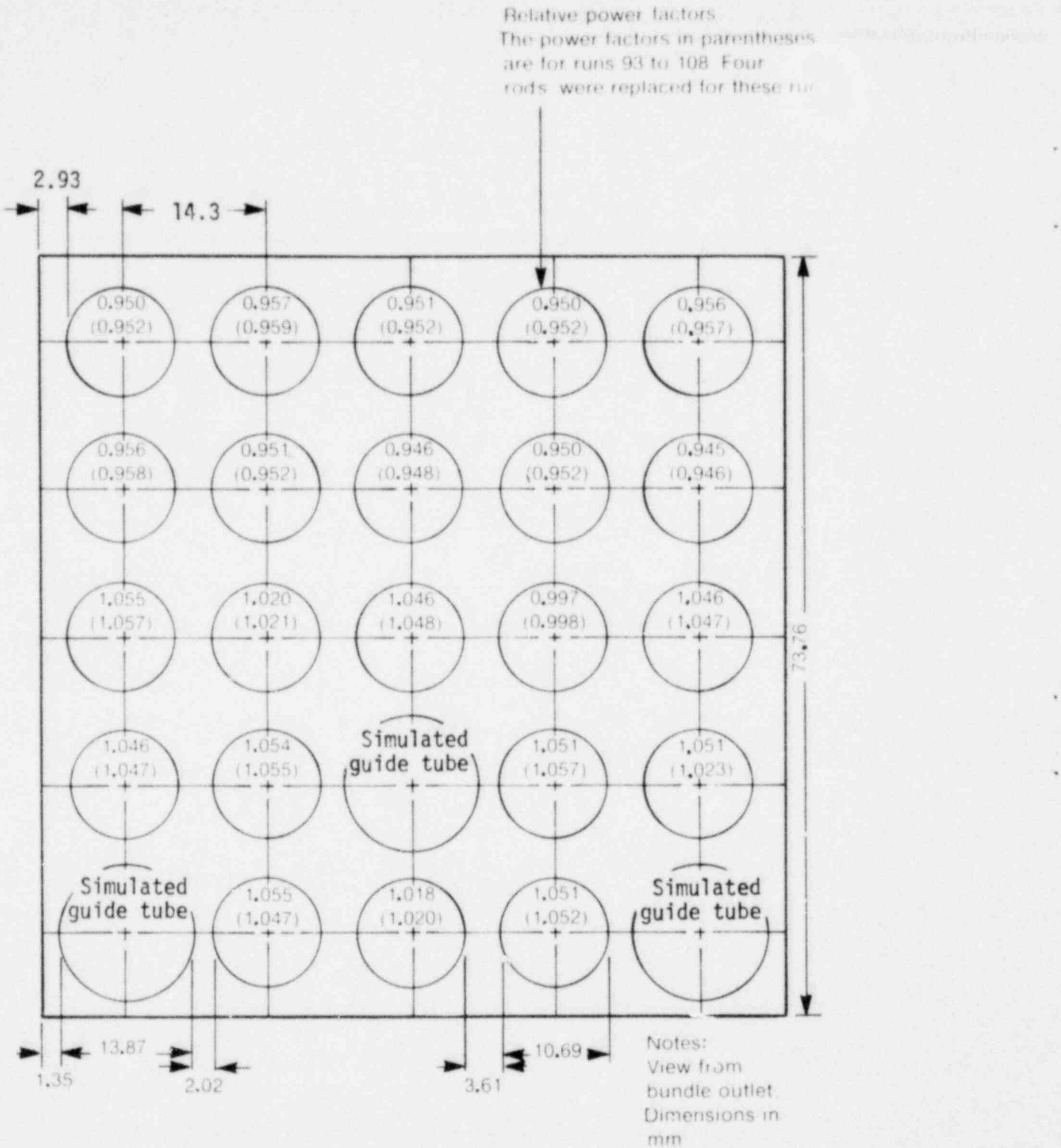

Figure 11 Configuration of rod bundle without external thermocouple simulators (ANC3).

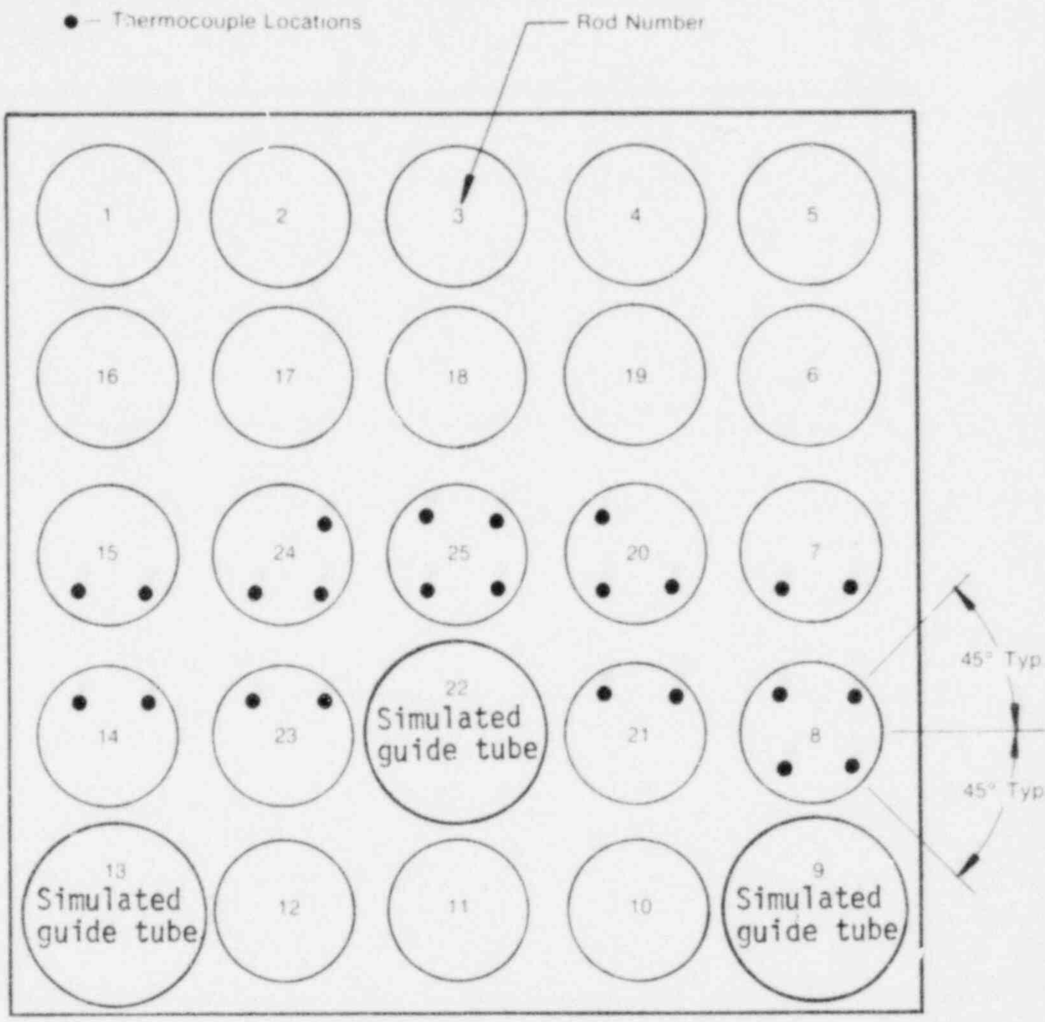

Notes: Axial Level 6.35 mm Upstream of Last Grid Spacer (0.152 m upstream from end of heated length)

View of Bundle Outlet

Figure 12 Azimuthal location in CHF detecting thermocouples in ANC3 test bundle.

The ANC3 bundle provided data at 13.8 MPa but failed prior to testing at 6.9 and 10.3 MPa.

The 25-rod bundle (designated ANC4) was used to obtain data at 6.9 and 10.3 MPa. The ANC4 bundle configuration was the same as the ANC3 bundle. The normalized rod power factors for the ANC4 bundle are shown in Figure 13. This bundle was primarily designed for transient (blowdown) CHF tests so the internal CHF sensing thermocouples were located differently than for the ANC3 bundle. Only one thermocouple was positioned in each rod at 12.7 and 152.4 mm from the end of the heated length. The azimuthal locations of these thermocouples are shown in Figure 14. These thermocouples were mounted in the ceramic plugs in the rods, the same as the azimuthal thermocouples in the ANC2 and ANC3 bundles.

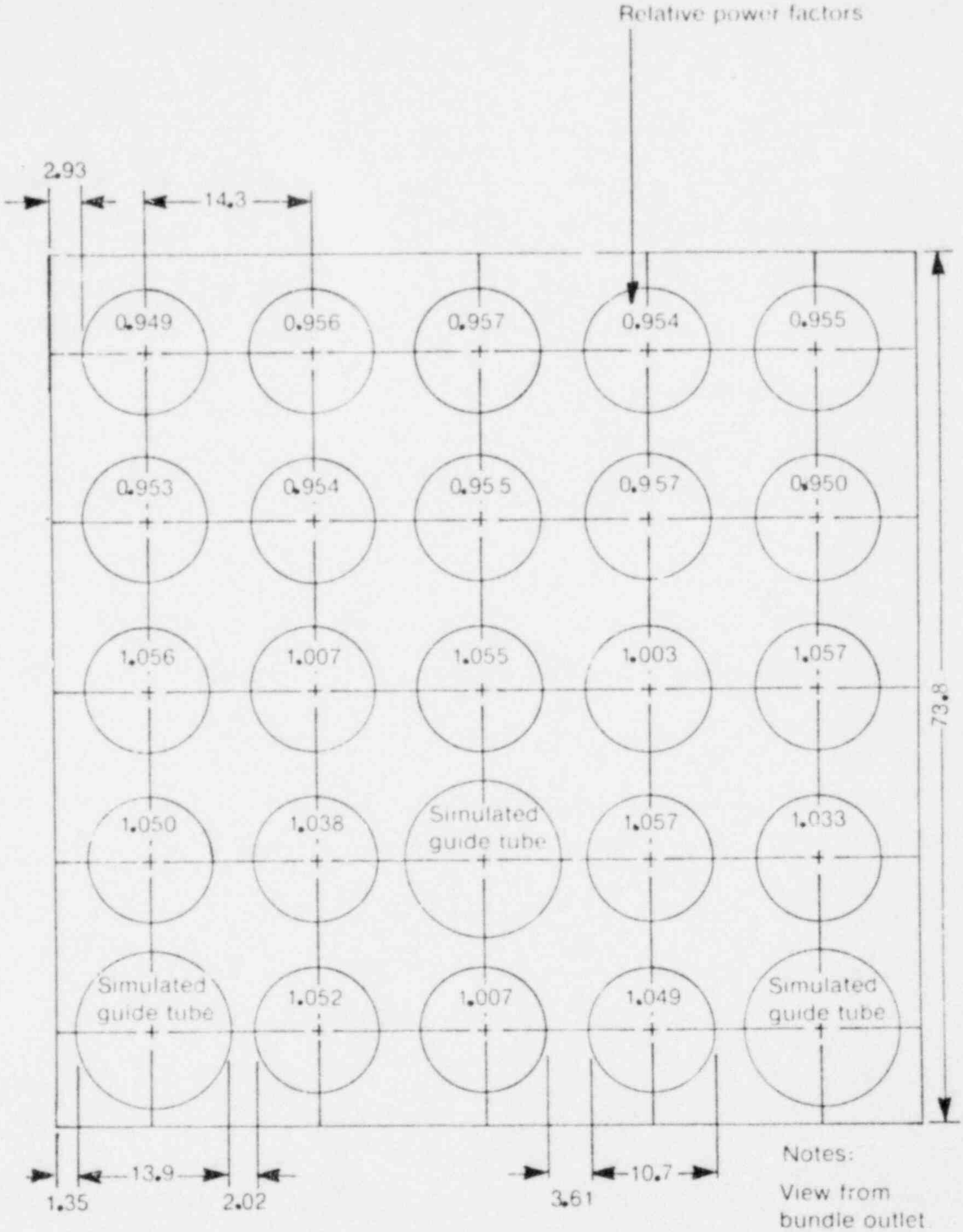

Figure 13 Configuration of rod bundle without external thermocouple simulators (ANC4).

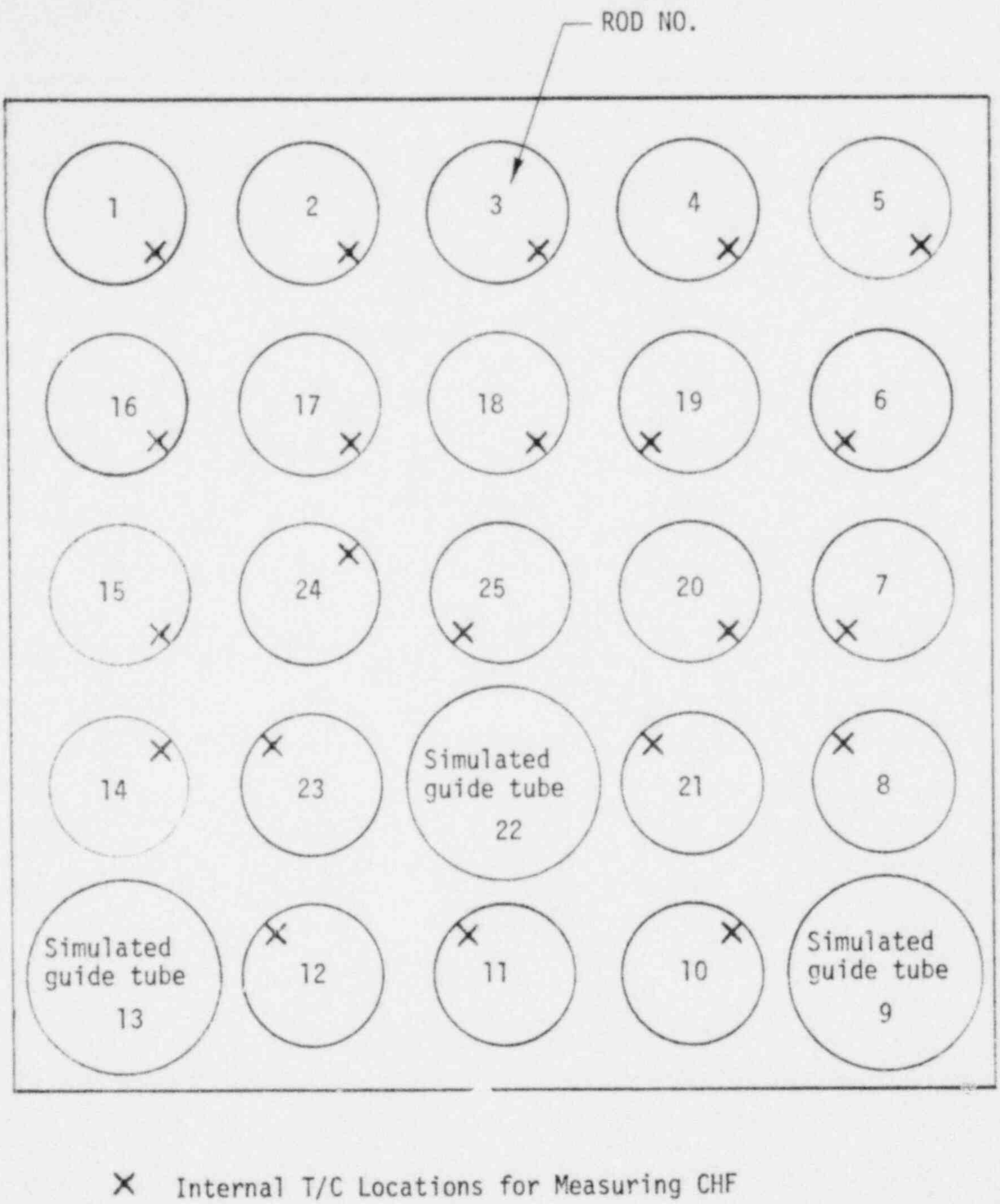

Figure 14 Azimuthal location of CHF detecting thermocouples in ANC4 test bundle

3. EXPERIMENT PERFORMANCE

Forty of the 157 data points for the rod bundles with rod external thermocouple simulators were obtained with the EXX2 bundle in 1973. These data points were taken at 10.3 and 13.8 MPa. The remaining 117 data points were obtained with the ANC2 bundle in November 1975. These data were taken at 6.9, 10.3 and 13.8 MPa.

Nineteen of the 53 data points for the rod bundles without rod external thermocouple simulators were obtained with the ANC3 bundle in December 1975. The ANC3 bundle failed beyond repair at this point (see Reference 2). These data were taken at 13.8 MPa. The remaining 34 data points were obtained with the ANC4 bundle in May 1977. Most of these data were taken at 6.9 and 10.3 MPa with only 3 data points taken at 13.8 MPa.

Pressure drop tests were conducted on all 4 of these bundles. The data were in excellent agreement.

III. ANALYSIS OF DATA

1. DISCUSSION

The data reduction method to be explained was used for all four sets of CHF data: EXX2, ANC2, ANC3 and ANC4. Any variations in the method for the different sets are explained fully. The objective of the data reduction was to arrive at accurate subchannel coolant conditions at each CHF location for each test run. This allowed a CHF correlation using local subchannel coolant conditions to be developed or the data to be compared with existing steady state CHF correlations.

The test data from the four sets of CHF tests were in the form of computer printouts of conditions during each run, strip charts indicating rod CHF occurrence, and electrical resistance measurements for the heated rods. The run conditions included the test section coolant inlet temperature, system pressure, flow rate, power level and pressure drop across various segments of the test bundle. The power was determined from voltage (bus-to-bus) and current measurements for the bundle. Each heated rod in a bundle had a 1.68 m segment of stainless steel, termed the heated length, and nickel and copper extensions at both ends. The bus-to-bus voltage measurement included the voltage drop across the nickel and copper extensions. In order to determine the power for the heated length portion of the test bundle, a voltage correction factor was used

$$F = \frac{V_{\text{bus-to-bus}}}{V_{\text{heated length}}}$$

where V = voltage.

Assuming the voltage across the heated length was the same for all of the heated rods, the power was corrected by

$$P_{\text{heated length}} = P_{\text{bus-to-bus}}/F$$

where P = power.

The heated length voltage was measured during the ANC3 tests, and the results, F as a function of inlet temperature, are shown in Figure 15. The ANC2, ANC3, and ANC4 power measurements were corrected using this function. The curve of F versus inlet temperature (Figure 15) was not applicable to the EXX2 bundle because of the differences in the heater rod wall thickness between the ANC2, ANC3, and ANC4 bundles, and the EXX2 bundle. For the EXX2 data the voltage correction factor was assumed to be a constant 1.025, regardless of inlet temperature because no $V_{\text{heated length}}$ measurements were available for these tests.

The inlet enthalpy, needed as input to COBRA-II, was determined from the inlet temperature and system pressure using the ASME Steam Tables[3]. The resulting run condition data for the four CHF tests are listed in Appendix A.

Internal thermocouple voltage readings during each test were recorded on strip charts. The occurrence of CHF near an internal thermocouple location resulted in a sharp rise in the thermocouple voltage reading. A typical strip chart indication of CHF is shown in Figure 16. From the charts, the rod(s) experiencing CHF was determined for each test run. When there were multiple CHF indications, either at different axial levels on one rod or on different rods, all indications were assumed to be independent CHF indications.

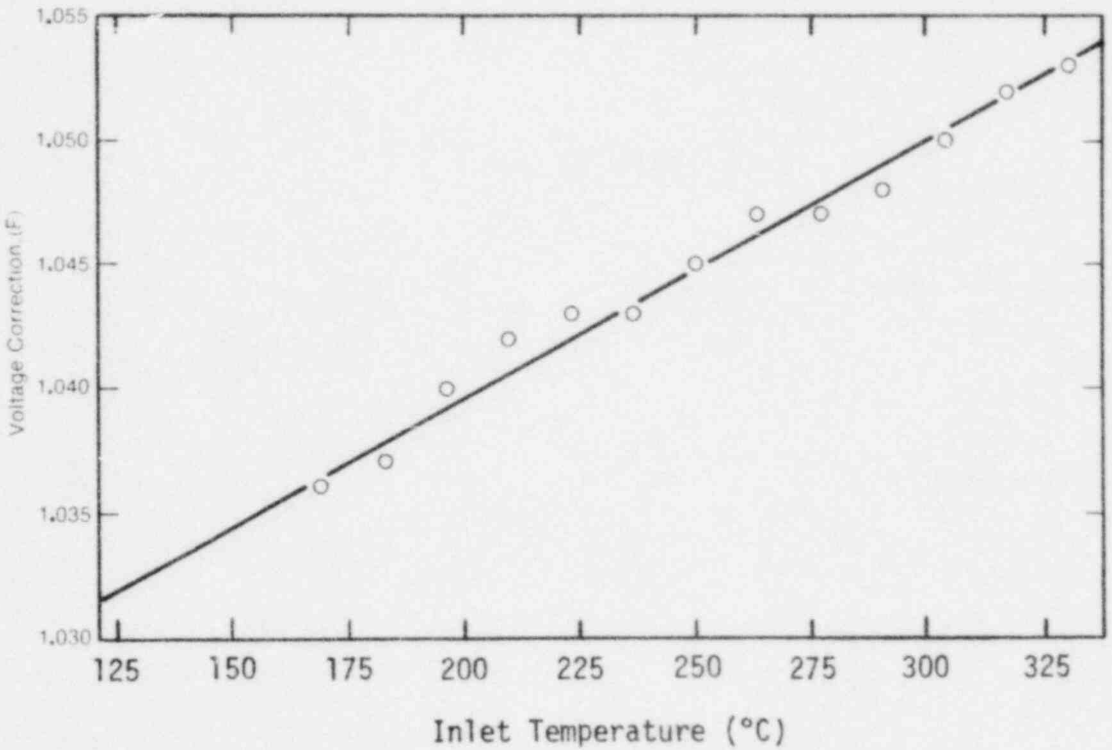

Figure 15 Voltage correction, F, versus inlet temperature for the ANC2, ANC3 and ANC4 test sections.

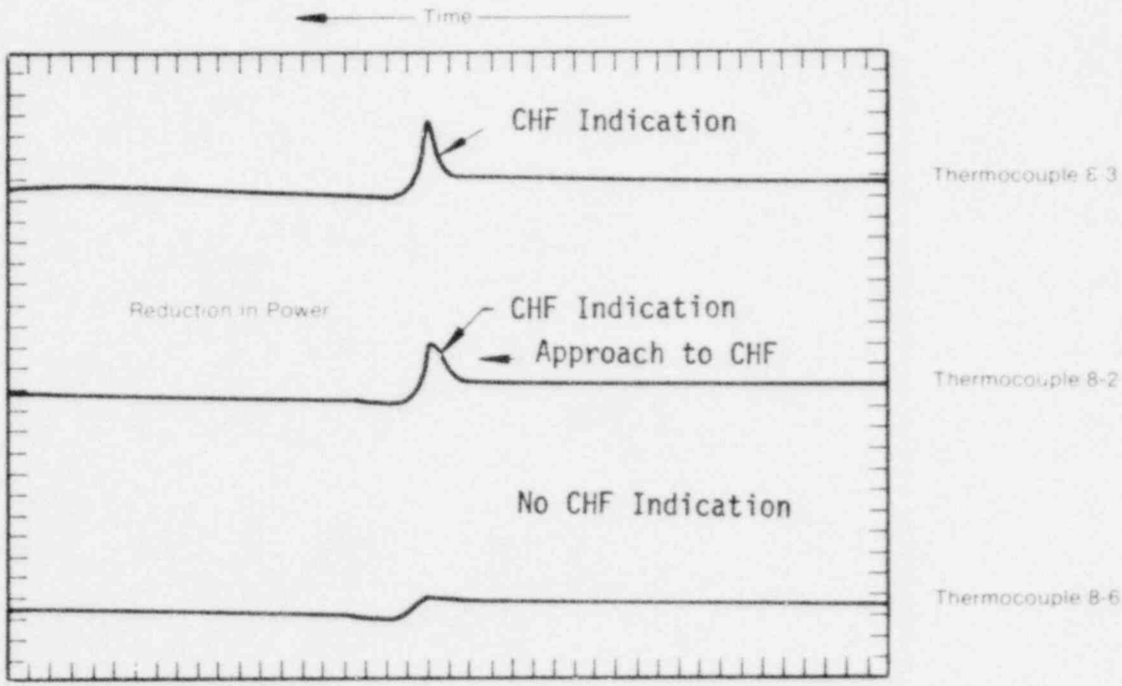

Figure 16 Thermocouple strip chart traces showing typical CHF indications.

CHF indications occurring significantly after the initial CHF indication were not included in the data base because they were usually the result of a system pressure drop when the power was reduced.

Once the CHF rod(s) was identified for each test run, a corresponding subchannel was chosen. Most of the ANC2 and ANC3 CHF indications came at axial locations in which the azimuthal thermocouples indicated the azimuthal CHF region[a]. If CHF occurred at the end of the bundle (1.68 m) where there were no azimuthal thermocouples, CHF was assumed to occur at the same azimuthal region as indicated by the thermocouples at the 1.52 m level. In cases where there was some doubt as to CHF region, one of the cooler subchannels adjacent to the CHF rod was chosen in order to be conservative. The EXX2 test was run with nondirectional thermocouples. CHF regions were chosen so that they agreed with those chosen for similar CHF indications in the ANC2 bundle.

With the system conditions for each CHF run and the location of CHF known, the subchannel code COBRA-II was used to predict the local subchannel conditions at CHF, such as mass flux and equilibrium quality.

---

[a] At times, two directional thermocouples would indicate CHF on the same rod at the same axial level, but in adjacent subchannels. In such cases, both indications were considered as independent CHF points. Actually, the CHF was probably occurring between the two subchannels.

2. SUBCHANNEL CODE AND MODEL

2.1 COBRA-II Description

The steady state subchannel analysis code COBRA-II[4] was used in the data analysis. COBRA-II ".... computes the flow and enthalpy in the subchannels of rod bundle nuclear fuel during both boiling and nonboiling conditions. It uses a mathematical model that considers two types of crossflow mixing. The first type is a net diversion crossflow caused by flow redistribution, and the second is a turbulent (fluctuating) crossflow caused by the random travel of coolant between adjacent subchannels. Each subchannel is assumed to contain one-dimensional, two-phase slip-flow and is assumed to have a sufficiently fine two-phase flow structure to permit specification of local void fraction as a function of enthalpy, flow, pressure and position. The equations of the mathematical model are solved as an initial-value problem by using finite differences."[4] COBRA-II was used rather than the newer version COBRA-IIIC[5], which also handles time-dependent problems, because of the difference in execution times. Both programs give essentially the same results for steady state problems. The program is listed in Reference 2.

2.2 Model of Test Bundle

Figure 8 shows the COBRA-II model of the test sections. There were 22 heated rods of 10.7 mm diameter, three unheated rods of 13.9-mm diameter, and an unheated shroud. The five grid spacer locations are shown in Figure 6. The COBRA-II calculations were started at the beginning of the heated lengths of the rods. Uniform enthalpy and mass flux were assumed at this level. This is a good assumption because there is a significant length of straight flow and one grid spacer upstream of the beginning of the heated length.

2.3 Single-Phase Friction Factor

The flow through the test bundle for the range of test conditions covered in the CHF test was turbulent. Therefore, a friction factor of the form

$$f = CRe^{-0.20}$$

where Re = Reynolds number for the test section, was used[6]. ΔP predictions for the highly subcooled test runs of ANC2 resulted in the value 0.213 for C. It should be noted that the ΔP comparisons were made only across the total heated length. Shorter incremental ΔP measurements were judged to be highly uncertain. The value 0.213 is slightly higher than the 0.203 used in previous data evaluations[7,8]. It is believed that 0.213 is more accurate than 0.203 because the data base used in this analysis is much larger than that used previously. The value 0.213, 16% above the smooth tube figure of 0.184, is not unusual. Tong and Weisman[9] indicate that for a bundle with a pitch-to-diameter ratio of 1.27 (the CHF bundles had a ratio of 1.33), the friction factor is 0 to 20% higher than the smooth tube correlation.

2.4 Grid Spacer Coefficients

COBRA-II computes the ΔP across grid spacers by using user-defined coefficients for each spacer and subchannel within the spacer. The coefficients are defined as:

$$C = \frac{\Delta P}{\frac{1}{2}\frac{\rho}{g_c}V^2}$$

where

v = velocity of the fluid

ρ = density of the fluid

g_c = Newton constant.

The spacer coefficients used for this work came from the results of velocity and pressure drop measurements made on a 15 x 15-rod LOFT central fuel assembly[7]. The spacers for the 15 x 15-rod test were similar to those for the CHF tests. For each spacer, four different spacer coefficients were used, depending on the type of subchannel:

$C = 2.91\ Re^{-0.142}$	Corner subchannels
$C = 2.25\ Re^{-0.142}$	Outer subchannels (bordering on shroud inner wall)
$C = 4.20\ Re^{-0.142}$	Inner subchannels
$C = 4.99\ Re^{-0.142}$	Inner subchannels adjacent to a simulated guide tube

where Re = Reynolds number for the subchannel.

In the 15 x 15-rod test large variations in flow were present at the inlet, so the lowest two sets of spacer coefficients were different from the others because of large flow redistributions. In the CHF tests the inlet flow was essentially uniform, so all of the spacers were assumed to have the same set of coefficients as Spacers 3 through 5 in Reference 7.

2.5 Turbulent Mixing Coefficient

COBRA-II models turbulent mixing momentum and enthalpy interchange between adjacent subchannels by the use of a turbulent mixing coefficient β[10]. Hot mixing results obtained before the CHF tests included outlet coolant temperature measurements for each subchannel. An evaluation of β using the hot mixing data resulted in

$$\beta = 0.0062 \frac{D}{S} Re^{-0.10}$$

where

D = average hydraulic diameter for the two subchannels in question

S = rod gap spacing between the two subchannels in question

Re = average Reynolds number for the two subchannels in question.

However, there was very little difference in the COBRA-II predictions over the range $\beta = (0.00 \text{ to } 0.0120) \frac{D}{S} Re^{-0.10}$. These results agree with previous estimates of β[7,11] for LOFT Core-1 fuel assemblies.

2.6 True Quality Correlation

COBRA-II has options for various two-phase correlations for true quality, void fraction, and friction multiplier. For true quality, the Levy model was used (in the program it is termed a subcooled void correlation, but it actually predicts only the true quality). Weisman and Bowring[12] believe the Levy model is more accurate than modified versions of the Bowring model, used in the subchannel codes HAMBO[13] and some versions of THINC[14], for mass fluxes greater than 680 kg/s-m^2 [the range for the CHF tests was 680 - 3400 kg/s-m^2]. Also Collier[15] states that the Levy correlation agrees well with the data of Egan, of Maurer, and of Rouhani.

2.7 Void Correlation

The Thom subcooled void correlation modified by Tong[9] was used for the subcooled region, and the Thom annular void model[9] was used for the positive equilibrium quality region. Several other void correlations investigated were the modified Armand[16], the homogeneous[4], the Levy, and the Bowring[15]. The Thom correlations were chosen because they generally predicted lower void fractions than the other models, which reduced the predicted pressure drops and improved the agreement with the ANC2 ΔP data. Castellana and Bonilla[17] indicate that the Thom and Bowring correlations are widely used and are generally recognized to show good agreement with available data. Also, Tong and Weisman[9] feel that the Thom subcooled correlation is somewhat more accurate than the Bowring model. These observations and the fact that the Thom correlations resulted in the most accurate ΔP predictions are justification for using the Thom models for the CHF data reduction.

2.8 Two-Phase Friction Multiplier

The Armand two-phase friction multiplier[4] was used in COBRA-II. Several other correlations investigated were the Thom, Levy, Baroczy, homogeneous (in COBRA-II), and Martinelli-Nelson[15]. The Armand Correlation generally predicted the lowest friction multipliers resulting in lower ΔP predictions, which agreed best with the ANC2 ΔP data.

For bulk boiling, the region in which the friction multiplier is the largest and has the most effect on the ΔP predictions, the Armand, Thom, and homogeneneous models are similar[17] and any of these three could have been used. The Martinelli-Nelson model was not used because it tends to overpredict the value of the friction multiplier for most of the mass fluxes involved, 680 to 3400 kg/s-m^2.

2.9 Pressure Drop Predictions

Pressure drop data were obtained for each run during the CHF tests. Although six ΔP values were recorded, corresponding with various lengths of the test section, only the ΔP across the total heated length of the bundle was compared with the COBRA-II predictions. The uncertainty in the other five measurements was large.

A comparison of measured to predicted test section pressure drops was made. The predicted pressure drops were generally lower than measured in the quality range of 0 to 30% and generally higher than measured in the quality range above 30%. The pressure drop predictions were an average of 4.6% low for all of the ANC4 runs and 2.3% low for all of the ANC2 runs. The change in the trend of measured to predicted pressure drop near a quality of 30% could be due to a change in flow regime from bubbly-slug flow to annular flow.

2.10 Power Generation In Rods

2.10.1 Rod Power Factors. The rod power factor determinations are an important part of the data reduction because they directly affect the experimental critical heat flux values and the COBRA-II predictions of local CHF conditions. Rod power factors represent the power generation in a rod relative to the average rod power generation in a test bundle. They were calculated from rod resistances measured at Columbia University before and after CHF testing. The conversion of resistances to power factors involved several steps and involved mostly simple electrical parallel and series resistance formulas. The first step was to determine the resistances at the test temperatures, which were assumed to be 640 K for the heated stainless steel sheaths and 590 K for the nickel extensions. The copper part of the extensions contributed a negligible amount to the resistance of the extensions. Then, power factors for the rods (heated length and extensions) were calculated using the formula

$$PF_{T,i} = \frac{R_{eq,T}}{R_{T,i}}$$

where

$$R_{eq,T} = \frac{1}{\sum_{j=1}^{22} \frac{1}{R_{T,i}}}$$

The subscript T denotes total rod (heated length and extensions) and i denotes the ith rod. All resistances used were those determined for the run temperatures mentioned previously.

Finally, the power factors were corrected to reflect only the power generated in the heated length of the rods. The formulas used are

$$PF_{HL,i} = PF_{T,i}\left(\frac{R_{HL,i}}{R_{T,i}}\right) \quad \text{(constant)}$$

$$22 = \left(\sum_{j=1}^{22} PF_{HL,j} \right) \text{ (constant)}$$

The subscript HL denotes heated length. All resistances used were those appropriate for the run temperatures. The original rod resistances at room temperature, intermediate calculations, and the final rod power factors are listed in Tables II through V for the four sets of CHF tests.

2.10.2 External Thermocouple Effect on Power Factors. Some of the power generated in a rod with external thermocouple simulators was actually generated in the simulators. This distinction was not needed for the COBRA-II calculations because predictions of enthalpy at the region of CHF do not distinguish between rod and thermocouple power generation. However, when determining the rod heat flux at the CHF location, the thermocouple power generation should not be included. The heat flux at the rod surface was much greater than at the thermocouple simulator surface. Therefore, the CHF probably started on the rod surface rather than on the simulator. In order to determine the surface heat flux at the point of CHF, the power generated by the thermocouple simulators was eliminated, and then the remaining power was assumed to be spread uniformly on the rod surface (excluding the thermocouple simulator surfaces).

It should be noted that some of the total power generation in a rod with external thermocouples also occurred within the welds attaching the thermocouples to the rod. Exxon Nuclear Company estimated that about

TABLE II

ROD RESISTANCES AND RELATIVE POWER FACTORS FOR THE EXX2 TEST BUNDLE

Rod Number	Resistances - 300 K (78°F) Heated Length (Ω)	Resistances - 300 K (78°F) Extensions (Ω)	Resistances - Run Temperatures[a] Heated Length (Ω)	Resistances - Run Temperatures[a] Extensions (Ω)	Rod Power Factors	Rod Power Factors With Thermocouple Effect Eliminated
1	0.1343	0.00090	0.1804	0.00287	0.945	
2	0.1334	0.00100	0.1792	0.00319	0.948	
3	0.1256	0.00090	0.1667	0.00287	1.020	0.967
4	0.1328	0.00100	0.1784	0.00319	0.953	
5	0.1255	0.00095	0.1665	0.00303	1.020	0.967
6	0.1335	0.00095	0.1795	0.00303	0.949	
7	0.1247	0.00100	0.1675	0.00319	1.012	
8	0.1150	0.00100	0.1526	0.00319	1.107	1.053
9	-	-	-	-	-	
10	0.1249	0.00120	0.1677	0.00382	1.004	
11	0.1266	0.00200	0.1700	0.00637	0.962	
12	0.1248	0.00120	0.1676	0.00382	1.005	
13	-	-	-	-	-	
14	0.1245	0.00170	0.1672	0.00541	0.988	
15	0.1252	0.00100	0.1681	0.00319	1.009	
16	0.1325	0.00110	0.1779	0.00350	0.952	
17	0.1258	0.00100	0.1669	0.00319	1.016	0.963
18	0.1274	0.00100	0.1691	0.00319	1.003	0.951
19	0.1263	0.00090	0.1676	0.00287	1.015	0.962
20	0.1276	0.00090	0.1714	0.00287	0.993	
21	0.1239	0.00100	0.1664	0.00319	1.019	
22	-	-	-	-	-	
23	0.1258	0.00085	0.1689	0.00271	1.010	
24	0.1273	0.00090	0.1710	0.00287	0.996	
25	0.1178	0.00120	0.1563	0.00382	1.074	1.021

[a] Run temperatures are defined as 640 K (700°F) for the heated lengths and 590 K (600°F) for the extensions.

TABLE III

ROD RESISTANCES AND RELATIVE POWER FACTORS FOR THE ANC2 TEST BUNDLE

Rod Number	Resistances - 300 K (78°F) Heated Length (Ω)	Resistances - 300 K (78°F) Extensions (Ω)	Resistances - Run Temperatures[a] Heated Length (Ω)	Resistances - Run Temperatures[a] Extensions (Ω)	Rod Power Factors	Rod Power Factors With Thermocouple Effect Eliminated
1	0.08660	0.00185	0.11630	0.00589	0.933	
2	0.08605	0.00170	0.11557	0.00541	0.946	
3	0.08225	0.00175	0.10964	0.00557	0.990	0.954
4	0.08675	0.00170	0.11651	0.00541	0.939	
5	0.08245	0.00180	0.10991	0.00573	0.985	0.950
6	0.08720	0.00160	0.11711	0.00510	0.939	
7	0.07810	0.00140	0.10489	0.00446	1.051	
8	0.07350	0.00195	0.09805	0.00621	1.081	1.045
9	-	-	-	-	-	
10	0.07970	0.00175	0.10704	0.00557	1.011	
11	0.08200	0.00175	0.11013	0.00557	0.986	
12	0.07780	0.00185	0.10449	0.00589	1.027	
13	-	-	-	-	-	
14	0.07785	0.00170	0.10455	0.00541	1.036	
15	0.07975	0.00160	0.10710	0.00510	1.019	
16	0.08865	0.00185	0.11637	0.00589	0.933	
17	0.08215	0.00170	0.10951	0.00541	0.993	0.957
18	0.08195	0.00155	0.10924	0.00494	1.004	0.[illegible]8
19	0.08205	0.00190	0.10937	0.00605	0.984	0.949
20	0.08100	0.00190	0.10878	0.00605	0.988	
21	0.07760	0.00160	0.10422	0.00510	1.045	
22	-	-	-	-	-	
23	0.07800	0.00155	0.10475	0.00494	1.043	
24	0.08160	0.00170	0.10959	0.00541	0.993	
25	0.07385	0.00195	0.09852	0.00621	1.076	1.040

[a] Run temperatures are defined as 640 K (700°F) for the heated lengths and 590 K (600°F) for the extensions

TABLE IV

ROD RESISTANCES AND RELATIVE POWER FACTORS FOR THE ANC3 TEST BUNDLE

Rod Number	Resistances - 300 K (78°F)		Resistances - Run Temperatures[a]		Rod Power Factors
	Heated Length (Ω)	Extensions (Ω)	Heated Length (Ω)	Extensions (Ω)	
1	0.08630	0.00175	0.11590	0.00557	0.950 (0.952)
2	0.08655	0.00155	0.11624	0.00494	0.957 (0.959)
3	0.08650	0.00170	0.11617	0.00541	0.951 (0.952)
4	0.08725	0.00155	0.11718	0.00494	0.950 (0.952)
5	0.08625	0.00165	0.11583	0.00526	0.956 (0.957)
6	0.08710	0.00170	0.11698	0.00541	0.945 (0.946)
7	0.07810	0.00165	0.10489	0.00526	0.046 (0.047)
8	0.07745(0.07970)[b]	0.00170(0.00175)	0.10402(0.10704)	0.00541(0.00557)	1.051 (1.023)
9	-	-	-	-	-
10	0.07795	0.00160	0.10469	0.00510	1.051 (1.052)
11	0.08170	0.00140	0.10972	0.00446	1.018 (1.020)
12	0.07780(0.07785)	0.00155(0.00170)	0.10449(0.10455)	0.00494(0.00541)	1.055 (1.047)
13	-	-	-	-	-
14	0.07735	0.00180	0.10388	0.00573	1.046 (1.047)
15	0.07830	0.00145	0.10516	0.00462	1.055 (1.057)
16	0.08640	0.00160	0.11604	0.00510	0.956 (0.958)
17	0.08650	0.00170	0.11617	0.00541	0.951 (0.952)
18	0.08670	0.00175	0.11644	0.00557	0.946 (0.948)
19	0.08655	0.00170	0.11624	0.00541	0.950 (0.952)
20	0.08160	0.00180	0.10959	0.00573	0.997 (0.998)
21	0.07795(0.07760)	0.00160(0.00160)	0.10469(0.10422)	0.00510(0.00510)	1.051 (1.057)
22	-	-	-	-	-
23	0.07795(0.07800)	0.00155(0.00155)	0.10469(0.10475)	0.00494(0.00494)	1.054 (1.055)
24	0.08205	0.00130	0.11019	0.00414	1.020 (1.021)
25	0.07805	0.00165	0.10487	0.00526	1.046 (1.048)

[a] Run temperatures are defined as 640 K (700°F) for the heated lengths and 590 K (600°F) for the extensions.

[b] All quantities in parentheses indicate changes for CHF runs 93 to 108 caused by the replacement of four rods.

TABLE V

ROD RESISTANCES AND RELATIVE POWER FACTORS FOR THE ANC4 TEST BUNDLE

Rod Number	Resistances - 300 K (78°F)		Resistances - Run Temperatures[a]		Rod Power Factors
	Heated Length (Ω)	Extensions (Ω)	Heated Length (Ω)	Extensions (Ω)	
1	0.08645	0.00155	0.11610	0.00494	0.949
2	0.08605	0.00150	0.11557	0.00478	0.956
3	0.08620	0.00145	0.11577	0.00462	0.957
4	0.08650	0.00145	0.11617	0.00462	0.954
5	0.08640	0.00145	0.11604	0.00462	0.955
6	0.08630	0.00155	0.11590	0.00494	0.950
7	0.07735	0.00145	0.10[illegible]68	0.00462	1.057
8	0.07905	0.00150	0.10616	0.00478	1.033
9	-	-	-	-	-
10	0.07730	0.00160	0.10381	0.00510	1.049
11	0.08080	0.00160	0.10851	0.00510	1.007
12	0.07755	0.00150	0.10415	0.00478	1.052
13	-	-	-	-	-
14	0.07765	0.00150	0.10428	0.00478	1.050
15	0.07715	0.00150	0.10361	0.00478	1.056
16	0.08610	0.00155	0.11563	0.00494	0.953
17	0.08650	0.00145	0.11617	0.00462	0.954
18	0.08565	0.00160	0.11503	0.00510	0.955
19	0.08595	0.00150	0.11543	0.00478	0.957
20	0.08165	0.00150	0.10966	0.00478	1.003
21	0.07760	0.00140	0.10422	0.00446	1.057
22	-	-	-	-	-
23	0.07640	0.00195	0.10261	0.00621	1.038
24	0.08160	0.00145	0.10959	0.00462	1.007
25	0.07705	0.00155	0.10348	0.00494	1.055

[a] Run temperatures are defined as 640 K (700°F) for the heated lengths and 590 K (600°F) for the extensions.

2% of a rod power generation occurred in the welds for the EXX2 bundle. This resulted in the estimate that the heat flux at the weld surfaces was twice that of the rod surface. A similar calculation for the ANC2 bundle indicated that the heat flux at the weld surfaces was less than at the rod surface. The reason for the difference between bundles is that the welds on the ANC2 bundle had much larger surface areas than did those on EXX2 and ANC1. Analysis of the CHF results (see Reference 2) indicated that no significant difference between bundles could be attributed to the difference in heat flux at the welds.

Assuming parallel electrical resistances for a rod and its four external thermocouple simulators, a formula for the total thermocouple simulator power generation in a rod was derived[a]

$$4\ P_{T/C} = P_w \left(1 - \frac{R_{T/C}}{R_{T/C}+4R_{w/o}}\right)$$

where P = power. The subscript T/C denotes one thermocouple simulator, w means a rod with thermocouple simulators, and w/o, an identical rod without thermocouple simulators. All quantities refer to the heated lengths only.

Using the preceding formula and assuming a test temperature of 640 K for the rod and thermocouple simulators resulted in a 3.3% power generation for the thermocouple simulators on Rods 8 and 25, and a 3.6% power generation for Rods 3, 5, 17, 18 and 19 for the ANC2 bundle. Since Rods 8 and 25 were high power rods, and their rod resistances were lower than the other rods, the thermocouple simulator effect was correspondingly smaller. Using the same formula for the EXX2 bundle

[a] It was assumed that whatever power was generated in the welds attaching the thermocouple simulator to the rod wall could be treated as though it were generated uniformly in the rod.

resulted in a 4.9% power generation in the simulators for Rods 8 and 25, and a 5.2% power generation for Rods 3, 5, 17, 18, and 19. Since the rod walls in the EXX2 bundle were thinner than those for ANC2, the thermocouple simulator power generation values were larger than those for ANC2. The resulting rod power factors with the thermocouple simulator power generation subtracted are listed in Table II for EXX2 and Table III for ANC2. ANC3 and ANC4 bundles had no thermocouple simulators, so the rod power factors for them are unchanged.

xon Nuclear Company[19] estimated, by another method, the thermocouple simulator power generation to be 4.6% for the EXX2 bundle using room temperature resistances. The equation in this report with room temperature resistances predicts 4.5% for the same rods. The major differences between Reference 19 and this analysis are that in this report an attempt was made to account for resistance changes when the bundles were heated up to actual run conditions and to account for minor differences between high power rods (8 and 25) and low power rods, (3, 5, 17, 18, and 19).

3. SUBCHANNEL RESULTS

The conditions for each test run and used as input to the COBRA II code are listed in Appendix A for the EXX2, ANC1, ANC2, ANC3, and ANC4 data sets.

The results of the data reduction work, critical heat flux, local quality, and mass flux for each CHF occurrence are listed in Appendix B for all four sets of tests.

IV. RESULTS

1. COMPARISON OF DATA BETWEEN BUNDLES WITH ROD EXTERNAL THERMOCOUPLE SIMULATORS (EXX2 AND ANC2) AND BUNDLES WITHOUT ROD EXTERNAL THERMOCOUPLE SIMULATORS (ANC3 AND ANC4)

The data from the bundles with rod external thermocouple simulators (EXX2, ANC1 and ANC2) have been compared with the data from the bundles without rod external thermocouple simulators (ANC3 and ANC4). In order to make this comparison, a new CHF correlation was developed (designated LOFT-2) based on the 157 data points from the bundles with rod external thermocouple simulators. The data base for the LOFT-2 correlation does not completely cover all combinations of pressure, quality and mass velocity over the pressure range of 6.9 to 13.8 MPa, however, the correlation does provide a valid means of comparing the data between the bundles because the data for the bundles with and without external thermocouple simulators were at approximately the same local fluid conditions. Since the data base for the LOFT-2 correlation is limited, the correlation does not provide a valid prediction of CHF for all combinations of pressure, quality and mass velocity that might occur in the LOFT reactor during blowdown. Therefore, the LOFT-2 correlation is not used for that application. The LOFT-2 correlation, however, satisfactorily predicts the 157 data points from the EXX2, ANC1 and ANC2 data sets as shown in Figures 17 through 20 with a mean value of measured to predicted CHF of 0.988 and a standard deviation of 0.106.

The data from the bundles without rod external thermocouple simulators (ANC3 and ANC4) have been compared with the LOFT-2 correlation as shown in Figures 21 through 24. Figure 21 indicates that data from the bundles without rod external thermocouple simulators is basically the

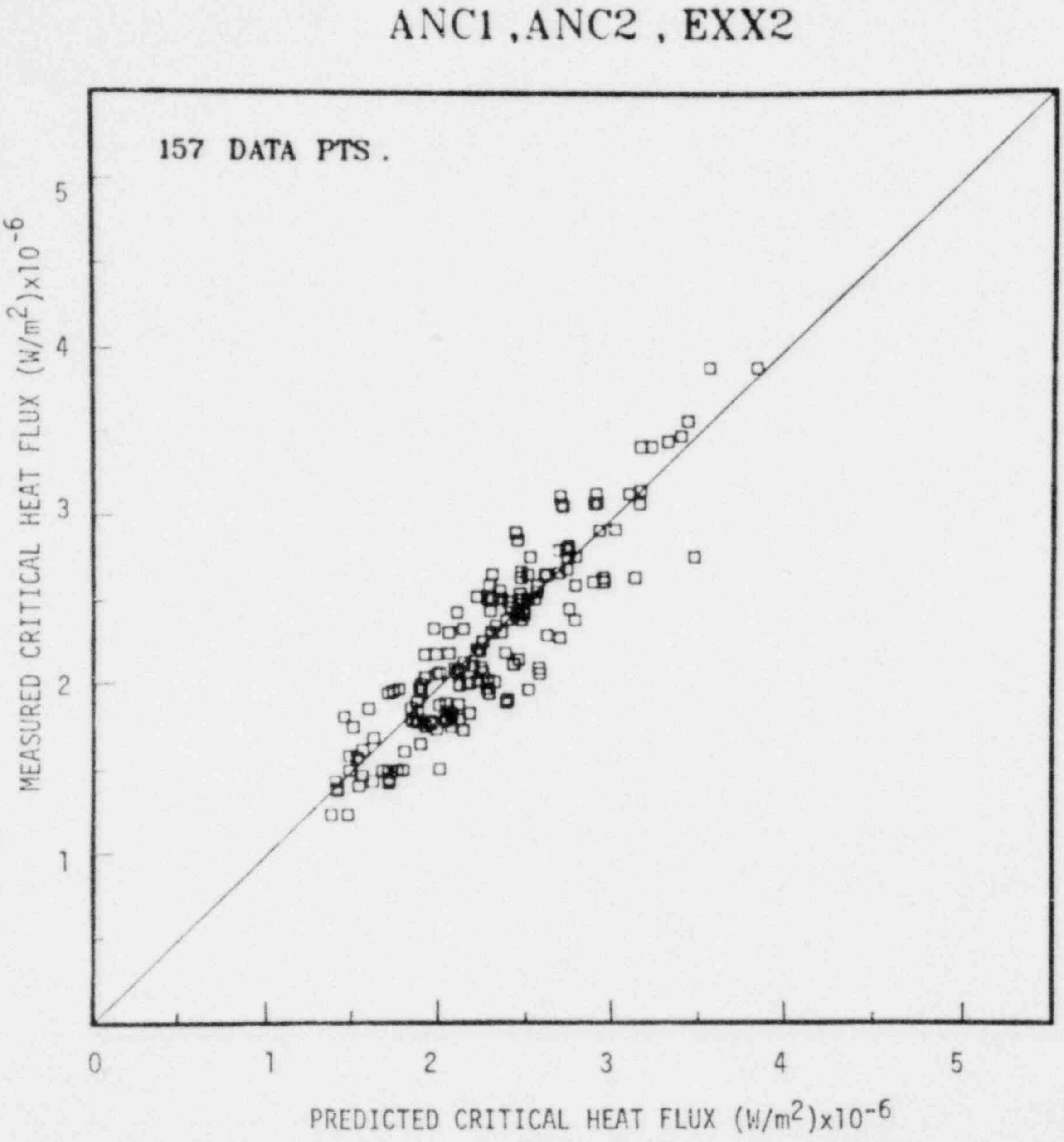

Figure 17 Comparison of measured to predicted critical heat flux. (LOFT-2 + COBRA-II) for LOFT bundles with external thermocouple simulators.

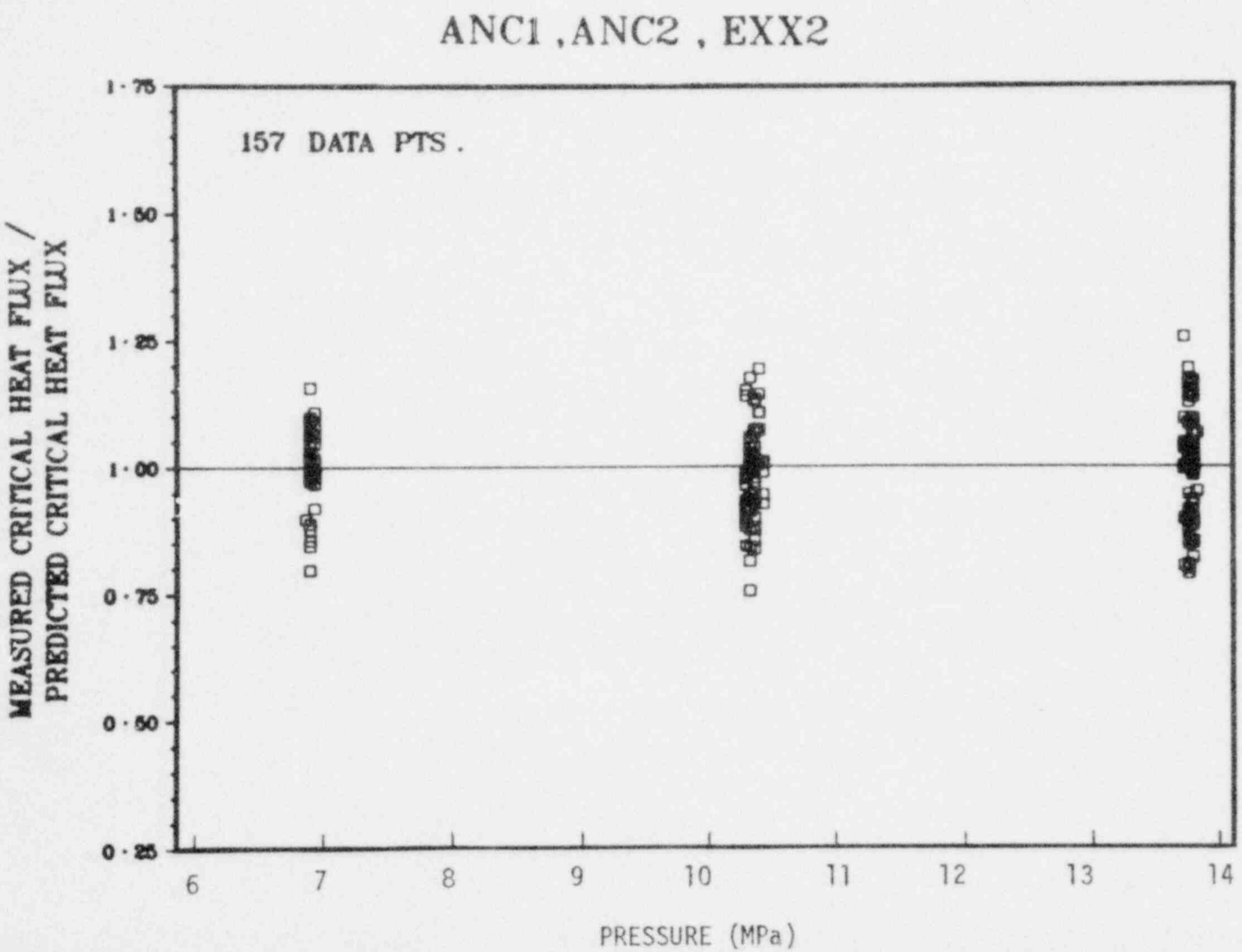

Figure 18 Ratio of measured to LOFT-2 predicted critical heat flux-vs-pressure for LOFT bundles with external thermocouple simulators.

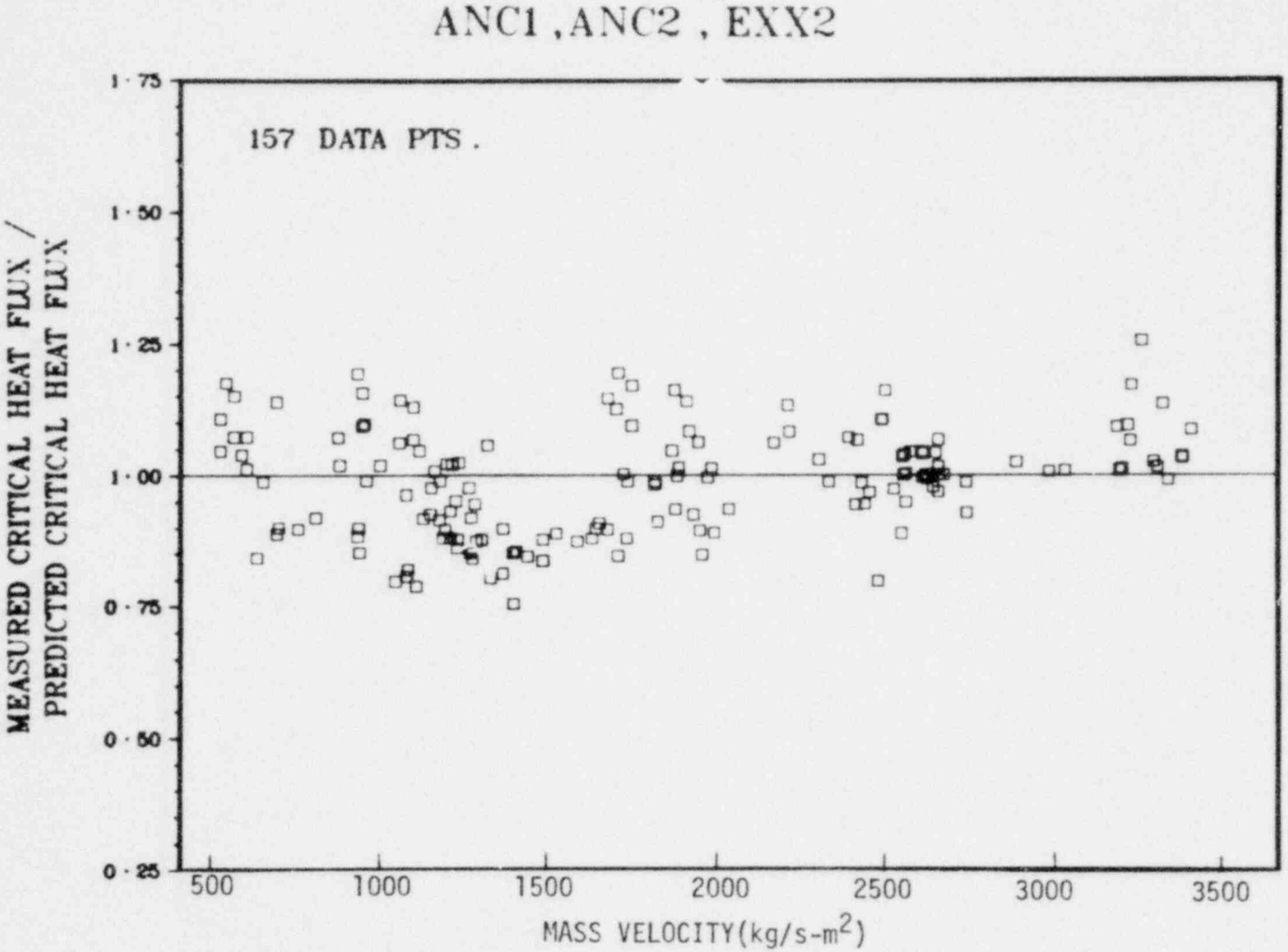

Figure 19 Ratio of measured to LOFT-2 predicted critical heat flux-vs-mass velocity for LOFT bundles with external thermocouple simulators.

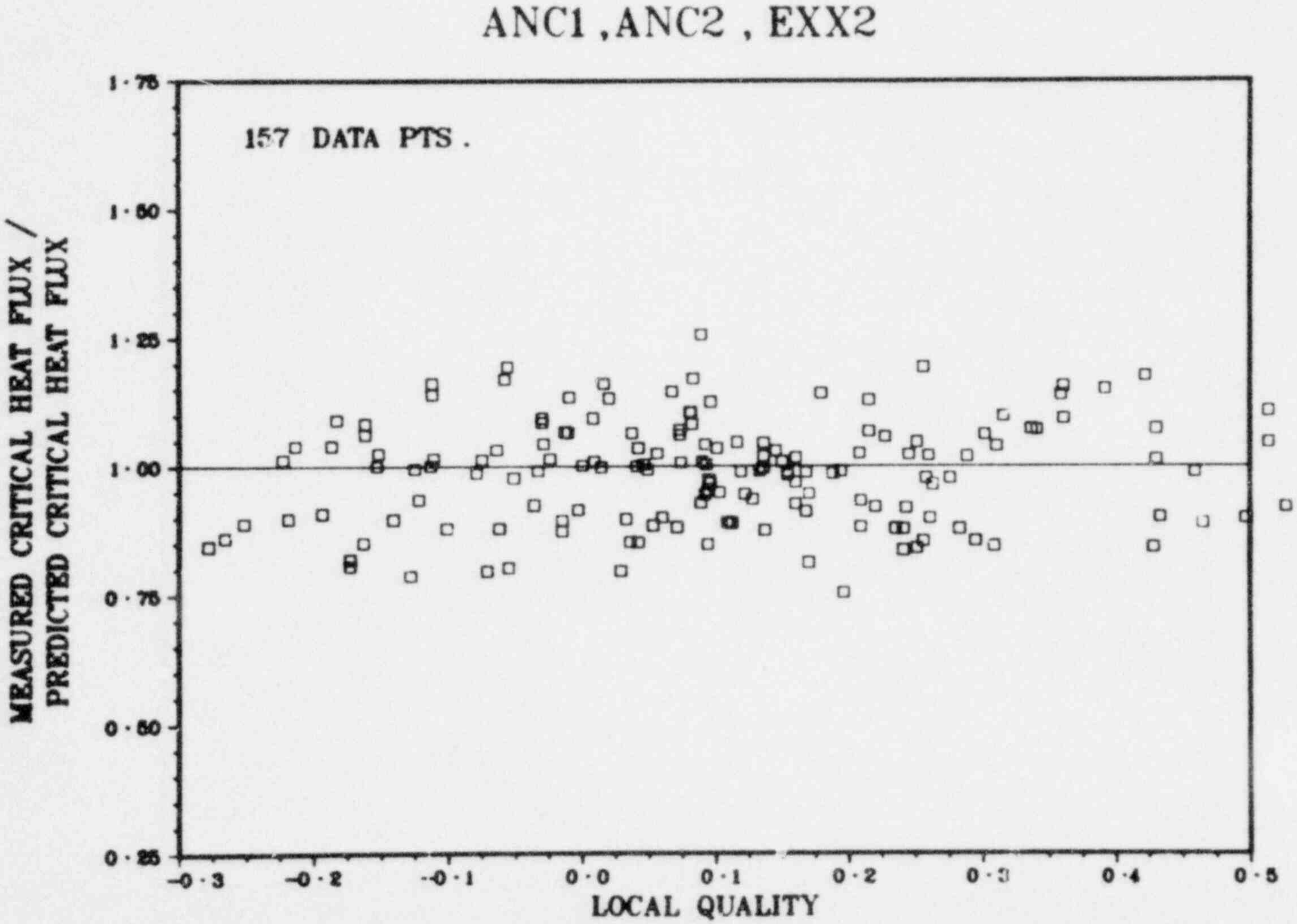

Figure 20 Ratio of measured to LOFT-2 predicted critical heat flux-vs-local quality for LOFT bundles with external thermocouple simulators.

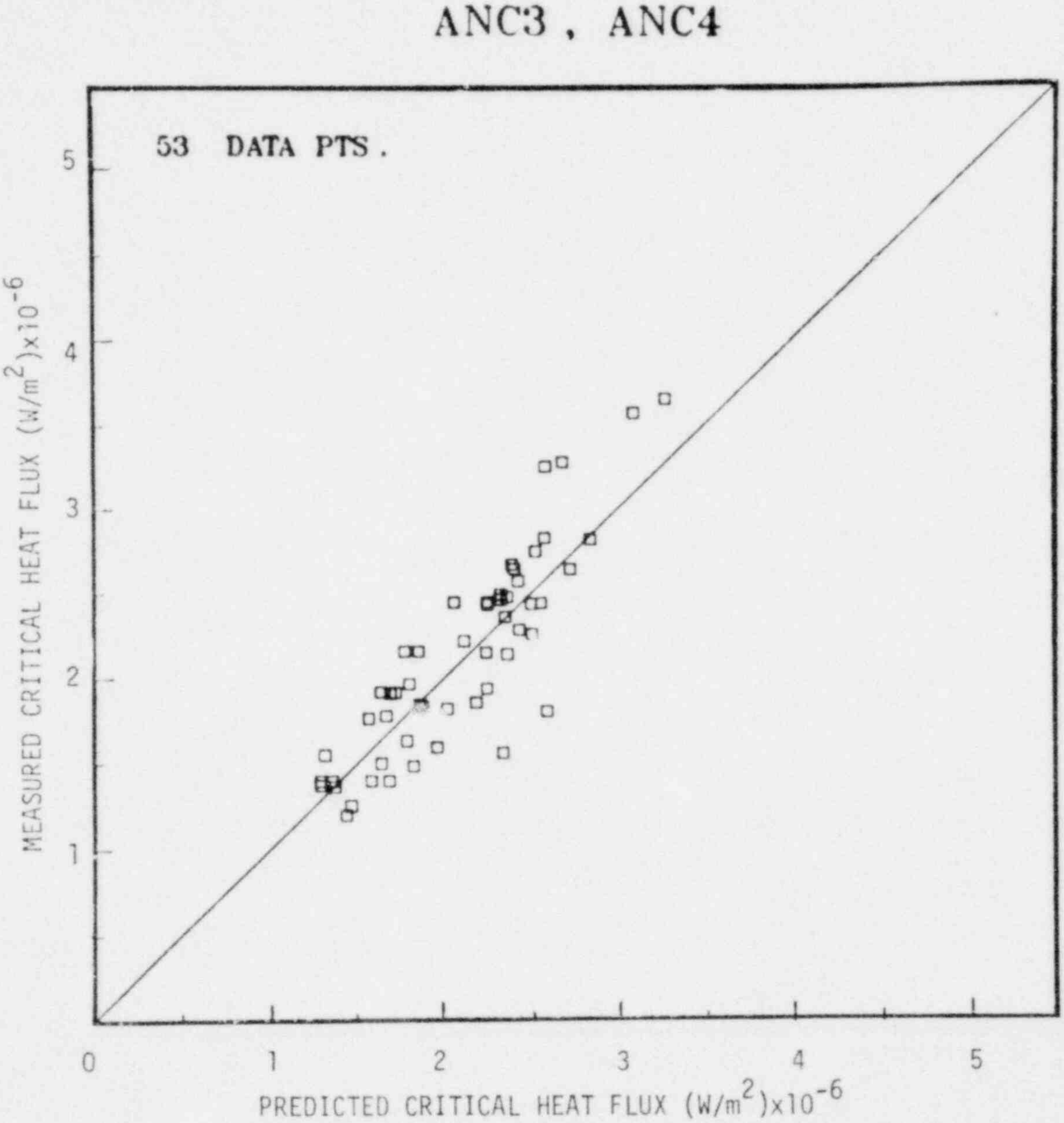

Figure 21 Comparison of measured to predicted critical heat flux. (LOFT-2 + COBRA-II) for LOFT bundles without external thermocouple simulators.

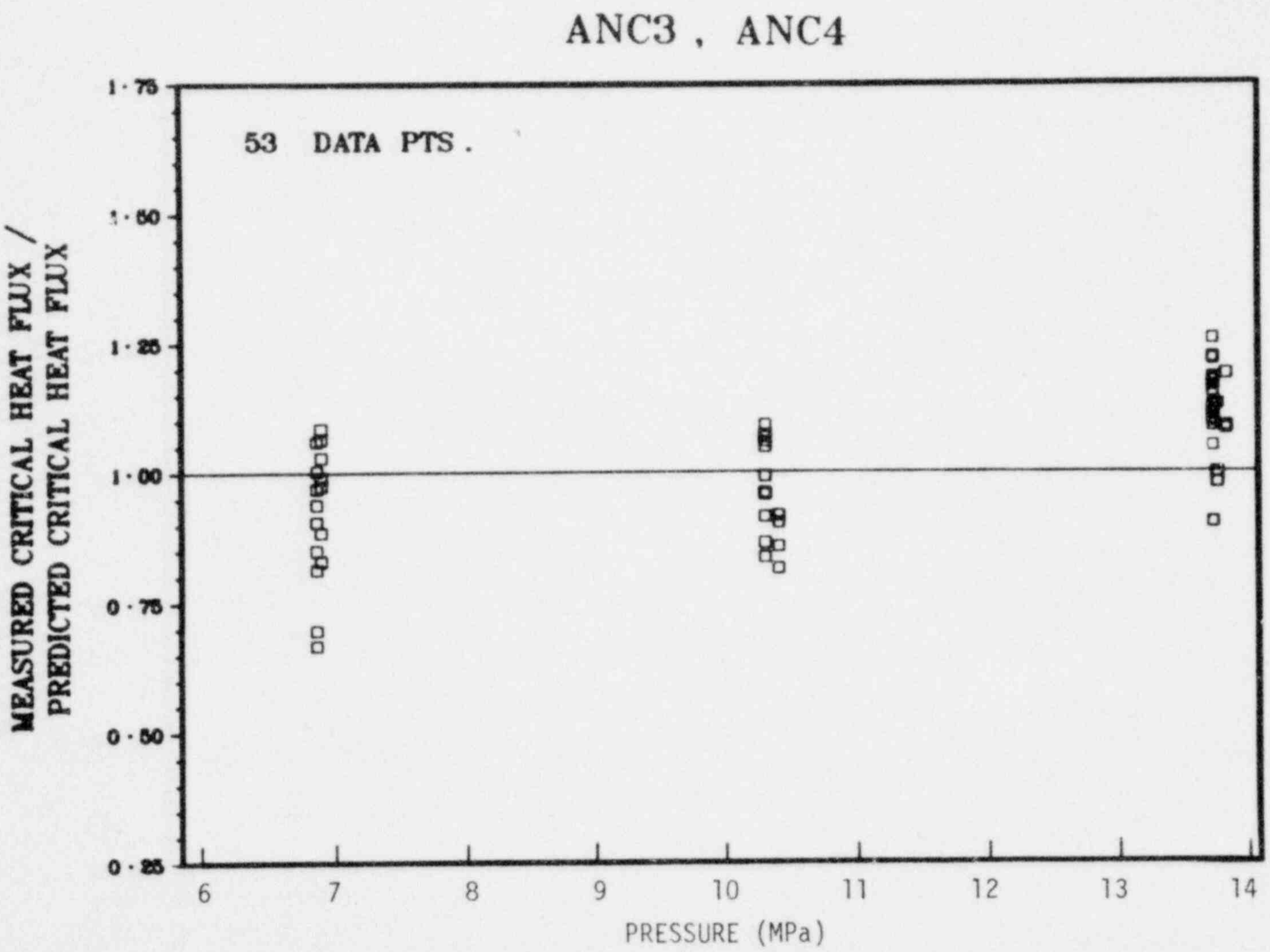

Figure 22 Ratio of measured to LOFT-2 predicted critical heat flux-vs-pressure for LOFT bundles without external thermocouple simulators.

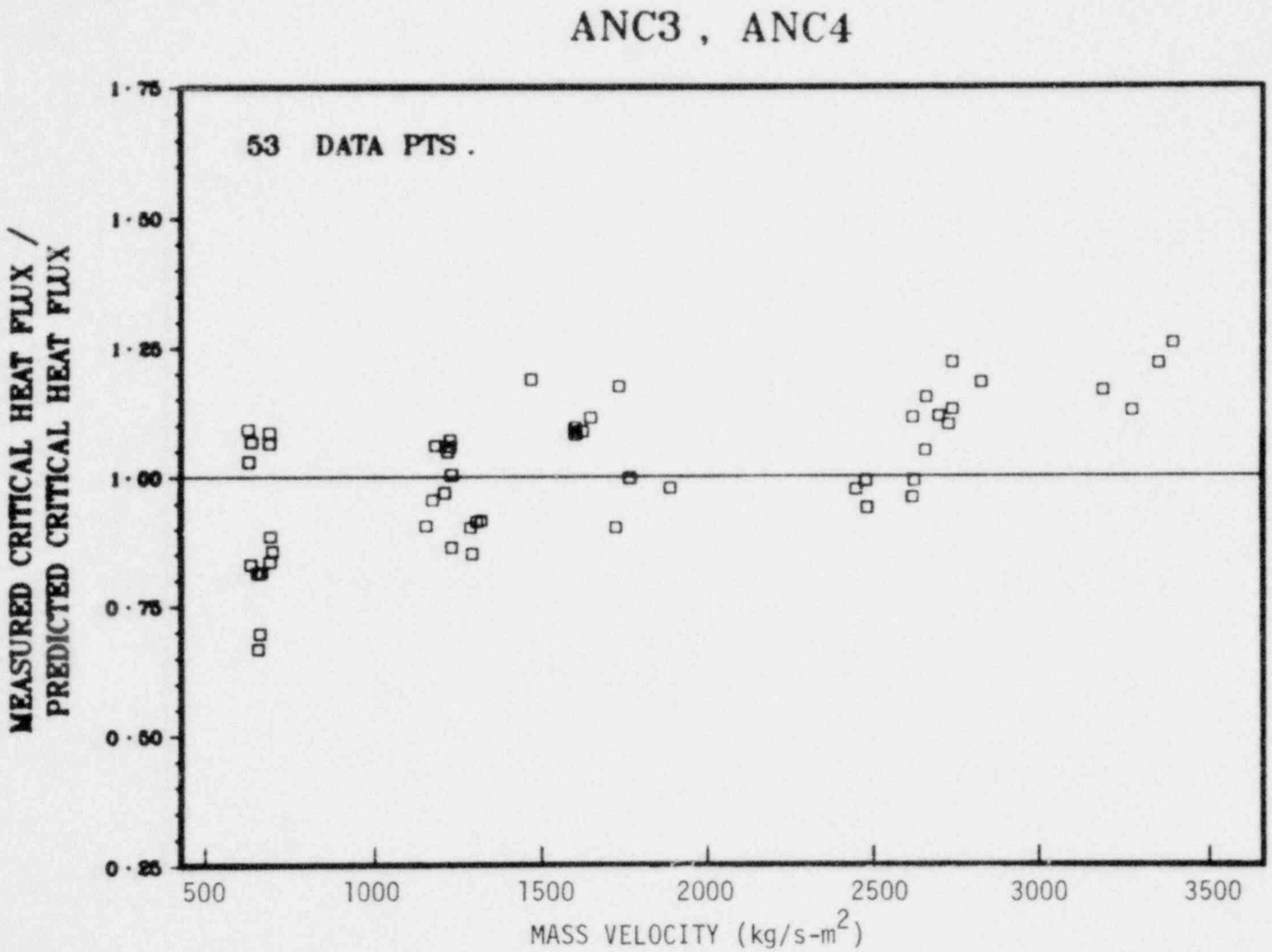

Figure 23 Ratio of measured to LOFT-2 predicted critical heat flux-vs-mass velocity for LOFT bundles without external thermocouple simulators.

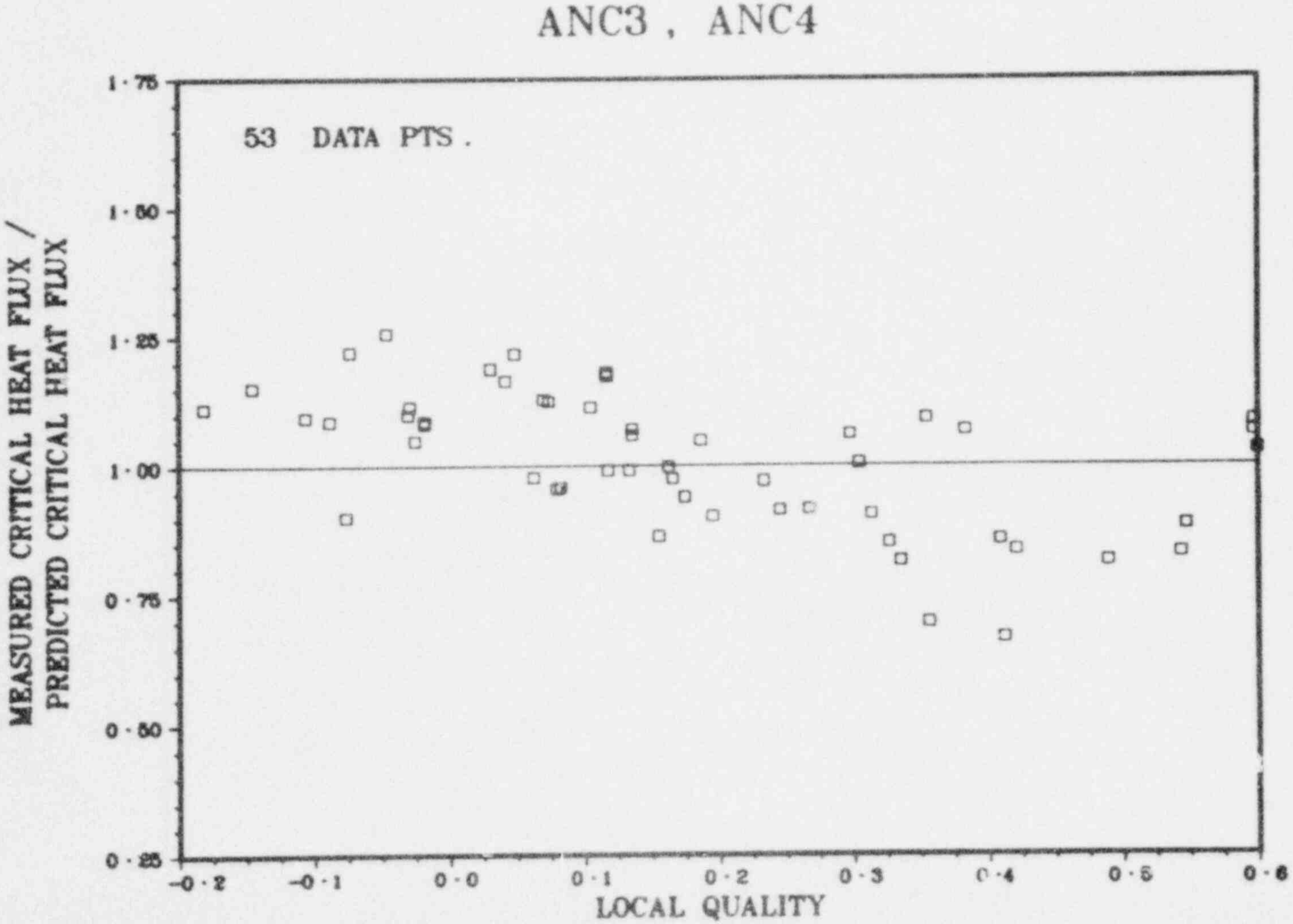

Figure 24 Ratio of measured to LOFT-2 predicted critical heat flux-vs-local quality for LOFT bundles without external thermocouple simulators.

same as the data from the bundles with rod external thermocouple simulators over the pressure range of 6.9 to 13.8 MPa. The mean value of measured to predicted CHF with the LOFT-2 correlation for these 53 data points is 1.015. Figures 22 and 24 indicate there is a slight trend with pressure and quality such that the data from the bundles with rod external thermocouples are an average of 13 percent lower at 13.8 MPa, an average of 2.5 percent higher at 10.3 MPa and an average of 7 percent higher at 6.9 MPa than the data from the bundles without rod external thermocouple simulators. This is consistent with earlier data[2] which showed that CHF in the bundles without the thermocouple simulators was increasingly higher than CHF in the bundles with the thermocouple simulators as the pressure increased above 13.8 MPa.

Although the data is limited over the ranges of pressure, mass velocity and quality tested, the range of the data is sufficient to draw conclusions regarding the effect of rod external thermocouple simulators on CHF in the bundles tested. Based on the test results, rod external thermocouple simulators do not have a significant effect on the magnitude of CHF in the bundles tested near 11 MPa and 30 to 40 percent quality, which is where CHF is predicted to occur during a blowdown in LOFT from 15.5 MPa. Thus, cladding surface thermocouples on LOFT fuel rods are not expected to have a significant effect on the transient critical heat flux or time-to-CHF in the LOFT core under blowdown conditions.

2. COMPARISON OF DATA FROM THE BUNDLES WITH ROD EXTERNAL THERMOCOUPLE SIMULATORS (EXX2 AND ANC2) WITH VARIOUS STEADY STATE CHF CORRELATIONS

The data from the bundles with external thermocouple simulators (EXX2 and ANC2) have been compared with the predicted critical heat fluxes of various steady state CHF correlations which are being used in codes such as RELAP and FRAP-T to predict CHF in the LOFT core under blowdown conditions. The ability of these correlations to predict CHF under blowdown conditions in the LOFT reactor has not been verified.

In Figures 25 through 28 the measured critical heat fluxes are compared with the predicted critical heat fluxes of the B&W-2 correlation (see Appendix C). This correlation overpredicts the data at qualities less than +0.10 and underpredicts the data at qualities greater than +0.15 and mass velocities less than 1360 kg/s-m^2. However, most of the data is outside the applicable range of the B&W-2 correlation.

Figures 29 through 32 show a comparison of the measured critical heat fluxes with the predicted critical heat fluxes of the Barnett correlation (see Appendix C). This correlation underpredicts almost all of the data, particularly at qualities higher than +0.10 and mass velocities less than 1632 kg/s-m^2.

Figures 33 through 36 show a comparison of the measured critical heat fluxes with the predicted critical heat fluxes of the General Electric CHF correlation (see Appendix C). This correlation does a good job of predicting the LOFT data except at qualities higher than +0.20 and mass velocities less than 1360 kg/s-m^2. The correlation underpredicts the data at those conditions.

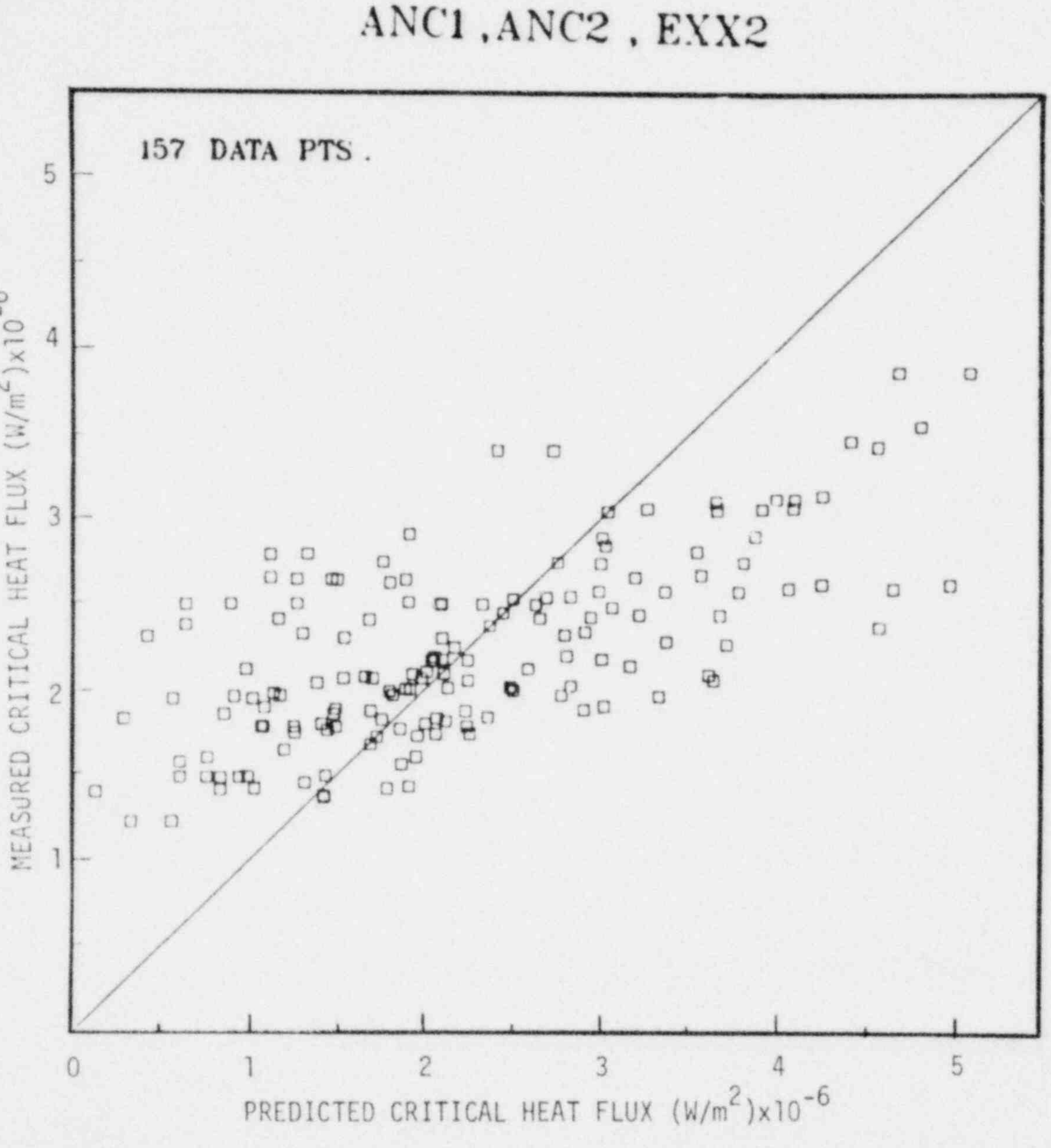

Figure 25 Comparison of measured to predicted critical heat flux. (B&W-2 + COBRA-II) for LOFT bundles with external thermocouple simulators.

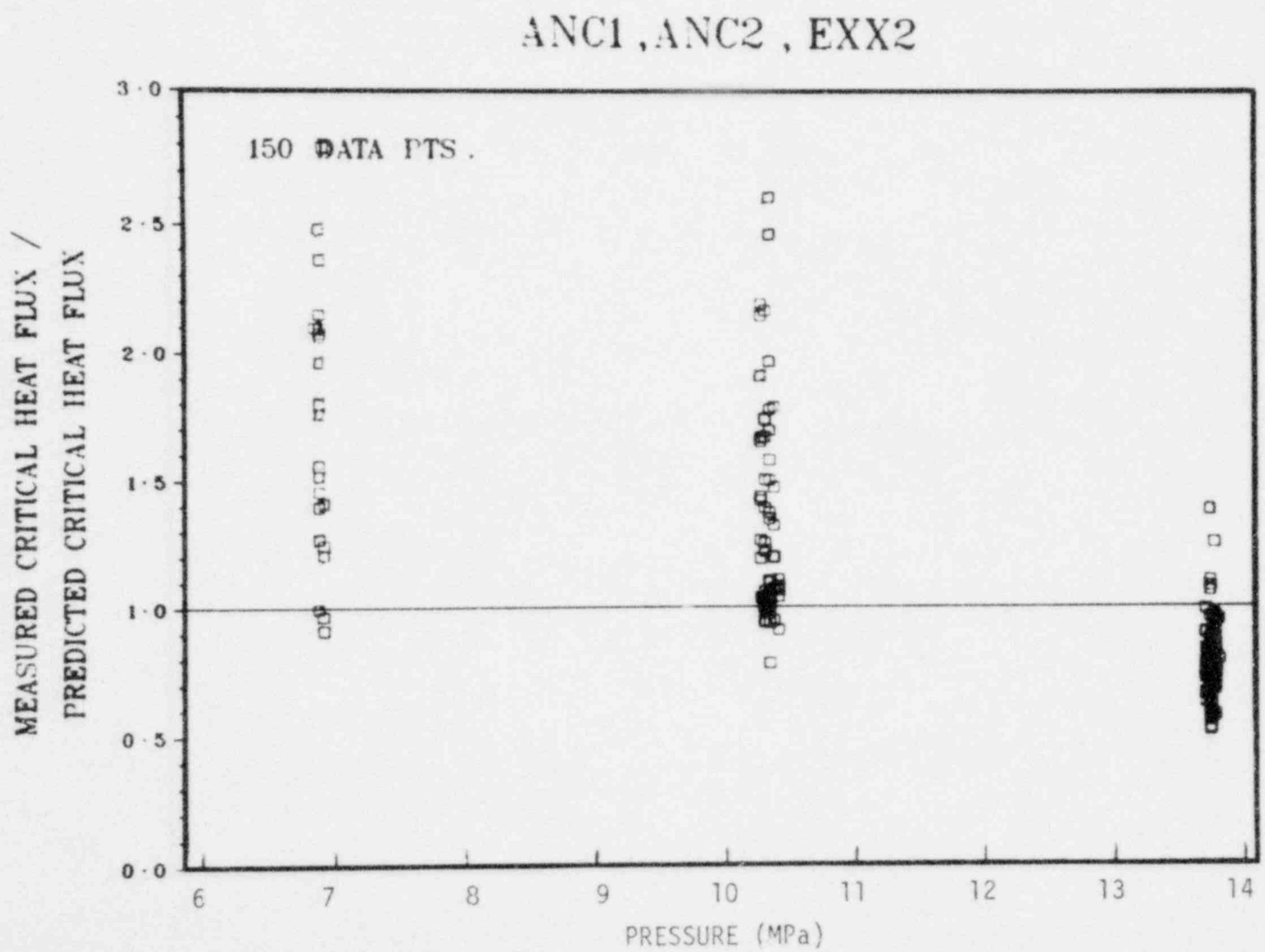

Figure 26 Ratio of measured to B&W-2 predicted critical heat flux-vs-pressure for LOFT bundles with external thermocouple simulators.

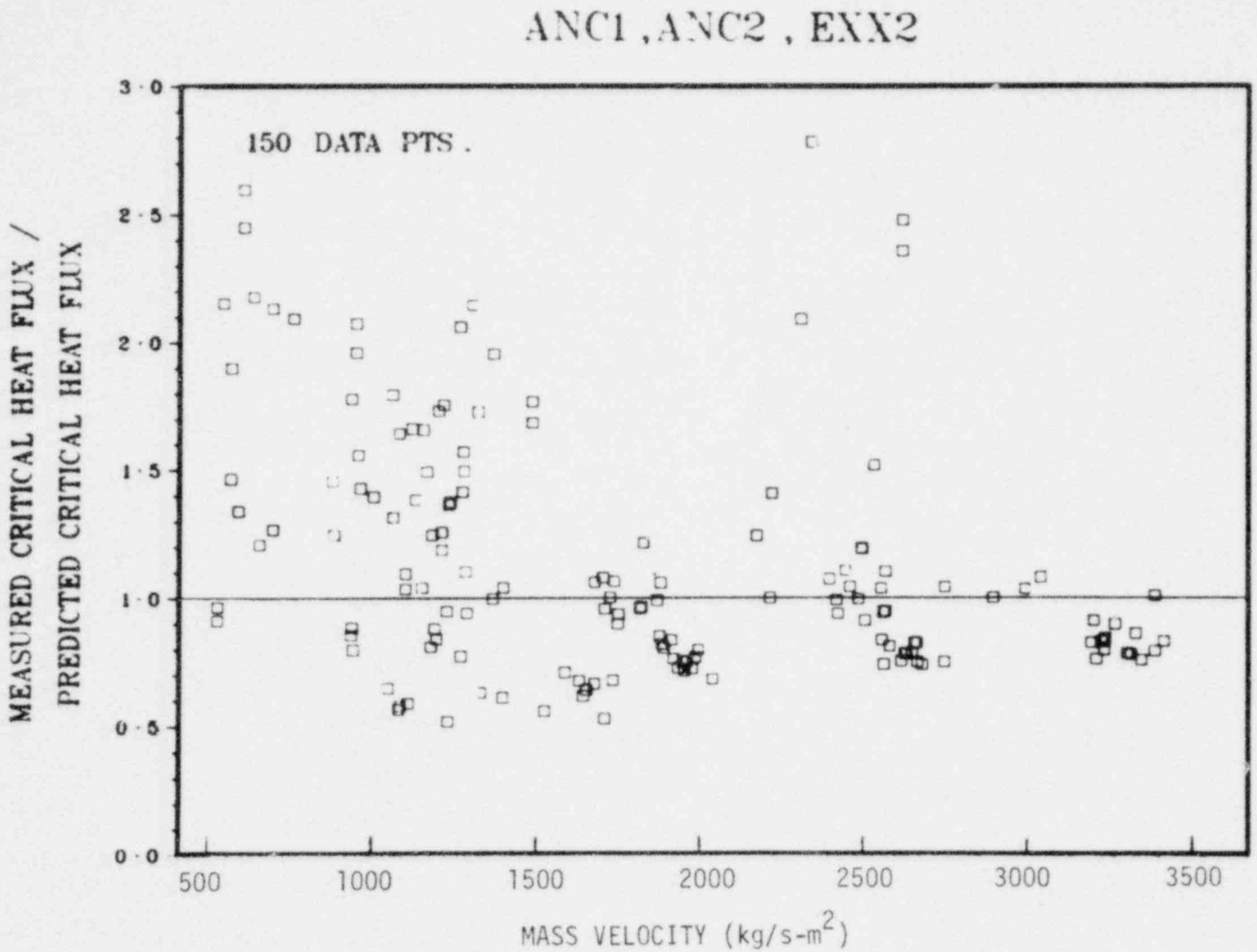

Figure 27 Ratio of measured to B&W-2 predicted critical heat flux-vs-mass velocity for LOFT bundles with external thermocouple simulators.

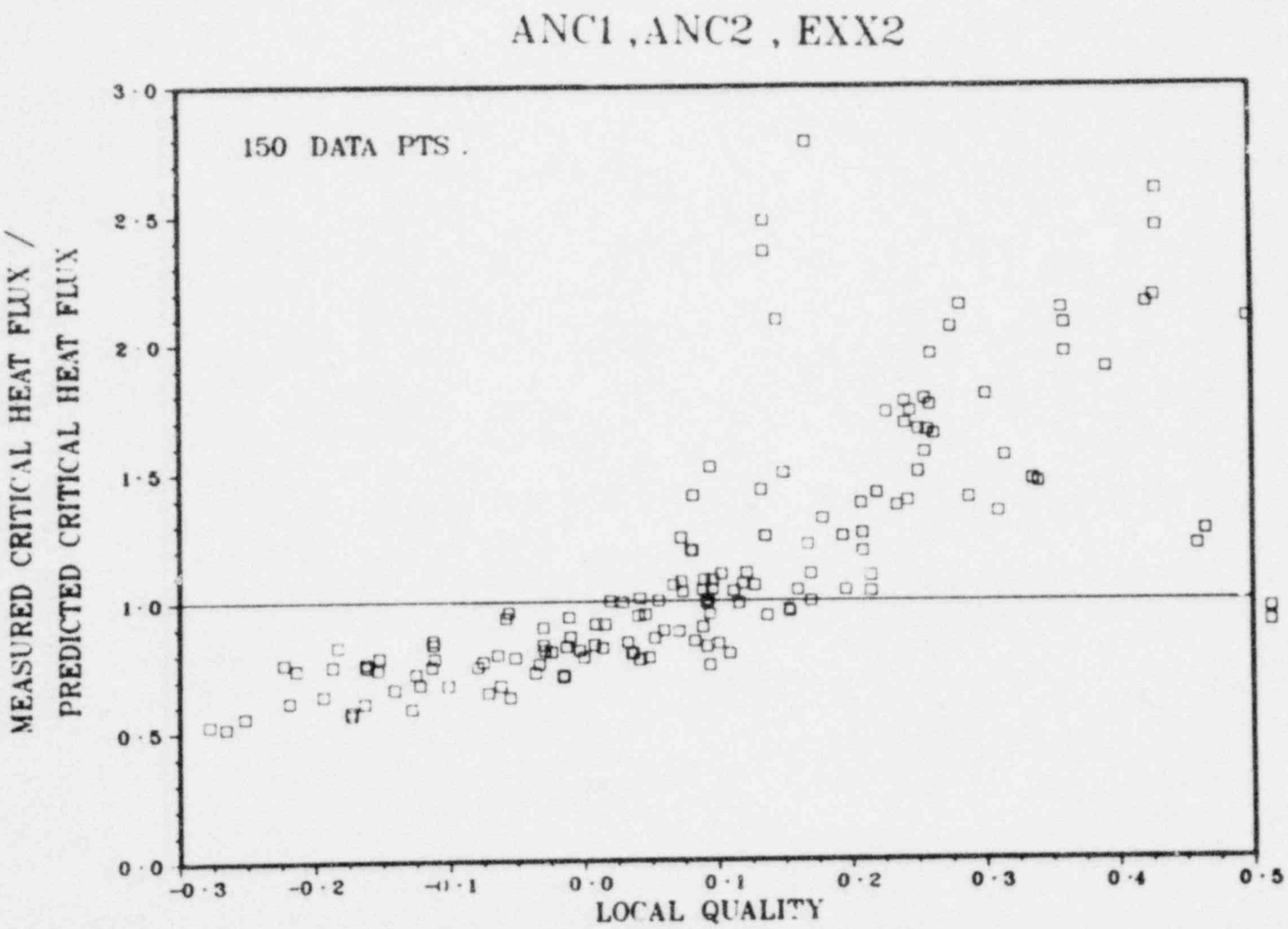

Figure 28 Ratio of measured to B&W-2 predicted critical heat flux-vs-local quality for LOFT bundles with external thermocouple simulators.

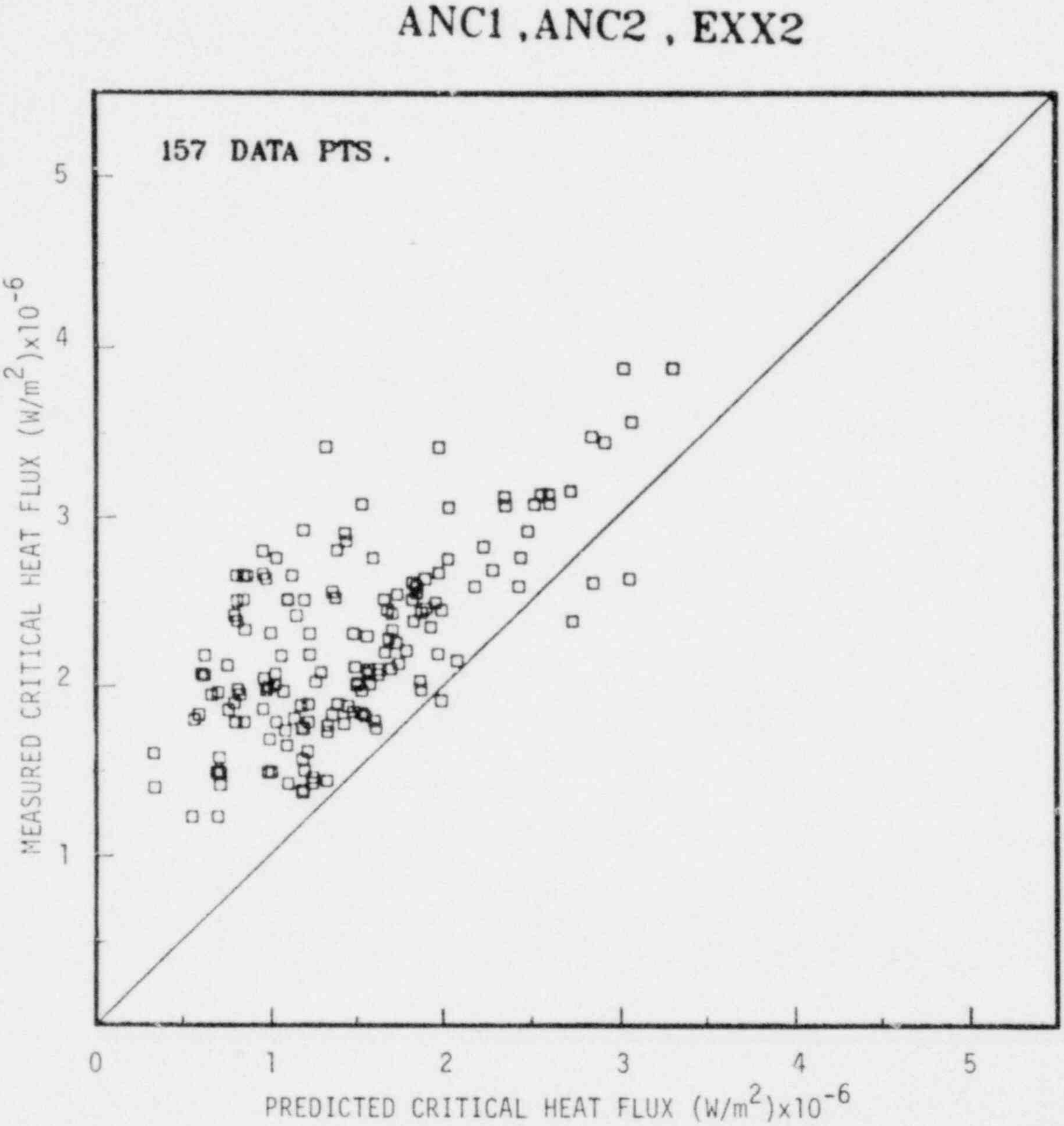

Figure 29 Comparison of measured to predicted critical heat flux. (Barnett + COBRA-II) for LOFT bundles with external thermocouple simulators.

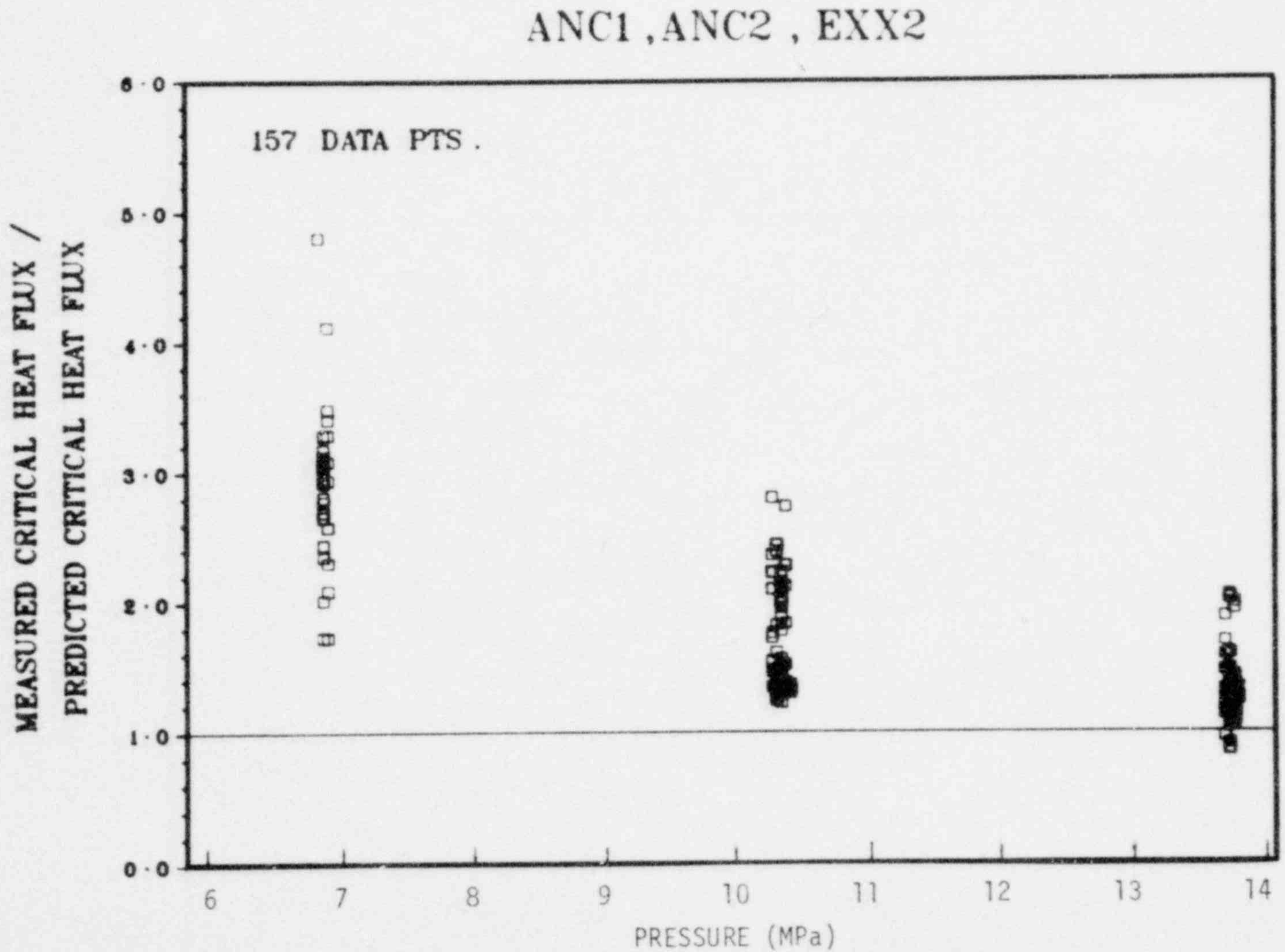

Figure 30 Ratio of measured to Barnett predicted critical heat flux-vs-pressure for LOFT bundles with external thermocouple simulators.

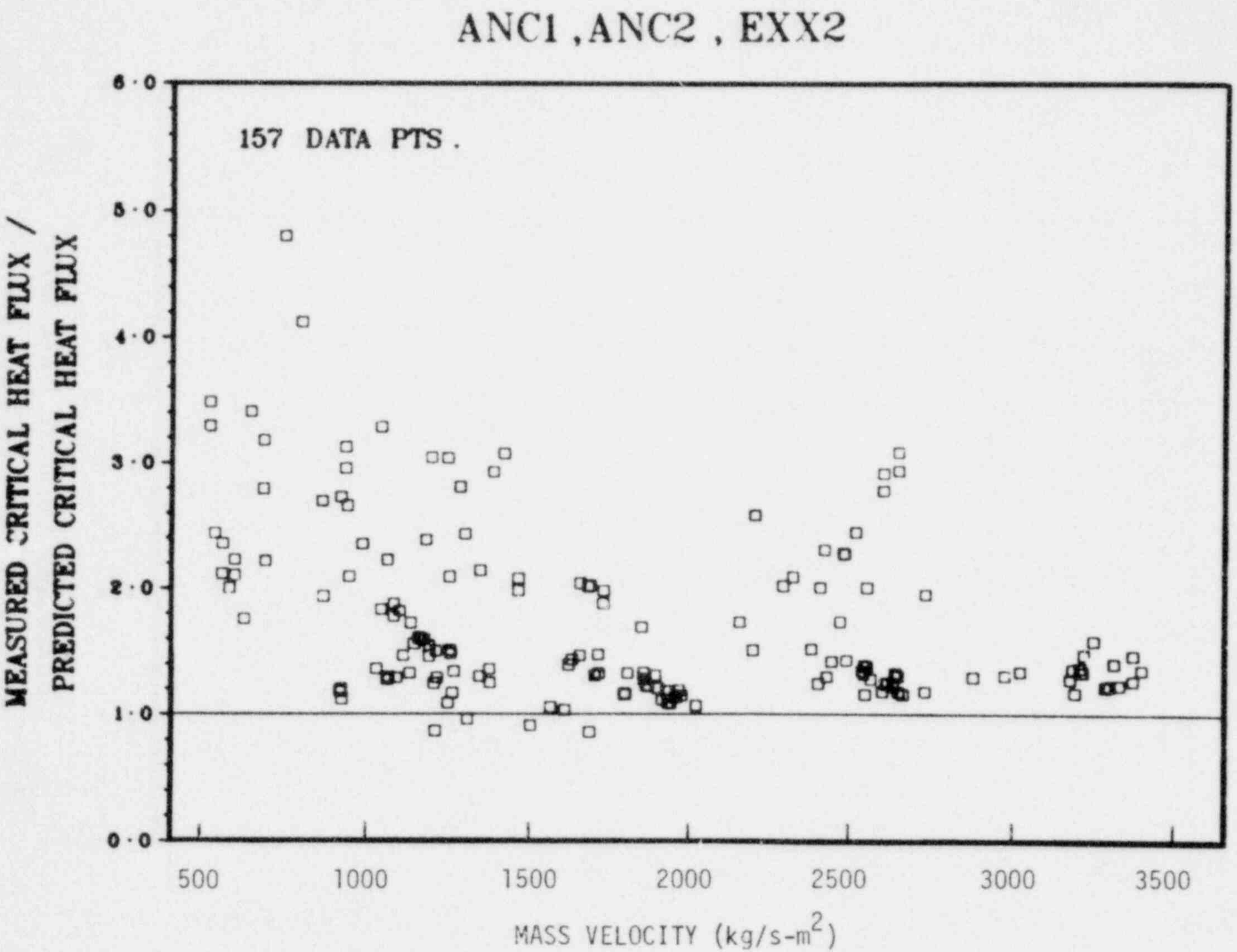

Figure 31 Ratio of measured to Barnett predicted critical heat flux-vs-mass velocity for LOFT bundles with external thermocouple simulators.

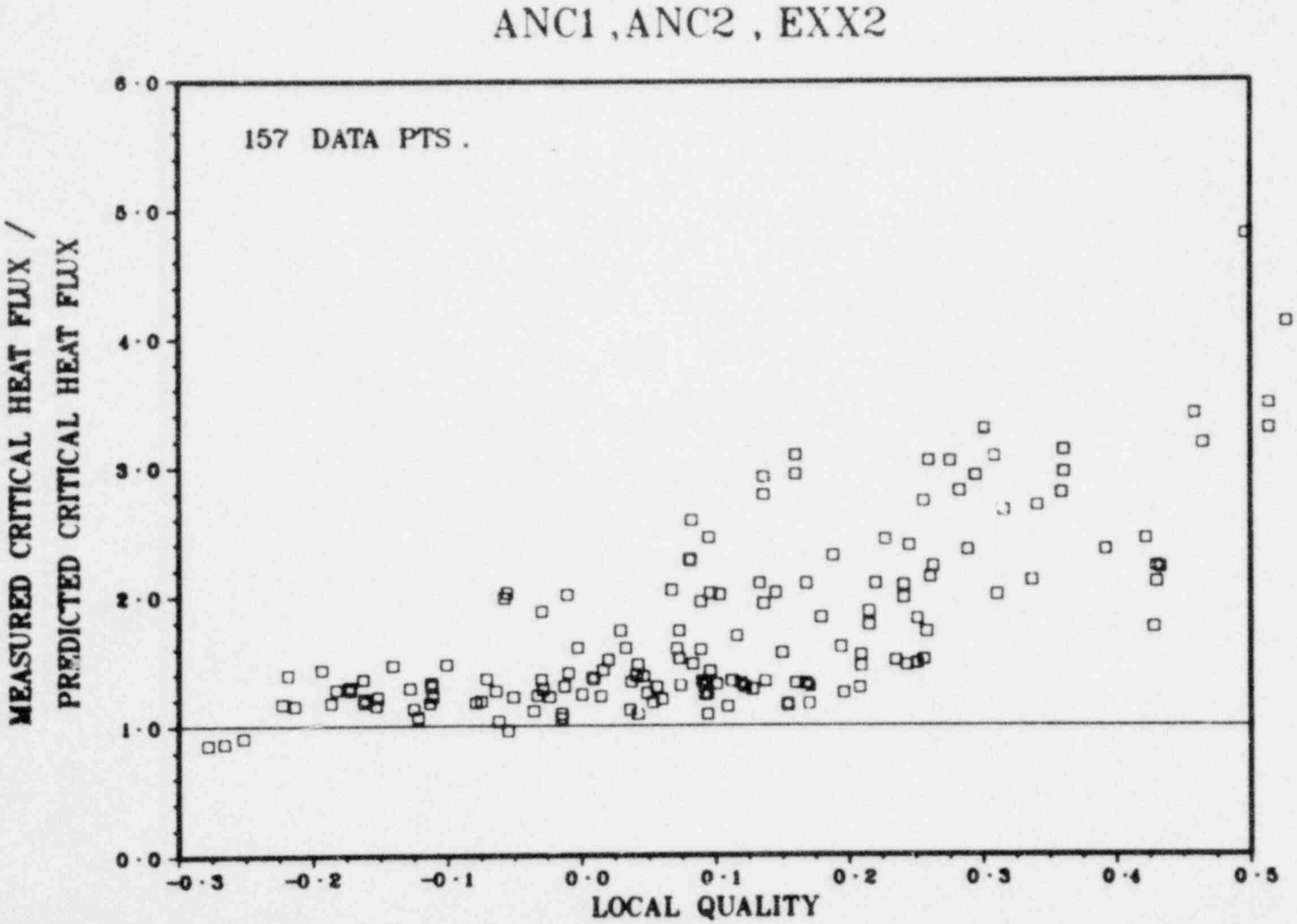

Figure 32 Ratio of measured to Barnett predicted critical heat flux-vs-local quality for LOFT bundles with external thermocouple simulators.

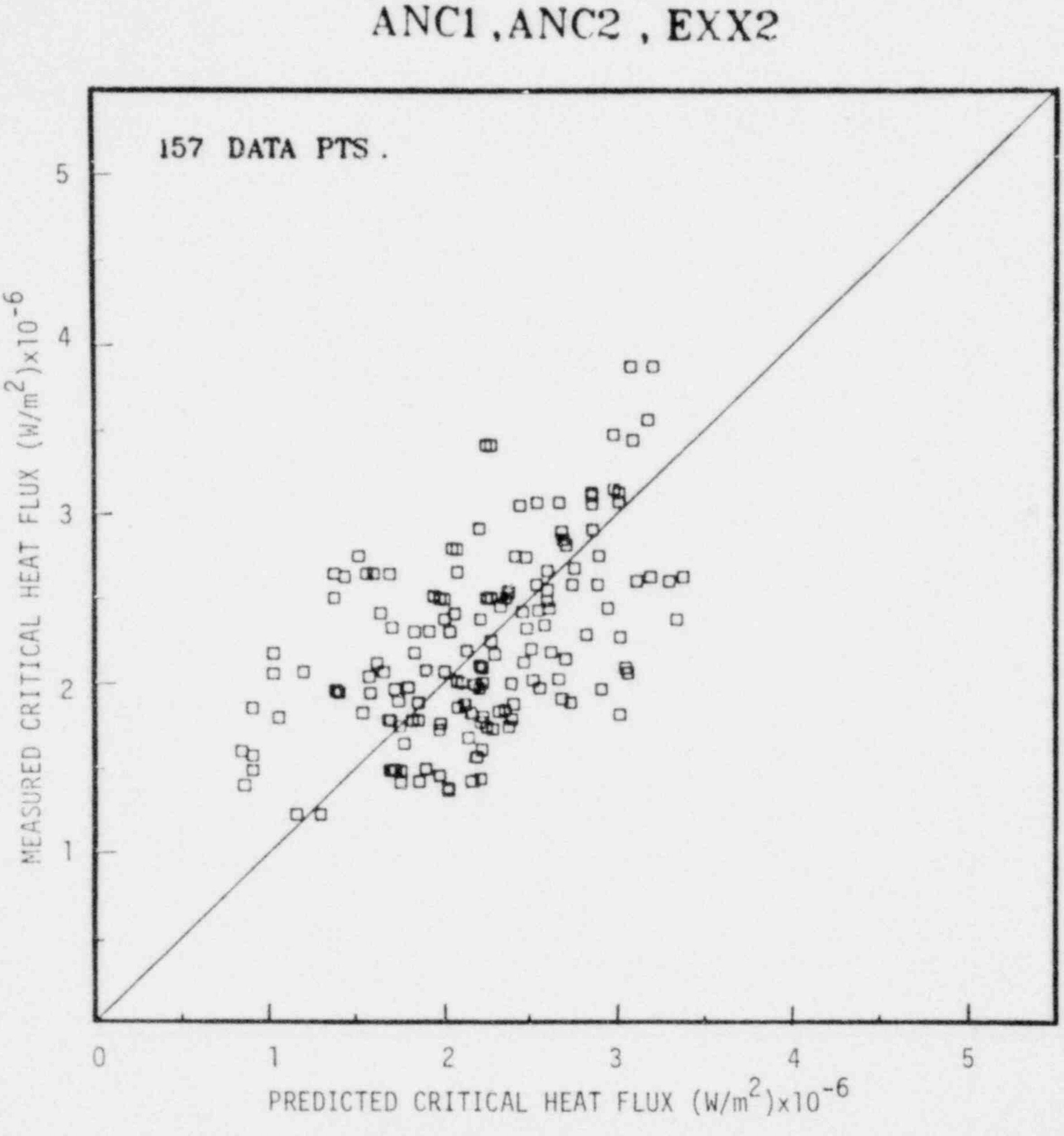

Figure 33 Comparison of measured to predicted critical heat flux. (GE + COBRA-II) for LOFT bundles with external thermocouple simulators.

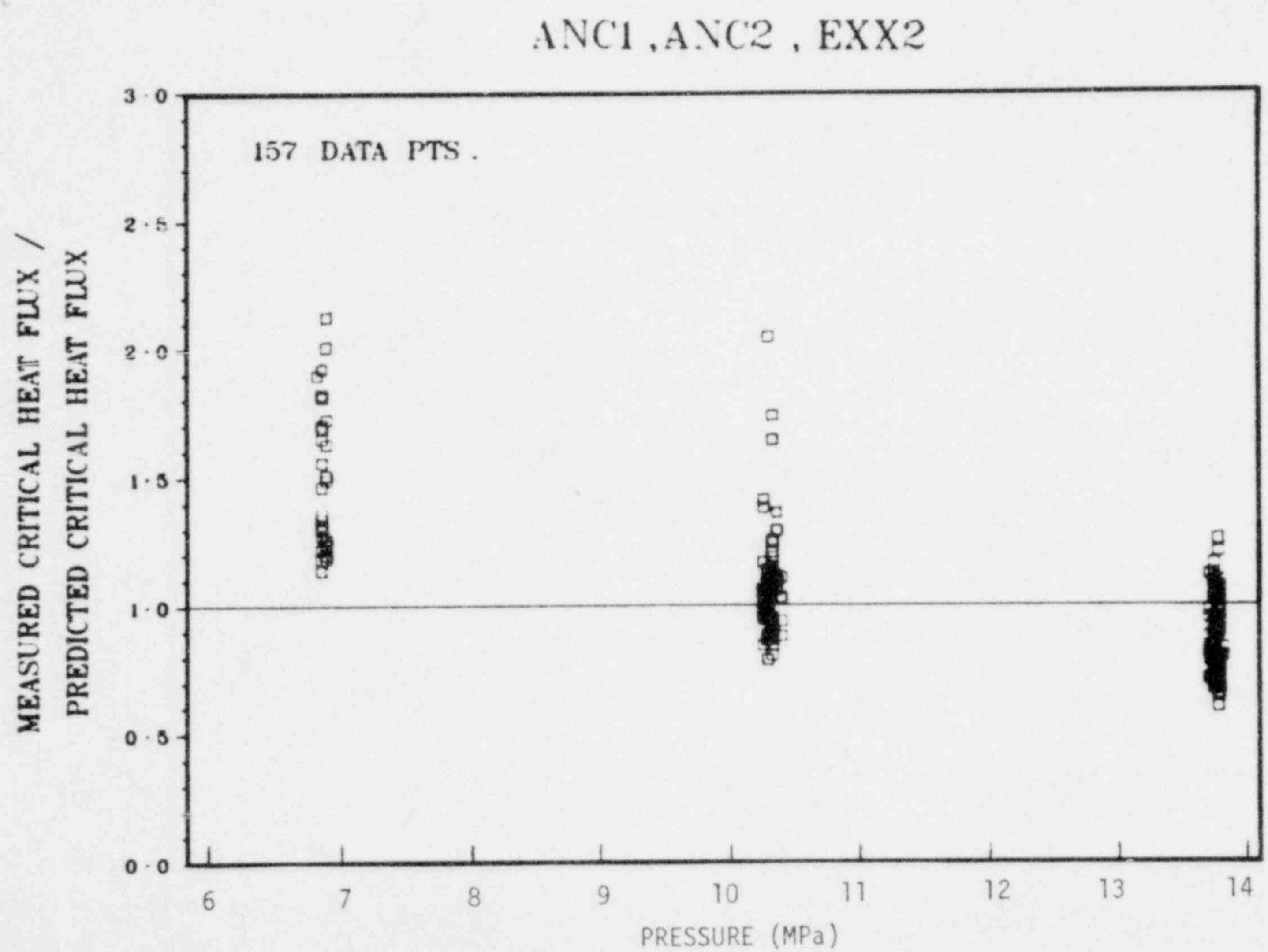

Figure 34 Ratio of measured to GE predicted critical heat flux-vs-pressure for LOFT bundles with external thermocouple simulators.

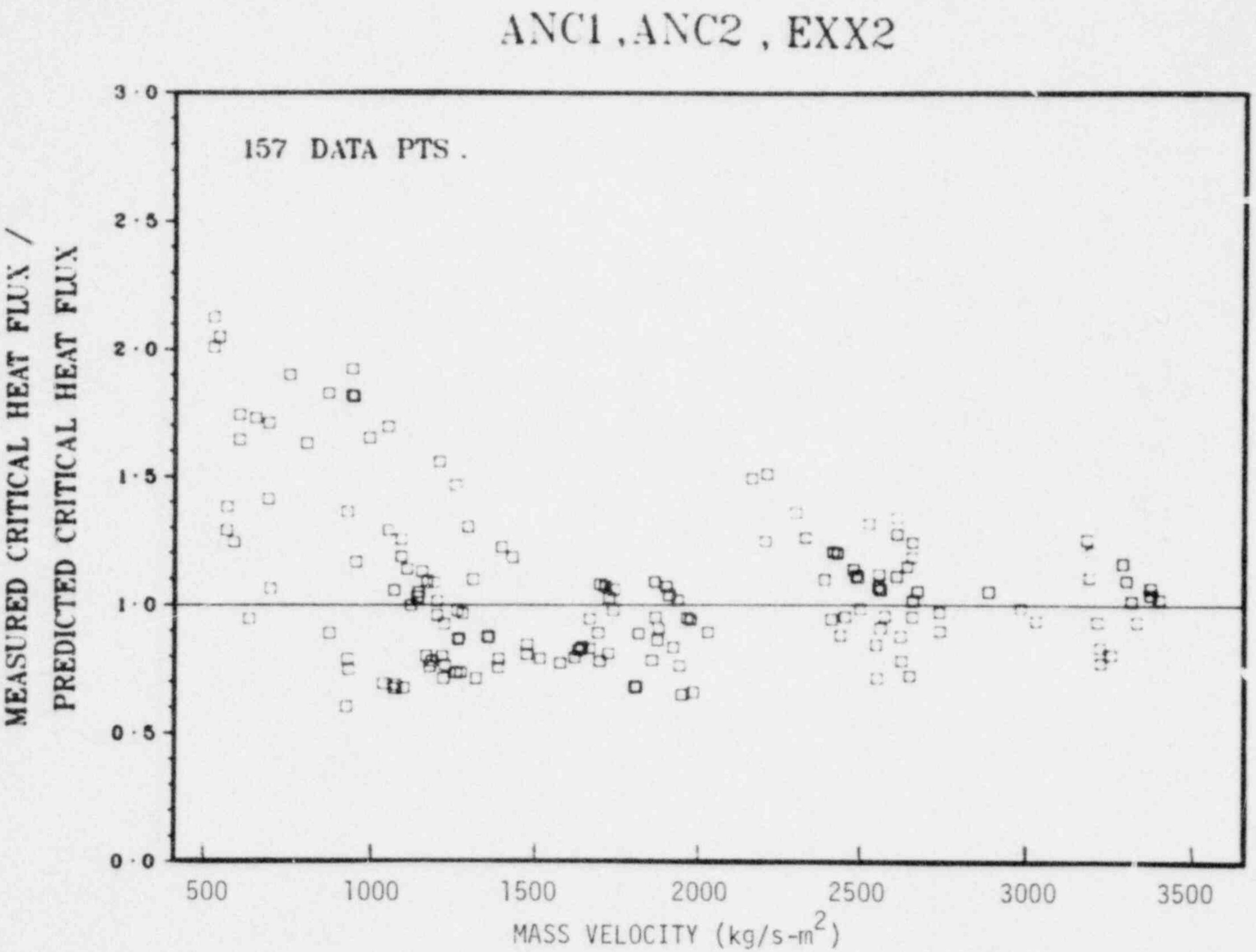

Figure 35 Ratio of measured to GE predicted critical heat flux-vs-mass velocity for LOFT bundles with external thermocouple simulators.

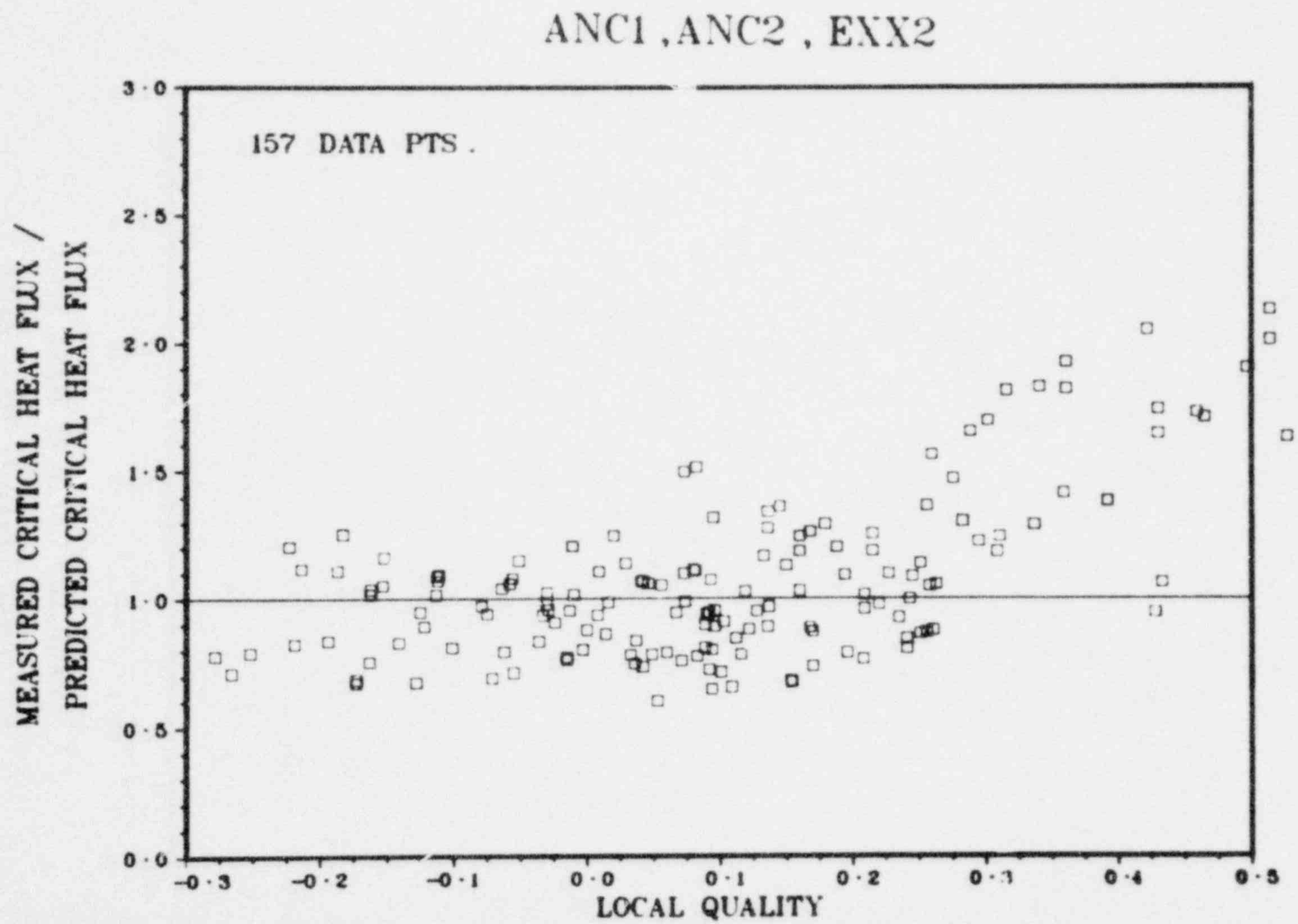

Figure 36 Ratio of measured to GE predicted critical heat flux-vs-local quality for LOFT bundles with external thermocouple simulators.

3. LOCATIONS OF CHF AND POSTULATED MECHANISMS

3.1 Bundles with Rod External Thermocouple Simulators

For the LOFT CHF tests at 13.8 to 16.5 MPa reported in Reference 2, 449 of the 455 data points from the bundles with rod external thermocouple simulators (EXX2, ANC1 and ANC2) were obtained on rods with the thermocouple simulators. The majority of this data was in the subcooled region (local quality < 0). The remaining six data points were obtained on rods that did not have thermocouple simulators. All six of these data points were obtained at local qualities higher than +10 percent.

For the EXX2 and ANC2 bundles at 13.8 MPa, 68 of 71 data points were obtained on rods with external thermocouple simulators. Sixty-three of the 71 data points were also at local qualities less than +10 percent. The remaining three data points which occurred on rods without external thermocouple simulators occurred at local qualities higher than +15 percent.

For the EXX2 and ANC2 bundles at 6.9 and 10.3 MPa, only 12 of 86 data points were obtained on rods with external thermocouple simulators. All but two of these 12 data points were at local qualities less than +10 percent. Of the remaining 74 of the 86 data points obtained on rods without external thermocouple simulators, almost all were at local qualities of +10 percent or higher.

It appears that thermocouples mounted externally on the cladding surface of LOFT fuel rods affect the steady state CHF mechanism on the rods they are attached to. The mechanism seems to change near +10 percent quality, probably due to a change in flow regime. For very low positive qualities and subcooled conditions the flow regime is bubbly flow. It is postulated that small bubbles form in the region directly between a rod with external thermocouple simulators and an adjacent rod. The external thermocouples reduce the ability of these bubbles to be swept away, causing CHF to be initiated at that location and resulting in a reduced magnitude of CHF. This is consistent with the high pressure low quality data reported in Reference 2. In these tests, burn marks were apparent on the rods with external thermocouple simulators in the region directly facing an adjacent rod and between the thermocouple simulators. It was also shown that in the low quality region, the critical heat fluxes in the bundles with rod external thermocouples were significantly lower than the CHF in the bundles without rod external thermocouples.

For fluid qualities higher than +10 percent, the flow regime changes to annular flow. In this flow regime a liquid film forms on the rods and thermocouple simulators. Due to the added surface area of the thermocouple simulators, the rods with the thermocouple simulators are cooled more than the rods without the thermocouple simulators. This would account for the fact that all of the CHF data points from the EXX2 and ANC2 bundles at qualities higher than +10 percent were all shifted to rods without the thermocouple simulators, even though these rods had lower power factors than the rods with the thermocouple simulators. Although the data points were shifted to the rods without thermocouple simulators in the EXX2 and ANC2 bundles, the critical heat fluxes were about the same magnitude as the critical heat fluxes in the ANC3 and ANC4 bundles in the high quality region.

The critical heat fluxes in the LOFT core under blowdown conditions will occur at high quality dry out conditions. The results of this test indicate that the LOFT rods with cladding surface thermocouples could have additional cooling due to the thermocouples and potentially shift the critical heat flux first to adjacent rod without cladding surface thermocouples. Whether or not this phenomena will occur will be determined from the LOFT transient (blowdown) CHF tests discussed in Section VI.

3.2 Bundles Without Rod External Thermocouple Simulators

For the bundles without rod external thermocouples (ANC3 and ANC4), critical heat fluxes were observed on a variety of rods both in the subcooled region and high quality region. For the ANC3 bundle in the high pressure low quality region, CHF burn marks generally extended completely around the rods and in some cases over several inches axially[2]. Compared to the ANC2 bundle, this also provides evidence that the rod external thermocouple simulators in the bundles tested affected the CHF mechanism.

V. CONCLUSIONS

Critical heat flux tests have been conducted on 25-rod bundles simulating the central region of the LOFT nuclear reactor core-1. The effect of fuel rod cladding surface thermocouples on CHF has been evaluated over the pressure range of 6.9 to 13.8 MPa. The following conclusions have been reached based on the test data:

(1) In the pressure and quality range where CHF is predicted to occur in the LOFT core during blowdown operation (11 MPa and 30 to 40 percent quality), the magnitudes of CHF between the bundles with and without external thermocouple simulators were about the same. Thus, cladding surface thermocouples on LOFT fuel rods are not expected to influence CHF or time-to-CHF on the LOFT fuel rods under loss-of-coolant conditions.

(2) An insufficient data base was obtained with the bundles with rod external thermocouple simulators to develop a new CHF correlation that could be used to predict CHF for LOFT under blowdown conditions. This resulted from experimental facility limitations on fluid quality during these tests. Additional tests at lower mass velocities are planned (see Section VI) to expand the data base in the range of 10.3 to 11.7 MPa and aid in developing a correlation for predicting transient CHF.

(3) Steady state correlations used in codes such as RELAP and FRAP-T to predict CHF for LOFT under blowdown conditions have been compared with the data from the bundles with rod external thermocouple simulators. The B&W-2, Barnett and GE CHF correlations do not satisfactorily predict this data and therefore, are not verified as adequate tools to predict CHF for LOFT blowdowns.

VI. FOLLOW-ON CHF TESTS

Additional CHF testing with the rod bundle with external thermocouple simulators is planned. The purpose of this testing is to extend the range of the data, in the pressure range of 10.3 to 11.7 MPa, to mass velocities as low as 136 kg/s-m^2 and higher qualities than have been previously tested. This data will aid in verifying the use of various steady state CHF correlations to predict time-to-CHF in LOFT during a blowdown or allow a new or modified correlation to be developed.

Also, transient (blowdown) CHF tests on bundles with and without rod external thermocouple simulators have been conducted. The purpose of these tests was to determine if the external thermocouples attached to the cladding surface of some of the LOFT fuel rods will affect CHF (or time-to-CHF) in the LOFT core under blowdown conditions. The rod bundles used for these tests were similar to those used for the steady state CHF tests. The results of these tests are reported in Reference 20.

VII. REFERENCES

1. M. L. Russell, LOFT Fuel Modules Design, Characterization, and Fabrication Program, ANCE-1223 (September 1975).

2. S. A. Eide and R. C. Gottula, Evaluation and Results of LOFT Steady State Departure from Nucleate Boiling Tests, TREE-NUREG-1043, (April 1977).

3. ASME Steam Tables, New York: The American Society of Mechanical Engineers, 1967.

4. D. S. Rowe, COBRA-II: A Digital Computer Program for Thermal-Hydraulic Subchannel Analysis of Rod Bundle Nuclear Fuel Elements, BNWL-1299 (February 1970).

5. D. S. Rowe, COBRA-IIIC: A Digital Computer Program for Steady State and Transient Thermal-Hydraulic Analysis of Rod Bundle Nuclear Fuel Elements, BNWL-1695 (March 1973).

6. W. W. Kays, Convective Heat and Mass Transfer, San Francisco: McGraw-Hill Book Company, 1966, p 73.

7. Internal Report.

8. Internal Report.

9. L. S. Tong and J. Weisman, Thermal Analysis of Pressurized Water Reactors, Hinsdale, Illinois: American Nuclear Society, 1970, pp. 123-128.

10. D. S. Rowe and C. W. Angle, Crossflow Mixing Between Parallel Flow Channels During Boiling, Part II, BNWL-371-PT2 (December 1967) p 35.

11. Internal Report.

12. J. Weisman and R. W. Bowring, "Methods for Detailed Thermal and Hydraulic Analysis of Water-Cooled Reactors," Nuclear Science and Engineering, 57 (1975) p 260.

13. R. W. Bowring, HAMBO: A Computer Programme for the Subchannel Analysis of the Hydraulic and Burnout Characteristics of Rod Clusters, Part 1: General Description, AEEW-R524 (1967).

14. H. Chelemer, J. Weisman, L. S. Tong, "Subchannel Thermal Analysis of Rod Bundle Cores," Nuclear Engineering and Design, 21 (1972) p 35.

15. J. G. Collier, Convective Boiling and Condensation, London: McGraw-Hill Book Company (UK) Limited, 1972, pp 28, 38 to 47, 180 to 185.

16. W. A. Massena, Steam Water Pressure Drop and Critical Discharge Flow - A Digital Computer Program, HW-65706 (June 1960).

17. F. S. Castellana and C. F. Bonilla, "Two-Phase Pressure Drop and Heat Trasnfer in Rod Bundles," in Two-Phase Flow and Heat Transfer in Rod Bundles, V. W. Schrock (ed), New York: The American Society of Mechanical Engineers, 1969.

18. F. E. Motley and F. F. Cadek, DNB Test Results for R Grid Thimble Cold Wall Cells, WCAP-7958, Addendum 1 (October 1972).

19. R. E. Collingham and C. E. Leach, LOFT Fuel Departure from Nucleate Boiling Test Analysis and Results, XN-73-36 (December 1973).

20. R. C. Gottula, LOFT Transient (Blowdown) Critical Heat Flux Tests, TREE-NUREG-1240 (May 1978).

APPENDIX A

TEST CONDITIONS

EXX2 RUN CONDITIONS

RUN	SYSTEM PRESSURE PSIA (PA)	INLET TEMPERATURE F (K)	INLET ENTHALPY BTU/LBM (J/KG)	INLET MASS FLUX LBM/HR-FT2 (KG/S-M2)	BUNDLE AVERAGE HEAT FLUX BTU/HR-FT2 (W/M2)
7.	2003. (1.38E 07)	600. (589.)	615. (1.43E 06)	1.51E 06 (2045.)	0.429E 06 (1.35E 06)
8.	2004. (1.38E 07)	606. (592.)	623. (1.45E 06)	2.01E 06 (2730.)	0.485E 06 (1.53E 06)
9.	1995. (1.38E 07)	610. (594.)	629. (1.46E 06)	2.47E 06 (3352.)	0.544E 06 (1.71E 06)
10.	2005. (1.38E 07)	603. (590.)	619. (1.44E 06)	1.44E 06 (1953.)	0.428E 06 (1.35E 06)
11.	2003. (1.38E 07)	581. (578.)	588. (1.37E 06)	2.01E 06 (2720.)	0.556E 06 (1.75E 06)
12.	2010. (1.39E 07)	587. (582.)	597. (1.39E 06)	2.47E 06 (3356.)	0.603E 06 (1.90E 06)
16.	2001. (1.38E 07)	543. (557.)	539. (1.25E 06)	2.56E 06 (3475.)	0.804E 06 (2.53E 06)
18.	2005. (1.38E 07)	565. (569.)	567. (1.32E 06)	2.46E 06 (3337.)	0.702E 06 (2.21E 06)
19.	2005. (1.38E 07)	548. (560.)	545. (1.27E 06)	2.50E 06 (3397.)	0.738E 06 (2.33E 06)
20.	1997. (1.38E 07)	547. (559.)	544. (1.26E 06)	1.99E 06 (2705.)	0.665E 06 (2.10E 06)
21.	1995. (1.38E 07)	545. (558.)	541. (1.26E 06)	1.51E 06 (2042.)	0.562E 06 (1.77E 06)
22.	1500. (1.03E 07)	553. (562.)	552. (1.28E 06)	1.01E 06 (1367.)	0.474E 06 (1.49E 06)
23.	1500. (1.03E 07)	550. (561.)	549. (1.28E 06)	1.51E 06 (2052.)	0.551E 06 (1.74E 06)
24.	1515. (1.04E 07)	556. (564.)	556. (1.29E 06)	1.99E 06 (2698.)	0.586E 06 (1.85E 06)
25.	1515. (1.04E 07)	552. (562.)	551. (1.28E 06)	2.50E 06 (3386.)	0.654E 06 (2.06E 06)
26.	1500. (1.03E 07)	515. (542.)	506. (1.18E 06)	9.85E 05 (1336.)	0.546E 06 (1.72E 06)
27.	1500. (1.03E 07)	519. (544.)	511. (1.19E 06)	1.57E 06 (2130.)	0.627E 06 (1.98E 06)
28.	1500. (1.03E 07)	530. (550.)	523. (1.22E 06)	2.01E 06 (2732.)	0.656E 06 (2.07E 06)
29.	1500. (1.03E 07)	537. (553.)	532. (1.24E 06)	2.48E 06 (3368.)	0.704E 06 (2.22E 06)
30.	1500. (1.03E 07)	518. (543.)	509. (1.18E 06)	2.44E 06 (3307.)	0.767E 06 (2.42E 06)
31.	1515. (1.04E 07)	493. (529.)	479. (1.11E 06)	1.48E 06 (2008.)	0.686E 06 (2.16E 06)
32.	1500. (1.03E 07)	497. (531.)	484. (1.13E 06)	1.99E 06 (2694.)	0.768E 06 (2.42E 06)
33.	1515. (1.04E 07)	501. (534.)	489. (1.14E 06)	2.46E 06 (3341.)	0.828E 06 (2.61E 06)
34.	1500. (1.03E 07)	467. (515.)	449. (1.05E 06)	9.86E 05 (1337.)	0.607E 06 (1.91E 06)
35.	1505. (1.04E 07)	467. (515.)	450. (1.05E 06)	1.50E 06 (2037.)	0.744E 06 (2.35E 06)
38.	2000. (1.38E 07)	562. (568.)	563. (1.31E 06)	1.02E 06 (1386.)	0.454E 06 (1.43E 06)
43.	2005. (1.38E 07)	483. (524.)	468. (1.09E 06)	9.83E 05 (1333.)	0.527E 06 (1.66E 06)
46.	2000. (1.38E 07)	513. (540.)	502. (1.17E 06)	2.01E 06 (2728.)	0.751E 06 (2.37E 06)
47.	2005. (1.38E 07)	509. (538.)	498. (1.16E 06)	1.53E 06 (2073.)	0.613E 06 (1.93E 06)
48.	2005. (1.38E 07)	487. (526.)	473. (1.10E 06)	1.50E 06 (2039.)	0.659E 06 (2.08E 06)
51.	1995. (1.38E 07)	432. (495.)	411. (9.57E 05)	1.02E 06 (1379.)	0.575E 06 (1.81E 06)

ANC1 RUN CONDITIONS

RUN	SYSTEM PRESSURE PSIA (PA)	INLET TEMPERATURE F (K)	INLET ENTHALPY BTU/LBM (J/KG)	INLET MASS FLUX LBM/HR-FT2 (KG/S-M2)	BUNDLE AVERAGE HEAT FLUX BTU/HR-FT2 (W/M2)
14.	1995. (1.38E 07)	607. (593.)	625. (1.45E 06)	1.93E 06 (2623.)	0.472E 06 (1.49E 06)
15.	2005. (1.38E 07)	593. (585.)	605. (1.41E 06)	1.48E 06 (2007.)	0.434E 06 (1.37E 06)
17.	2000. (1.38E 07)	609. (594.)	628. (1.46E 06)	2.45E 06 (3329.)	0.528E 06 (1.66E 06)

ANC2 RUN CONDITIONS

RUN	SYSTEM PRESSURE PSIA (PA)	INLET TEMPERATURE F (K)	INLET ENTHALPY BTU/LBM (J/KG)	INLET MASS FLUX LBM/HR-FT2 (KG/S-M2)	BUNDLE AVERAGE HEAT FLUX BTU/HR-FT2 (W/M2)
27.	2005. (1.38E 07)	530. (550.)	523. (1.22E 06)	2.03E 06 (2755.)	0.742E 06 (2.34E 06)
32.	2005. (1.38E 07)	493. (529.)	479. (1.11E 06)	2.03E 06 (2758.)	0.817E 06 (2.58E 06)
37.	2005. (1.38E 07)	466. (514.)	448. (1.04E 06)	2.01E 06 (2728.)	0.887E 06 (2.80E 06)
44.	2005. (1.38E 07)	436. (498.)	416. (9.67E 05)	2.03E 06 (2754.)	0.960E 06 (3.03E 06)
56.	2000. (1.38E 07)	504. (535.)	492. (1.14E 06)	1.49E 06 (2025.)	0.648E 06 (2.04E 06)
61.	2000. (1.38E 07)	471. (517.)	455. (1.06E 06)	1.49E 06 (2015.)	0.715E 06 (2.25E 06)
66.	2005. (1.38E 07)	435. (497.)	415. (9.65E 05)	1.51E 06 (2054.)	0.788E 06 (2.48E 06)
73.	1995. (1.38E 07)	398. (477.)	375. (8.72E 05)	1.51E 06 (2043.)	0.840E 06 (2.65E 06)
78.	2005. (1.38E 07)	356. (453.)	330. (7.69E 05)	1.51E 06 (2050.)	0.938E 06 (2.96E 06)
80.	2000. (1.38E 07)	346. (448.)	321. (7.46E 05)	1.49E 06 (2020.)	0.954E 06 (3.01E 06)
82.	2000. (1.38E 07)	403. (479.)	380. (8.85E 05)	2.00E 06 (2719.)	0.105E 07 (3.31E 06)
83.	1995. (1.38E 07)	383. (468.)	359. (8.34E 05)	1.99E 06 (2694.)	0.108E 07 (3.42E 06)
106.	2005. (1.38E 07)	549. (560.)	546. (1.27E 06)	2.54E 06 (3446.)	0.788E 06 (2.48E 06)
111.	2005. (1.38E 07)	519. (543.)	509. (1.18E 06)	2.52E 06 (3412.)	0.859E 06 (2.71E 06)
116.	2005. (1.38E 07)	487. (526.)	473. (1.10E 06)	2.51E 06 (3398.)	0.954E 06 (3.01E 06)
123.	2000. (1.38E 07)	454. (508.)	436. (1.01E 06)	2.51E 06 (3404.)	0.106E 07 (3.33E 06)
128.	2005. (1.38E 07)	410. (483.)	387. (9.01E 05)	2.53E 06 (3428.)	0.118E 07 (3.72E 06)
150.	2000. (1.38E 07)	443. (501.)	423. (9.84E 05)	1.03E 06 (1394.)	0.569E 06 (1.79E 06)
155.	2000. (1.38E 07)	405. (480.)	383. (8.90E 05)	1.02E 06 (1390.)	0.618E 06 (1.95E 06)
162.	2000. (1.38E 07)	366. (459.)	341. (7.94E 05)	1.01E 06 (1374.)	0.664E 06 (2.09E 06)
167.	2000. (1.38E 07)	330. (439.)	304. (7.07E 05)	1.01E 06 (1370.)	0.694E 06 (2.19E 06)
172.	2000. (1.38E 07)	293. (418.)	266. (6.19E 05)	9.93E 05 (1347.)	0.725E 06 (2.29E 06)
183.	2005. (1.38E 07)	382. (468.)	358. (8.33E 05)	7.58E 05 (1028.)	0.562E 06 (1.77E 06)
190.	2000. (1.38E 07)	341. (445.)	315. (7.32E 05)	7.47E 05 (1013.)	0.575E 06 (1.81E 06)
195.	2000. (1.38E 07)	307. (426.)	280. (6.51E 05)	7.57E 05 (1026.)	0.599E 06 (1.89E 06)
201.	2000. (1.38E 07)	266. (403.)	238. (5.54E 05)	7.46E 05 (1012.)	0.629E 06 (1.98E 06)
203.	2005. (1.38E 07)	260. (400.)	233. (5.41E 05)	7.44E 05 (1009.)	0.638E 06 (2.01E 06)
204.	2005. (1.38E 07)	379. (466.)	354. (8.25E 05)	7.52E 05 (1020.)	0.568E 06 (1.79E 06)
226.	2005. (1.38E 07)	379. (466.)	354. (8.25E 05)	7.52E 05 (1020.)	0.548E 06 (1.73E 06)
235.	2000. (1.38E 07)	475. (519.)	459. (1.07E 06)	1.25E 06 (1695.)	0.601E 06 (1.89E 06)
240.	2000. (1.38E 07)	440. (500.)	420. (9.78E 05)	1.25E 06 (1702.)	0.654E 06 (2.06E 06)
247.	2000. (1.38E 07)	405. (480.)	383. (8.90E 05)	1.23E 06 (1675.)	0.698E 06 (2.20E 06)
252.	1995. (1.38E 07)	371. (462.)	347. (8.06E 05)	1.23E 06 (1673.)	0.745E 06 (2.35E 06)
257.	2000. (1.38E 07)	327. (437.)	301. (7.00E 05)	1.21E 06 (1648.)	0.794E 06 (2.50E 06)
259.	2000. (1.38E 07)	315. (430.)	288. (6.70E 05)	1.22E 06 (1657.)	0.802E 06 (2.53E 06)
321.	2010. (1.39E 07)	482. (523.)	466. (1.08E 06)	1.02E 06 (1383.)	0.542E 06 (1.71E 06)
334.	2005. (1.38E 07)	380. (467.)	356. (8.28E 05)	7.52E 05 (1020.)	0.557E 06 (1.76E 06)
278.	1000. (6.89E 06)	516. (542.)	507. (1.18E 06)	1.02E 06 (1387.)	0.563E 06 (1.77E 06)
279.	1000. (6.89E 06)	496. (531.)	483. (1.12E 06)	1.02E 06 (1389.)	0.593E 06 (1.87E 06)
280.	1000. (6.89E 06)	458. (510.)	439. (1.02E 06)	1.00E 06 (1360.)	0.646E 06 (2.04E 06)
281.	1000. (6.89E 06)	416. (486.)	393. (9.13E 05)	1.01E 06 (1364.)	0.737E 06 (2.32E 06)
282.	1000. (6.89E 06)	371. (462.)	345. (8.03E 05)	9.96E 05 (1351.)	0.808E 06 (2.55E 06)
283.	1000. (6.89E 06)	337. (442.)	309. (7.19E 05)	1.01E 06 (1375.)	0.839E 06 (2.64E 06)
284.	1000. (6.89E 06)	318. (432.)	289. (6.73E 05)	9.51E 05 (1290.)	0.848E 06 (2.67E 06)
285.	1500. (1.03E 07)	559. (566.)	560. (1.30E 06)	1.05E 06 (1420.)	0.454E 06 (1.43E 06)
286.	1505. (1.04E 07)	562. (567.)	563. (1.31E 06)	1.04E 06 (1417.)	0.453E 06 (1.43E 06)
287.	1505. (1.04E 07)	534. (552.)	528. (1.23E 06)	1.03E 06 (1401.)	0.500E 06 (1.58E 06)
288.	1495. (1.03E 07)	493. (529.)	479. (1.11E 06)	1.03E 06 (1394.)	0.574E 06 (1.81E 06)
289.	1500. (1.03E 07)	460. (511.)	442. (1.03E 06)	1.02E 06 (1378.)	0.633E 06 (2.00E 06)
290.	1505. (1.04E 07)	411. (483.)	388. (9.02E 05)	1.01E 06 (1372.)	0.702E 06 (2.21E 06)

ANC2 RUN CONDITIONS

RUN	SYSTEM PRESSURE PSIA (PA)	INLET TEMPERATURE F (K)	INLET ENTHALPY BTU/LBM (J/KG)	INLET MASS FLUX LBM/HR-FT2 (KG/S-M2)	BUNDLE AVERAGE HEAT FLUX BTU/HR-FT2 (W/M2)
291.	1510. (1.04E 07)	359. (455.)	333. (7.74E 05)	9.96E 05 (1351.)	0.767E 06 (2.42E 06)
292.	1495. (1.03E 07)	314. (430.)	287. (6.67E 05)	9.62E 05 (1304.)	0.793E 06 (2.50E 06)
293.	1005. (6.93E 06)	518. (543.)	509. (1.18E 06)	2.01E 06 (2728.)	0.703E 06 (2.22E 06)
294.	1005. (6.93E 06)	493. (529.)	479. (1.11E 06)	1.98E 06 (2681.)	0.763E 06 (2.40E 06)
295.	1000. (6.89E 06)	461. (511.)	442. (1.03E 06)	2.00E 06 (2707.)	0.853E 06 (2.69E 06)
296.	1000. (6.89E 06)	420. (489.)	398. (9.25E 05)	1.99E 06 (2693.)	0.936E 06 (2.95E 06)
297.	1005. (6.93E 06)	380. (466.)	354. (8.24E 05)	1.98E 06 (2689.)	0.104E 07 (3.27E 06)
298.	1495. (1.03E 07)	555. (564.)	555. (1.29E 06)	2.03E 06 (2759.)	0.556E 06 (1.75E 06)
299.	1505. (1.04E 07)	532. (551.)	525. (1.22E 06)	2.01E 06 (2730.)	0.642E 06 (2.02E 06)
300.	1510. (1.04E 07)	499. (533.)	487. (1.13E 06)	2.02E 06 (2734.)	0.764E 06 (2.41E 06)
301.	1500. (1.03E 07)	461. (512.)	443. (1.03E 06)	2.02E 06 (2745.)	0.839E 06 (2.64E 06)
302.	1505. (1.04E 07)	419. (488.)	396. (9.22E 05)	1.96E 06 (2665.)	0.936E 06 (2.95E 06)
311.	1005. (6.93E 06)	521. (545.)	512. (1.19E 06)	5.40E 05 (732.)	0.448E 06 (1.41E 06)
312.	995. (6.86E 06)	444. (502.)	423. (9.85E 05)	5.43E 05 (736.)	0.513E 06 (1.62E 06)
313.	1000. (6.89E 06)	344. (447.)	317. (7.37E 05)	5.08E 05 (689.)	0.576E 06 (1.82E 06)
314.	1495. (1.03E 07)	543. (557.)	539. (1.25E 06)	5.25E 05 (712.)	0.373E 06 (1.18E 06)
315.	1505. (1.04E 07)	443. (501.)	423. (9.83E 05)	5.40E 05 (732.)	0.479E 06 (1.51E 06)
316.	1500. (1.03E 07)	333. (440.)	306. (7.12E 05)	5.00E 05 (678.)	0.565E 06 (1.78E 06)
317.	1510. (1.04E 07)	246. (392.)	217. (5.05E 05)	5.00E 05 (678.)	0.621E 06 (1.96E 06)
318.	1005. (6.93E 06)	246. (392.)	216. (5.03E 05)	4.99E 05 (677.)	0.663E 06 (2.09E 06)
319.	1505. (1.04E 07)	246. (392.)	217. (5.05E 05)	5.22E 05 (708.)	0.630E 06 (1.99E 06)
320.	1495. (1.03E 07)	277. (409.)	249. (5.79E 05)	5.13E 05 (696.)	0.627E 06 (1.98E 06)

ANC3 RUN CONDITIONS

RUN	SYSTEM PRESSURE PSIA (PA)	INLET TEMPERATURE F (K)	INLET ENTHALPY BTU/LBM (J/KG)	INLET MASS FLUX LBM/HR-FT2 (KG/S-M2)	BUNDLE AVERAGE HEAT FLUX BTU/HR-FT2 (W/M2)
25.	2000. (1.38E 07)	609. (593.)	627. (1.46E 06)	2.07E 06 (2808.)	0.470E 06 (1.48E 06)
28.	2005. (1.38E 07)	576. (575.)	581. (1.35E 06)	2.04E 06 (2770.)	0.579E 06 (1.83E 06)
38.	2005. (1.38E 07)	596. (587.)	609. (1.42E 06)	1.28E 06 (1740.)	0.415E 06 (1.31E 06)
42.	2000. (1.38E 07)	528. (549.)	521. (1.21E 06)	1.36E 06 (1841.)	0.582E 06 (1.83E 06)
45.	2015. (1.39E 07)	431. (495.)	410. (9.54E 05)	1.24E 06 (1686.)	0.744E 06 (2.35E 06)
48.	2000. (1.38E 07)	364. (458.)	339. (7.89E 05)	1.21E 06 (1646.)	0.835E 06 (2.63E 06)
51.	2000. (1.38E 07)	341. (445.)	315. (7.34E 05)	1.18E 06 (1599.)	0.859E 06 (2.71E 06)
57.	2000. (1.38E 07)	500. (533.)	487. (1.13E 06)	2.02E 06 (2745.)	0.812E 06 (2.56E 06)
62.	2000. (1.38E 07)	447. (504.)	428. (9.95E 05)	2.02E 06 (2739.)	0.995E 06 (3.14E 06)
67.	2000. (1.38E 07)	417. (487.)	395. (9.20E 05)	2.03E 06 (2754.)	0.108E 07 (3.40E 06)
70.	2000. (1.38E 07)	396. (475.)	373. (8.68E 05)	2.01E 06 (2732.)	0.110E 07 (3.48E 06)
80.	2005. (1.38E 07)	545. (558.)	541. (1.26E 06)	1.50E 06 (2031.)	0.555E 06 (1.75E 06)
99.	2000. (1.38E 07)	603. (590.)	618. (1.44E 06)	2.54E 06 (3439.)	0.533E 06 (1.68E 06)
100.	2000. (1.38E 07)	577. (576.)	582. (1.35E 06)	2.51E 06 (3405.)	0.653E 06 (2.06E 06)
107.	2000. (1.38E 07)	495. (530.)	481. (1.12E 06)	2.53E 06 (3428.)	0.991E 06 (3.12E 06)

ANC4 RUN CONDITIONS

RUN	SYSTEM PRESSURE PSIA (PA)	INLET TEMPERATURE F (K)	INLET ENTHALPY BTU/LBM (J/KG)	INLET MASS FLUX LBM/HR-FT2 (KG/S-M2)	BUNDLE AVERAGE HEAT FLUX BTU/HR-FT2 (W/M2)
10.	1005. (6.93E 06)	530. (550.)	524. (1.22E 06)	4.91E 05 (666.)	0.422E 06 (1.33E 06)
11.	1000. (6.89E 06)	450. (506.)	431. (1.00E 06)	5.01E 05 (679.)	0.482E 06 (1.52E 06)
12.	1515. (1.04E 07)	530. (550.)	524. (1.22E 06)	5.16E 05 (700.)	0.379E 06 (1.19E 06)
13.	1500. (1.03E 07)	541. (556.)	537. (1.25E 06)	5.10E 05 (692.)	0.363E 06 (1.14E 06)
14.	1515. (1.04E 07)	434. (496.)	413. (9.61E 05)	4.99E 05 (677.)	0.449E 06 (1.42E 06)
15.	1500. (1.03E 07)	336. (442.)	309. (7.19E 05)	5.00E 05 (678.)	0.547E 06 (1.72E 06)
16.	1000. (6.89E 06)	358. (454.)	332. (7.71E 05)	4.96E 05 (673.)	0.558E 06 (1.76E 06)
21.	1515. (1.04E 07)	561. (567.)	562. (1.31E 06)	9.97E 05 (1352.)	0.454E 06 (1.43E 06)
22.	1500. (1.03E 07)	537. (554.)	533. (1.24E 06)	1.00E 06 (1363.)	0.493E 06 (1.55E 06)
23.	1000. (6.89E 06)	513. (540.)	503. (1.17E 06)	1.01E 06 (1364.)	0.565E 06 (1.78E 06)
24.	1515. (1.04E 07)	494. (530.)	481. (1.12E 06)	1.01E 06 (1374.)	0.550E 06 (1.73E 06)
25.	1500. (1.03E 07)	468. (515.)	451. (1.05E 06)	9.83E 05 (1333.)	0.590E 06 (1.86E 06)
26.	1000. (6.89E 06)	456. (509.)	437. (1.02E 06)	9.82E 05 (1332.)	0.651E 06 (2.05E 06)
27.	1500. (1.03E 07)	415. (486.)	392. (9.12E 05)	1.02E 06 (1383.)	0.675E 06 (2.13E 06)
28.	1500. (1.03E 07)	560. (566.)	561. (1.30E 06)	1.98E 06 (2679.)	0.561E 06 (1.77E 06)
29.	1500. (1.03E 07)	535. (553.)	530. (1.23E 06)	2.04E 06 (2765.)	0.653E 06 (2.06E 06)
89.	1000. (6.89E 06)	347. (448.)	320. (7.44E 05)	1.08E 06 (1471.)	0.799E 06 (2.52E 06)
90.	1500. (1.03E 07)	322. (434.)	295. (6.86E 05)	1.00E 06 (1357.)	0.751E 06 (2.37E 06)
91.	1500. (1.03E 07)	360. (456.)	335. (7.79E 05)	1.05E 06 (1421.)	0.758E 06 (2.39E 06)
92.	1000. (6.89E 06)	379. (466.)	354. (8.23E 05)	1.05E 06 (1424.)	0.783E 06 (2.47E 06)
93.	1000. (6.89E 06)	417. (487.)	395. (9.18E 05)	1.05E 06 (1428.)	0.718E 06 (2.26E 06)
95.	2000. (1.38E 07)	425. (492.)	404. (9.40E 05)	1.25E 06 (1692.)	0.684E 06 (2.16E 06)
96.	1005. (6.93E 06)	455. (508.)	436. (1.01E 06)	2.04E 06 (2773.)	0.851E 06 (2.68E 06)
97.	1005. (6.93E 06)	501. (534.)	489. (1.14E 06)	1.98E 06 (2690.)	0.737E 06 (2.32E 06)
98.	2000. (1.38E 07)	501. (534.)	489. (1.14E 06)	2.04E 06 (2761.)	0.800E 06 (2.52E 06)
100.	2000. (1.38E 07)	509. (538.)	498. (1.16E 06)	1.98E 06 (2689.)	0.750E 06 (2.36E 06)
102.	1000. (6.89E 06)	515. (542.)	506. (1.18E 06)	1.99E 06 (2698.)	0.691E 06 (2.18E 06)
104.	1500. (1.03E 07)	267. (404.)	239. (5.55E 05)	4.98E 05 (675.)	0.605E 06 (1.91E 06)

APPENDIX B

LOCAL SUBCHANNEL CONDITIONS FOR ALL CHF DATA POINTS

LOCAL SUBCHANNEL CHF CONDITIONS (SI UNITS)
EXX2 DATA

RUN NO.	CHF ROD NO.	CHF CHANNEL	PRESSURE (KPA) X 10-4	MASS VEL. (KG/S-M2) X 10-3	EQUILIBRIUM QUALITY	PREDICTED CHF (W/M2) X 10-6 LOFT2	BEW-2	BARNETT	GE	MEASURED CHF (W/M2) X 10-6 HFLUX
22	12-2	30	1.034	1.391	0.196	1.99	1.44	1.20	1.90	1.50
23	21-2	35	1.034	1.818	0.168	1.94	1.46	1.34	1.99	1.77
24	21-2	35	1.045	2.435	0.122	1.99	1.70	1.45	2.14	1.88
25	21-2	35	1.045	3.032	0.090	2.08	1.94	1.57	2.24	2.10
26.1	21-2	35	1.034	1.124	0.243	1.91	1.27	1.20	1.76	1.75
26.2	12-2	30	1.034	1.359	0.170	2.13	1.74	1.33	1.99	1.73
27	21-2	35	1.034	1.870	0.128	2.16	1.90	1.58	2.12	2.01
28	21-2	35	1.034	2.408	0.092	2.23	2.12	1.70	2.23	2.11
29.1	21-2	35	1.034	2.985	0.074	2.24	2.18	1.73	2.29	2.26
29.2	12-2	30	1.034	3.379	0.042	2.46	2.52	1.74	2.39	2.55
30	21-2	35	1.034	2.888	0.056	2.40	2.46	1.91	2.35	2.46
31	21-2	35	1.045	1.729	0.119	2.23	2.07	1.66	2.15	2.20
32	8-2	27	1.034	2.552	0.041	2.56	2.71	1.85	2.39	2.56
33	8-2	27	1.045	3.193	0.009	2.73	3.03	2.03	2.49	2.76
34.1	8-2	27	1.034	1.281	0.137	2.31	2.15	1.51	2.09	2.02
34.2	20-0	26	1.034	1.192	0.245	1.86	1.10	0.80	1.75	1.90
35	21-2	35	1.038	1.717	0.093	2.38	2.39	1.83	2.23	2.39
52	21-2	35	1.045	1.144	0.160	2.24	2.00	1.57	2.02	2.08
7	8-2	27	1.382	1.987	0.109	1.60	1.80	1.25	2.18	1.43
8	8-2	27	1.382	2.647	0.092	1.55	1.96	1.22	2.23	1.61
9	8-2	27	1.376	3.258	0.089	1.44	2.02	1.14	2.24	1.81
10.1	21-2	35	1.382	1.810	0.154	1.40	1.43	1.19	2.04	1.37
10.2	25-2	35	1.382	1.810	0.154	1.40	1.43	1.19	2.04	1.38
11	8-2	27	1.382	2.623	0.049	1.86	2.37	1.48	2.37	1.85
12	8-2	27	1.386	3.226	0.037	1.88	2.52	1.50	2.40	2.01
16	8-2	27	1.379	3.406	-0.030	2.46	3.22	1.98	2.62	2.68
18	8-2	27	1.382	3.218	0.008	2.13	2.82	1.71	2.50	2.34
19	8-2	27	1.382	3.338	-0.033	2.48	3.24	2.00	2.63	2.46
20	8-2	27	1.376	2.620	0.0	2.21	2.33	1.79	2.52	2.21
21	18-0	34	1.376	1.860	0.116	1.61	1.70	1.00	2.16	1.69
38.1	21-2	35	1.379	1.276	0.170	1.54	1.32	1.25	1.99	1.46
38.2	24-0	36	1.379	1.229	0.208	1.39	1.04	1.11	1.87	1.42
43	8-1	27	1.382	1.262	0.042	2.06	2.27	1.61	2.39	1.75
46	8-1	27	1.379	2.572	-0.029	2.39	3.09	1.96	2.61	2.50
47	8-1	27	1.382	1.945	-0.015	2.27	2.85	1.87	2.68	2.03
48	8-1	27	1.382	1.926	-0.036	2.37	3.03	1.97	2.64	2.19
51	8-1	27	1.376	1.323	-0.055	2.39	3.04	1.99	2.69	1.92

LOCAL SUBCHANNEL CHF CONDITIONS (SI UNITS)
ANCI DATA

RUN NO.	CHF ROD NO.	CHF CHANNEL	PRESSURE (KPA) X 10-4	MASS VEL. (KG/S-M2) X 10-3	EQUILIBRIUM QUALITY	PREDICTED CHF (W/M2) X 10-6 LOFT2	BEW-2	BARNETT	GE	MEASURED CHF (W/M2) X 10-6 HFLUX
14	8-2	27	1.376	2.548	0.101	1.52	1.88	1.19	2.20	1.57
15	8-2	27	1.392	1.951	0.094	1.70	1.92	1.33	2.23	1.44
17	8-2	27	1.379	3.229	0.083	1.49	2.08	1.19	2.26	1.75

LOCAL SUBCHANNEL CHF CONDITIONS (SI UNITS)
ANC2 DATA

RUN NO.	CHF ROD NO.	CHF CHANNEL	PRESSURE (KPA) X 10-4	MASS VEL. (KG/S-M2) X 10-3	EQUILIBRIUM QUALITY	PREDICTED CHF (W/M2) X 10-6 LOFT2	B&W-2	BARNETT	GE	MEASURED CHF (W/M2) X 10-6 HFLUX
278	23-2	31	0.689	1.433	0.309	2.17	0.29	0.60	1.55	1.83
279	23-2	31	0.689	1.399	0.295	2.28	0.57	0.67	1.59	1.95
280	23-2	31	0.689	1.296	0.283	2.42	0.99	0.76	1.63	2.12
281	23-2	31	0.689	1.258	0.276	2.48	[illegible]	0.80	1.65	2.42
282.1	20-1	35	0.689	0.942	0.361	2.30	1.28	0.85	1.38	2.52
282.2	21-1	35	0.689	0.942	0.361	2.30	1.28	0.85	1.38	2.66
282.3	21-2	35	0.689	0.995	0.289	2.61	1.91	1.13	1.61	2.66
282.4	21-3	26	0.689	1.052	0.302	2.51	1.48	0.81	1.57	2.66
282.5	23-2	31	0.689	1.208	0.260	2.60	1.51	0.87	1.70	2.66
283	21-1	35	0.689	0.949	0.316	2.52	1.77	1.04	1.53	2.76
284	20-1	35	0.689	0.871	0.341	2.46	1.82	0.98	1.45	2.64
285	21-2	35	1.034	1.271	0.251	1.78	1.00	1.01	1.73	1.49
286.1	21-2	35	1.038	1.268	0.256	1.75	0.95	0.99	1.71	1.49
286.2	21-3	26	1.038	1.360	0.261	1.66	0.76	0.70	1.70	1.49
286.3	23-2	31	1.038	1.478	0.241	1.70	0.84	0.72	1.76	1.49
286.4	24-2	31	1.038	1.478	0.241	1.70	0.84	0.72	1.76	1.42
287	21-2	35	1.038	1.226	0.235	1.88	1.21	1.10	1.78	1.65
288.1	20-1	35	1.031	1.146	0.258	1.83	1.08	1.04	1.71	1.79
288.2	20-2	34	1.031	1.073	0.263	1.86	1.09	0.80	1.69	1.79
288.3	20-3	26	1.031	1.265	0.220	1.94	1.26	0.85	1.83	1.79
288.4	20-4	35	1.031	1.203	0.209	2.03	1.50	1.23	1.86	1.79
288.5	21-2	35	1.031	1.203	0.209	2.03	1.50	1.23	1.86	1.89
289.1	20-1	35	1.034	1.112	0.251	1.88	1.19	1.08	1.73	1.97
289.2	21-2	35	1.034	1.173	0.194	2.11	1.67	1.30	1.91	2.08
289.3	24-1	31	1.034	1.313	0.227	1.88	1.15	0.82	1.81	1.98
290.1	20-1	35	1.038	1.093	0.215	2.05	2.11	1.23	1.84	2.19
290.2	21-1	35	1.038	1.093	0.215	2.05	2.11	1.23	1.84	2.31
290.3	21-2	35	1.038	1.157	0.150	2.29	1.55	1.48	2.05	2.31
291.1	18-1	34	1.041	0.929	0.256	1.96	1.31	0.86	1.71	2.34
291.2	21-1	35	1.041	1.055	0.179	2.21	1.92	1.38	1.96	2.53
292	18-1	34	1.031	0.955	0.133	2.45	1.70	1.16	2.08	2.42
293	21-2	35	0.693	2.426	0.188	2.35	0.43	1.01	1.93	2.32
294.1	21-2	35	0.693	2.328	0.168	2.54	0.90	1.20	1.99	2.51
294.2	23-2	31	0.693	2.655	0.160	2.47	0.64	0.81	2.02	2.51
294.3	24-2	31	0.693	2.655	0.160	2.47	0.64	0.81	2.02	2.39
295.1	21-2	35	0.689	2.298	0.145	2.73	1.34	1.39	2.06	2.81
295.2	23-2	31	0.689	2.609	0.136	2.68	1.13	0.96	2.09	2.81
295.3	24-2	31	0.689	2.609	0.136	2.68	1.13	0.96	2.09	2.67
296	24-2	31	0.689	2.524	0.095	3.01	1.93	1.20	2.22	2.93
297.1	8-3	26	0.693	2.210	0.082	3.16	2.43	1.33	2.26	3.42
297.2	21-2	35	0.693	2.164	0.073	3.22	2.75	1.98	2.29	3.42
298	21-2	35	1.031	2.545	0.112	2.06	1.77	1.36	2.17	1.83
299.1	20-3	26	1.038	2.559	0.103	2.11	1.81	1.00	2.20	2.00
299.2	21-2	35	1.038	2.450	0.096	2.19	2.03	1.49	2.22	2.11
299.3	24-2	31	1.038	2.740	0.089	2.17	1.93	1.03	2.24	2.01
300.1	8-2	27	1.041	2.559	0.046	2.51	2.65	1.83	2.38	2.52
300.2	8-3	26	1.041	2.487	0.081	2.28	2.11	1.11	2.27	2.52
300.3	21-2	35	1.041	2.387	0.073	2.35	2.35	1.66	2.29	2.52
300.4	21-3	26	1.041	2.487	0.081	2.28	2.11	1.11	2.27	2.52
301	8-3	26	1.034	2.476	0.029	2.64	2.78	1.60	2.43	2.76

LOCAL SUBCHANNEL CHF CONDITIONS (SI UNITS)
ANC2 DATA

RUN NO.	CHF ROD NO.	CHF CHANNEL	PRESSURE (KPA) X 10-4	MASS VEL. (KG/S-M2) X 10-3	EQUILIBRIUM QUALITY	P R E D I C T E D C H F (W/M2) X 10-6 LOFT2	BEW-2	BARNETT	GE	MEASURED CHF (W/M2) X 10-6 HFLUX
302.1	8-2	27	1.038	2.640	-0.051	3.16	3.95	2.53	2.68	3.08
302.2	9-3	26	1.038	2.414	-0.011	2.89	3.29	1.54	2.56	3.08
302.3	25-1	36	1.038	2.206	0.020	2.71	3.07	2.04	2.46	3.07
311	24-1	31	0.693	0.805	0.527	1.53	0.13	0.34	0.86	1.40
312	24-1	31	0.686	0.753	0.497	1.79	0.77	0.33	0.84	1.60
313	24-1	31	0.689	0.690	0.465	2.03	1.42	0.57	1.06	1.80
314.1	21-2	35	1.031	0.632	0.428	1.46	0.56	0.70	1.30	1.23
314.2	21-3	26	1.031	0.696	0.433	1.36	0.33	0.55	1.16	1.23
315.1	20-1	35	1.038	0.601	0.430	1.47	0.61	0.71	0.91	1.49
315.2	21-1	35	1.038	0.601	0.430	1.47	0.61	0.71	0.91	1.58
316	21-1	35	1.034	0.540	0.422	1.58	0.86	0.76	0.91	1.86
317	21-1	35	1.041	0.563	0.337	1.91	1.40	0.97	1.59	2.05
318.1	20-1	35	0.693	0.523	0.514	1.97	2.26	0.63	1.03	2.06
318.2	21-1	35	0.693	0.523	0.514	1.97	2.26	0.63	1.03	2.18
318.3	24-1	31	0.693	0.650	0.459	2.10	1.71	0.61	1.20	2.07
319	21-1	35	1.038	0.586	0.311	2.00	1.55	1.03	1.67	2.07
320.1	20-1	35	1.031	0.564	0.392	1.70	1.03	0.83	1.41	1.95
320.2	24-1	31	1.031	0.689	0.359	1.72	0.92	0.70	1.39	1.96
27.1	8-2	27	1.382	2.655	-0.013	2.29	2.97	1.88	2.56	2.44
27.2	25-5	35	1.382	2.496	0.016	2.10	2.68	1.71	2.47	2.43
32	8-2	27	1.382	2.739	-0.079	2.73	3.60	2.29	2.77	2.69
37	8-2	27	1.382	2.658	-0.113	2.92	3.91	2.49	2.88	2.92
44	8-2	27	1.382	2.671	-0.153	3.16	4.29	2.74	3.00	3.16
56.1	8-1	27	1.379	1.877	0.014	2.14	2.61	1.75	2.48	2.13
56.2	18-1	34	1.379	1.695	0.096	1.76	1.83	0.98	2.22	1.98
61.1	18-1	34	1.379	1.669	0.067	1.90	2.06	1.07	2.31	2.18
61.2	8-1	27	1.379	1.881	-0.024	2.32	2.93	1.93	2.60	2.35
66.1	8-2	27	1.382	2.031	-0.122	2.78	3.81	2.44	2.91	2.59
66.2	8-1	27	1.382	1.978	-0.075	2.56	3.39	2.19	2.76	2.59
73.1	8-1	27	1.376	1.968	-0.125	2.78	3.84	2.45	2.92	2.77
73.2	18-1	34	1.376	1.741	-0.030	2.34	2.85	1.36	2.62	2.56
78.1	8-1	27	1.382	1.939	-0.162	2.91	4.13	2.62	3.03	3.09
78.2	18-1	34	1.382	1.742	-0.058	2.45	3.06	1.44	2.70	2.86
78.3	25-1	36	1.382	1.904	-0.112	2.70	3.69	2.36	2.87	3.08
80.1	8-1	27	1.379	1.912	-0.162	2.90	4.13	2.61	3.03	3.14
80.2	18-1	34	1.379	1.700	-0.056	2.44	3.04	1.44	2.70	2.91
80.3	25-1	36	1.379	1.869	-0.112	2.69	3.68	2.36	2.87	3.13
82	8-2	27	1.379	2.608	-0.187	3.32	4.60	2.94	3.11	3.45
83	8-2	27	1.376	2.555	-0.214	3.44	4.84	3.09	3.20	3.57
106	8-2	27	1.382	3.321	-0.010	2.29	3.02	1.85	2.55	2.59
111	8-2	27	1.382	3.379	-0.064	2.74	3.57	2.24	2.72	2.83
116	8-2	27	1.382	3.306	-0.111	3.09	4.03	2.57	2.87	3.14
123	8-2	27	1.379	3.295	-0.152	3.40	4.45	2.86	3.00	3.49
128.1	8-1	27	1.382	3.187	-0.183	3.56	4.72	3.05	3.10	3.89
128.2	8-2	27	1.382	3.202	-0.223	3.84	5.12	3.33	3.22	3.89
150	18-1	34	1.379	1.182	0.071	1.97	1.97	1.09	2.30	1.74
155	18-1	34	1.379	1.188	0.033	2.10	2.25	1.18	2.42	1.88
162	18-1	34	1.379	1.172	-0.003	2.22	2.51	1.27	2.53	2.03
167	8-3	26	1.379	1.390	-0.163	2.69	3.74	1.69	3.04	2.29
172	8-2	27	1.379	1.223	-0.266	2.77	4.61	2.75	3.36	2.39

LOCAL SUBCHANNEL CHF CONDITIONS (SI UNITS)
ANC2 DATA

RUN NO.	CHF ROD NO.	CHF CHANNEL	PRESSURE (KPA) X 10-4	MASS VEL. (KG/S-M2) X 10-3	EQUILIBRIUM QUALITY	PREDICTED CHF (W/M2) X 10-6 LOFT2	BGW-2	BARNETT	GE	MEASURED CHF (W/M2) X 10-6 HFLUX
183	25-1	36	1.382	0.932	0.060	2.05	2.08	1.53	2.33	1.84
190	8-3	26	1.379	1.041	-0.071	2.38	2.93	1.39	2.75	1.89
195	8-3	26	1.379	1.102	-0.128	2.51	3.35	1.53	2.93	1.97
201	8-3	26	1.379	1.074	-0.173	2.57	3.67	1.63	3.08	2.07
203	8-3	26	1.382	1.078	-0.173	2.57	3.64	1.62	3.07	2.10
204	25-1	34	1.382	0.876	0.136	1.83	1.49	0.96	2.09	1.86
226	25-1	36	1.382	0.934	0.036	2.11	2.25	1.60	2.41	1.80
235	8-1	27	1.379	1.580	-0.015	2.27	2.80	1.88	2.57	1.98
240	8-1	27	1.379	1.623	-0.062	2.45	3.19	2.08	2.72	2.15
247	8-3	26	1.379	1.726	-0.101	2.61	3.40	1.56	2.84	2.30
252	8-3	26	1.376	1.669	-0.141	2.74	3.71	1.68	2.97	2.46
257.1	8-2	27	1.379	1.517	-0.252	2.94	4.69	2.87	3.32	2.62
257.2	8-3	26	1.379	1.645	-0.194	2.88	4.10	1.83	3.13	2.62
259.1	8-2	27	1.379	1.700	-0.278	3.12	5.01	3.08	3.40	2.64
2[illegible]9.2	8-3	26	1.379	1.635	-0.219	2.94	4.29	1.90	3.21	2.64
321	25-1	36	1.386	1.219	0.094	1.87	1.88	1.43	2.23	1.78
334	25-1	36	1.382	0.929	0.053	2.06	2.13	1.55	3.03	1.83

LOCAL SUBCHANNEL CHF CONDITIONS (SI UNITS)
ANC3 DATA

RUN NO.	CHF RCD NO.	CHF CHANNEL	PRESSURE (KPA) X 10-4	MASS VEL. (KG/S-M2) X 10-3	EQUILIBRIUM QUALITY	PREDICTED CHF (W/M2) X 10-6 LOFT2	BSW-2	BARNETT	GE	MEASURED CHF (W/M2) X 10-6 HFLUX
25	23-2	31	1.379	2.818	0.116	1.32	1.67	0.74	2.16	1.56
28	23-2	31	1.382	2.730	0.069	1.70	2.10	0.95	2.30	1.92
38	21-3	26	1.382	1.755	0.162	1.38	1.29	0.76	2.01	1.37
42.1	21-1	35	1.379	1.637	0.104	1.73	1.83	1.35	2.19	1.93
42.2	23-1	31	1.379	1.722	0.116	1.65	1.65	0.90	2.16	1.93
45.1	8-2	26	1.389	1.591	-0.019	2.27	2.68	1.30	2.58	2.46
45.2	7-2	26	1.389	1.591	-0.019	2.27	2.68	1.30	2.58	2.45
45.3	21-1	35	1.389	1.458	0.030	2.07	2.39	1.66	2.43	2.46
48	8-2	26	1.379	1.612	-0.089	2.54	3.26	1.51	2.80	2.77
51	8-2	26	1.379	1.589	-0.107	2.60	3.39	1.56	2.86	2.85
57	8-2	26	1.379	2.689	-0.030	2.41	2.99	1.36	2.62	2.69
62	8-2	26	1.379	2.731	-0.074	2.70	[illegible]	1.54	2.75	3.30
67	12-2	30	1.379	2.651	-0.146	3.11	[illegible]	5.84	2.98	3.59
70	12-2	30	1.379	2.610	-0.182	3.30	4.27	6.05	3.10	3.67
80	12-1	30	1.382	1.877	0.062	1.89	2.19	1.51	2.33	1.85
99	21-2	35	1.379	3.271	0.073	1.58	2.18	[illegible]	2.29	1.77
100.1	21-2	35	1.379	3.184	0.041	1.87	2.49	1.49	2.39	2.17
100.2	21-3	26	1.379	3.351	0.048	1.79	2.33	[illegible]	2.37	2.17
107	14-2	31	1.379	3.394	-0.047	2.60	3.26	[illegible]	2.58	3.27

LOCAL SUBCHANNEL CHF CONDITIONS (SI UNITS)
ANC4 DATA

RUN NO.	CHF ROD NO.	CHF CHANNEL	PRESSURE (KPA) X 10-4	MASS VEL. (KG/S-M2) X 10-3	EQUILIBRIUM QUALITY	PREDICTED CHF (W/M2) X 10-6 LOFT2	B&W-2	BARNETT	GE	MEASURED CHF (W/M2) X 10-6 HFLUX
10.1	15-1	31	0.693	0.671	0.597	1.30	0.31	0.29	0.77	1.41
10.2	15-2	31	0.693	0.674	0.547	1.59	0.76	0.40	0.92	1.41
10.3	23-1	31	0.693	0.671	0.597	1.30	0.31	0.29	0.77	1.38
10.4	21-1	35	0.693	0.610	0.600	1.36	0.76	0.28	0.76	1.41
10.5	21-2	35	0.693	0.616	0.543	1.69	1.25	0.45	0.94	1.41
11.1	15-2	31	0.689	0.635	0.489	1.97	1.56	0.55	1.11	1.60
11.2	8-2	27	0.689	0.637	0.412	2.35	2.34	0.86	.35	1.57
12.	15-2	31	1.045	0.681	0.409	1.47	0.51	0.62	1.23	1.26
13.	15-2	31	1.034	0.673	0.421	1.44	0.47	0.59	1.32	1.21
14.	15-2	31	1.045	0.647	0.335	1.83	1.14	0.75	1.59	1.49
15.	23-1	31	1.034	0.617	0.383	1.68	0.90	0.68	1.44	1.79
16.	8-2	27	0.689	0.643	0.356	2.60	2.84	1.04	1.53	1.82
21.	15-2	31	1.045	1.306	0.267	1.65	0.75	0.69	1.68	1.51
22.	15-2	31	1.034	1.292	0.245	1.80	0.99	0.77	1.75	1.64
23.	14-2	31	0.689	1.280	0.326	2.20	0.49	0.61	1.49	1.87
24.	15-2	31	1.045	1.275	0.195	2.03	1.48	0.92	1.91	1.83
25.	10-2	28	1.034	1.218	0.155	2.26	2.02	1.45	2.03	1.95
26.	14-2	31	0.689	1.140	0.313	2.38	1.07	0.73	1.54	2.16
27.	14-1	31	1.034	1.205	0.186	2.13	1.65	0.96	1.94	2.23
28.	14-2	31	1.034	2.614	0.133	1.87	1.39	0.84	2.10	1.86
29.	12-2	30	1.034	2.609	0.082	2.26	2.15	1.56	2.26	2.17
89.	15-1	31	0.689	1.196	0.233	2.74	1.88	0.97	1.79	2.66
90.	23-1	31	1.034	1.159	0.079	2.57	2.69	1.27	2.27	2.46
91.1	23-1	31	1.034	1.212	0.135	2.34	2.12	1.11	2.10	2.48
91.2	14-1	31	1.034	1.212	0.135	2.34	2.12	1.11	2.10	2.51
92.	14-1	31	0.689	1.169	0.297	2.44	1.18	0.77	1.59	2.59
93.	14-1	31	0.689	1.216	0.304	2.37	0.94	0.72	1.56	2.38
95.	15-2	31	1.379	1.713	-0.077	2.52	3.19	1.49	2.76	2.28
96.	21-2	35	0.693	2.468	0.117	2.86	1.68	1.56	2.15	2.84
97.	21-2	35	0.693	2.438	0.165	2.52	0.82	1.17	2.00	2.46
98.	15-2	31	1.379	2.719	-0.031	2.42	3.01	1.36	2.62	2.66
100.	15-2	31	1.379	2.648	-0.026	2.38	2.95	1.34	2.60	2.50
102.	21-2	35	0.689	2.472	0.174	2.45	0.62	1.09	1.97	2.30
104.	23-1	31	1.034	0.607	0.354	1.81	1.13	0.73	1.53	1.98

LOCAL SUBCHANNEL CHF CONDITIONS (ENGLISH UNITS)
EXX2 DATA

RUN NO.	CHF ROD NO.	CHF CHANNEL	PRESSURE (PSIA)	MASS VEL. (LBM/HR-FT2) X 10-6	EQUILIBRIUM QUALITY	PREDICTED CHF (BTU/HR-FT2) X 10-6 LOFT2	BGW-2	BARNETT	GE	MEASURED CHF (BTU/HR-FT2) X 10-6 HFLUX
22	12-2	30	1500.	1.026	0.196	0.631	0.458	0.381	0.604	0.476
23	21-2	35	1500.	1.341	0.168	0.616	0.462	0.424	0.632	0.561
24	21-2	35	1515.	1.796	0.122	0.632	0.540	0.461	0.678	0.597
25	21-2	35	1515.	2.236	0.090	0.660	0.617	0.498	0.710	0.666
26.1	21-2	35	1500.	0.829	0.243	0.606	0.402	0.380	0.557	0.556
26.2	12-2	30	1500.	1.002	0.170	0.676	0.551	0.423	0.630	0.549
27	21-2	35	1500.	1.377	0.128	0.684	0.604	0.501	0.672	0.639
28	21-2	35	1500.	1.776	0.092	0.708	0.674	0.539	C.708	0.668
29.1	21-2	35	1500.	2.201	0.074	0.712	0.693	0.549	0.726	0.717
29.2	12-2	30	1500.	2.492	0.042	0.780	0.801	0.551	0.758	0.808
30	21-2	35	1500.	2.130	0.056	0.763	0.782	0.605	C.744	0.782
31	21-2	35	1515.	1.275	0.119	0.707	0.657	0.528	0.681	0.699
32	8-2	27	1500.	1.882	0.041	0.811	0.861	0.587	0.759	0.811
33	8-2	27	1515.	2.355	0.009	0.867	0.961	0.645	0.791	0.875
34.1	8-2	27	1500.	0.945	0.137	0.733	0.681	0.479	0.663	0.641
34.2	20-0	26	1500.	0.879	0.245	0.590	0.348	0.253	0.555	0.603
35	21-2	35	1505.	1.266	0.093	0.756	0.757	0.581	0.707	0.758
52	21-2	35	1515.	0.844	0.160	0.712	0.634	0.498	0.640	0.659
7	8-2	27	2005.	1.465	0.109	0.509	0.570	0.396	0.691	0.453
8	8-2	27	2005.	1.952	0.092	0.491	0.623	0.387	0.708	0.512
9	8-2	27	1995.	2.403	0.089	0.457	0.640	0.363	C.711	0.574
10.1	21-2	35	2005.	1.335	0.154	0.444	0.455	0.378	0.646	0.436
10.2	25-2	35	2005.	1.335	0.154	0.444	0.455	0.378	0.646	0.439
11	8-2	27	2005.	1.934	0.049	0.591	0.753	0.471	C.751	0.587
12	8-2	27	2010.	2.379	0.037	0.598	0.801	0.477	0.763	0.637
16	8-2	27	2000.	2.512	-0.030	0.782	1.022	0.628	0.830	0.849
18	8-2	27	2005.	2.373	0.008	0.677	0.894	0.542	0.792	0.741
19	8-2	27	2005.	2.462	-0.033	0.786	1.029	0.633	0.833	0.779
20	8-2	27	1995.	1.932	C.0	0.701	0.898	0.568	0.800	0.702
21	18-0	34	1995.	1.372	0.116	0.511	0.540	0.317	0.684	0.535
38.1	21-2	35	2000.	0.941	0.170	0.490	0.420	0.397	0.630	0.463
38.2	24-0	36	2000.	0.906	0.208	0.441	0.329	0.351	0.592	0.452
43	8-1	27	2005.	0.931	0.042	0.653	0.720	0.512	0.758	0.556
46	8-1	27	2000.	1.897	-0.029	0.759	0.981	0.622	0.829	0.793
47	8-1	27	2005.	1.434	-0.015	0.721	0.905	0.593	0.849	0.645
48	8-1	27	2005.	1.420	-0.036	0.753	0.962	0.626	0.836	0.696
51	8-1	27	1995.	0.976	-0.055	0.757	0.966	0.632	0.855	0.608

LOCAL SUBCHANNEL CHF CONDITIONS (ENGLISH UNITS)
ANC1 DATA

RUN NO.	CHF ROD NO.	CHF CHANNEL	PRESSURE (PSIA)	MASS VEL. (LBM/HR-FT2) X 10-6	EQUILIBRIUM QUALITY	PREDICTED CHF (BTU/HR-FT2) X 10-6 LOFT2	B&W-2	BARNETT	GE	MEASURED CHF (BTU/HR-FT2) X 10-6 HFLUX
14	8-2	27	1995.	1.879	0.101	0.481	0.597	0.378	0.699	0.498
15	8-2	27	2005.	1.439	0.094	0.539	0.610	0.422	0.706	0.457
17	8-2	27	2000.	2.381	0.083	0.474	0.659	0.377	0.717	0.555

LOCAL SUBCHANNEL CHF CONDITIONS (ENGLISH UNITS)
ANC2 DATA

RUN NO.	CHF ROD NO.	CHF CHANNEL	PRESSURE (PSIA)	MASS VEL. (LBM/HR-FT2) X 10-6	EQUILIBRIUM QUALITY	PREDICTED CHF (BTU/HR-FT2) X 10-6 LOFT2	B&W-2	BARNETT	GE	MEASURED CHF (BTU/HR-FT2) X 10-6 HFLUX
278	23-2	31	1000.	1.057	0.309	0.688	0.093	0.189	0.491	0.581
279	23-2	31	1000.	1.032	0.295	0.723	0.181	0.211	0.505	0.618
280	23-2	31	1000.	0.956	0.283	0.768	0.314	0.240	0.517	0.674
281	23-2	31	1000.	0.928	0.276	0.788	0.373	0.253	0.524	0.769
282.1	20-1	35	1000.	0.695	0.361	0.730	0.407	0.270	0.439	0.798
282.2	21-1	35	1000.	0.695	0.361	0.730	0.407	0.270	0.439	0.844
282.3	21-2	35	1000.	0.734	0.289	0.828	0.505	0.359	0.511	0.844
282.4	21-3	26	1000.	0.776	0.302	0.795	0.470	0.257	0.478	0.844
282.5	23-2	31	1000.	0.891	0.260	0.826	0.480	0.277	0.540	0.843
283	21-1	35	1000.	0.700	0.316	0.799	0.563	0.330	0.484	0.877
284	20-1	35	1000.	0.642	0.341	0.782	0.576	0.311	0.459	0.838
285	21-2	35	1500.	0.937	0.251	0.564	0.317	0.321	0.549	0.474
286.1	21-2	35	1505.	0.935	0.256	0.554	0.301	0.314	0.544	0.473
286.2	21-3	26	1505.	1.003	0.261	0.527	0.242	0.221	0.539	0.473
286.3	23-2	31	1505.	1.090	0.241	0.538	0.267	0.227	0.559	0.472
286.4	24-2	31	1505.	1.090	0.241	0.538	0.267	0.227	0.559	0.450
287	21-2	35	1505.	0.904	0.235	0.596	0.383	0.349	0.565	0.523
288.1	20-1	35	1495.	0.845	0.258	0.581	0.342	0.329	0.541	0.567
288.2	20-2	34	1495.	0.791	0.263	0.589	0.345	0.255	0.537	0.567
288.3	20-3	26	1495.	0.933	0.220	0.617	0.401	0.271	0.580	0.567
288.4	20-4	35	1495.	0.887	0.209	0.644	0.477	0.389	0.591	0.567
288.5	21-2	35	1495.	0.887	0.209	0.644	0.477	0.389	0.591	0.600
289.1	20-1	35	1500.	0.820	0.251	0.597	0.376	0.343	0.549	0.625
289.2	21-2	35	1500.	0.865	0.194	0.668	0.530	0.412	0.606	0.661
289.3	24-1	31	1500.	0.968	0.227	0.595	0.364	0.259	0.573	0.629
290.1	20-1	35	1505.	0.806	0.215	0.650	0.671	0.391	0.585	0.694
290.2	21-1	35	1505.	0.806	0.215	0.650	0.671	0.391	0.585	0.734
290.3	21-2	35	1505.	0.853	0.150	0.728	0.492	0.471	0.650	0.734
291.1	18-1	34	1510.	0.685	0.256	0.622	0.417	0.272	0.544	0.742
291.2	21-1	35	1510.	0.778	0.179	0.702	0.610	0.438	0.621	0.802
292	18-1	34	1495.	0.704	0.133	0.776	0.538	0.367	0.659	0.768
293	21-2	35	1005.	1.789	0.188	0.746	0.135	0.319	0.612	0.735
294.1	21-2	35	1005.	1.717	0.168	0.807	0.286	0.381	0.632	0.797
294.2	23-2	31	1005.	1.958	0.160	0.783	0.204	0.258	0.640	0.796
294.3	24-2	31	1005.	1.958	0.160	0.783	0.204	0.258	0.640	0.758
295.1	21-2	35	1000.	1.695	0.145	0.865	0.426	0.441	0.655	0.891
295.2	23-2	31	1000.	1.924	0.136	0.851	0.359	0.305	0.664	0.890
295.3	24-2	31	1000.	1.924	0.136	0.851	0.359	0.305	0.664	0.847
296	24-2	31	1000.	1.861	0.095	0.955	0.612	0.380	0.705	0.929
297.1	8-3	26	1005.	1.630	0.082	1.003	0.772	0.421	0.718	1.086
297.2	21-2	35	1005.	1.596	0.073	1.023	0.874	0.629	0.727	1.086
298	21-2	35	1495.	1.877	0.112	0.654	0.561	0.433	0.688	0.581
299.1	20-3	26	1505.	1.887	0.103	0.669	0.575	0.316	0.697	0.634
299.2	21-2	35	1505.	1.807	0.096	0.694	0.643	0.474	0.704	0.671
299.3	24-2	31	1505.	2.021	0.089	0.688	0.613	0.327	0.711	0.638
300.1	8-2	27	1510.	1.887	0.046	0.795	0.842	0.579	0.754	0.798
300.2	8-3	26	1510.	1.834	0.081	0.722	0.669	0.351	0.719	0.798
300.3	21-2	35	1510.	1.760	0.073	0.745	0.744	0.527	0.727	0.798
300.4	21-3	26	1510.	1.834	0.081	0.722	0.669	0.351	0.719	0.798
301	8-3	26	1500.	1.826	0.029	0.838	0.882	0.507	0.771	0.877

LOCAL SUBCHANNEL CHF CONDITIONS (ENGLISH UNITS)
ANC2 DATA

RUN NO.	CHF ROD NO.	CHF CHANNEL	PRESSURE (PSIA)	MASS VEL. (LBM/HR-FT2) X 10-6	EQUILIBRIUM QUALITY	P R E D I C T E D C H F (BTU/HR-FT2) X 10-6 LOFT2	BEW-2	BARNETT	GE	MEASURED CHF (BTU/HR-FT2) X 10-6 HFLUX
302.1	8-2	27	1505.	1.947	-0.051	1.001	1.252	0.802	0.851	0.978
302.2	8-3	26	1505.	1.780	-0.011	0.917	1.044	0.487	0.811	0.978
302.3	25-1	36	1505.	1.627	0.020	0.859	0.974	0.647	0.780	0.973
311	24-1	31	1005.	0.594	0.527	0.484	0.042	0.108	0.273	0.445
312	24-1	31	995.	0.555	0.497	0.567	0.243	0.106	0.268	0.509
313	24-1	31	1000.	0.509	0.465	0.644	0.451	0.180	0.335	0.572
314.1	21-2	35	1495.	0.466	0.428	0.463	0.179	0.222	0.412	0.390
314.2	21-3	26	1495.	0.513	0.433	0.433	0.106	0.176	0.367	0.390
315.1	20-1	35	1505.	0.443	0.430	0.467	0.193	0.225	0.288	0.473
315.2	21-1	35	1505.	0.443	0.430	0.467	0.193	0.225	0.288	0.501
316	21-1	35	1500.	0.398	0.422	0.502	0.274	0.242	0.288	0.590
317	21-1	35	1510.	0.415	0.337	0.605	0.443	0.307	0.503	0.649
318.1	20-1	35	1005.	0.386	0.514	0.626	0.717	0.199	0.326	0.655
318.2	21-1	35	1005.	0.386	0.514	0.626	0.717	0.199	0.326	0.693
318.3	24-1	31	1005.	0.479	0.459	0.666	0.544	0.193	0.381	0.658
319	21-1	35	1505.	0.432	0.311	0.633	0.491	0.328	0.529	0.658
320.1	20-1	35	1495.	0.416	0.392	0.538	0.326	0.263	0.448	0.619
320.2	24-1	31	1495.	0.508	0.359	0.547	0.292	0.223	0.441	0.623
27.1	8-2	27	2005.	1.958	-0.013	0.726	0.942	0.596	0.813	0.775
27.2	25-5	35	2005.	1.841	0.016	0.665	0.849	0.542	0.784	0.772
32	8-2	27	2005.	2.020	-0.079	0.866	1.142	0.726	0.879	0.854
37	8-2	27	2005.	1.960	-0.113	0.926	1.240	0.790	0.913	0.927
44	8-2	27	2005.	1.970	-0.153	1.002	1.362	0.869	0.953	1.003
56.1	8-1	27	2000.	1.384	0.014	0.678	0.828	0.554	0.786	0.677
56.2	18-1	34	2000.	1.250	0.096	0.557	0.581	0.311	0.704	0.627
61.1	18-1	34	2000.	1.231	0.067	0.604	0.652	0.339	0.733	0.692
61.2	8-1	27	2000.	1.387	-0.024	0.736	0.931	0.613	0.824	0.747
66.1	8-2	27	2005.	1.498	-0.122	0.881	1.210	0.773	0.922	0.823
66.2	8-1	27	2005.	1.459	-0.075	0.812	1.076	0.694	0.875	0.823
73.1	8-1	27	1995.	1.451	-0.125	0.882	1.219	0.777	0.925	0.878
73.2	18-1	34	1995.	1.284	-0.030	0.743	0.905	0.433	0.830	0.813
78.1	8-1	27	2005.	1.430	-0.162	0.922	1.309	0.830	0.962	0.980
78.2	18-1	34	2005.	1.285	-0.358	0.776	0.970	0.458	0.858	0.908
78.3	25-1	36	2005.	1.404	-0.112	0.856	1.171	0.749	0.912	0.976
80.1	8-1	27	2000.	1.410	0.162	0.920	1.311	0.829	0.962	0.997
80.2	18-1	34	2000.	1.254	-0.056	0.773	0.964	0.456	0.856	0.923
80.3	25-1	36	2000.	1.378	-0.112	0.854	1.169	0.748	0.912	0.992
82	8-2	27	2000.	1.923	-0.187	1.053	1.460	0.932	0.987	1.096
83	8-2	27	1995.	1.884	-0.214	1.090	1.537	0.981	1.014	1.134
106	8-2	27	2005.	2.449	-0.010	0.725	0.957	0.587	0.810	0.823
111	8-2	27	2005.	2.492	-0.064	0.869	1.134	0.710	0.864	0.898
116	8-2	27	2005.	2.433	-0.111	0.981	1.278	0.814	0.911	0.997
123	8-2	27	2000.	2.430	-0.152	1.078	1.412	0.908	0.952	1.106
128.1	8-1	27	2005.	2.350	-0.183	1.131	1.497	0.967	0.983	1.234
128.2	8-2	27	2005.	2.361	-0.223	1.218	1.625	1.056	1.023	1.234
150	18-1	34	2000.	0.872	0.071	0.626	0.626	0.346	0.729	0.551
155	18-1	34	2000.	0.876	0.033	0.667	0.713	0.375	0.767	0.598
162	18-1	34	2000.	0.864	-0.003	0.703	0.795	0.402	0.803	0.643
167	8-3	26	2000.	1.025	-0.163	0.852	1.188	0.535	0.963	0.725
172	8-2	27	2000.	0.902	-0.266	0.880	1.463	0.872	1.066	0.758

LOCAL SUBCHANNEL CHF CONDITIONS (ENGLISH UNITS)
ANC2 DATA

RUN NO.	CHF ROD NO.	CHF CHANNEL	PRESSURE (PSIA)	MASS VEL. (LBM/HR-FT2) X 10-6	EQUILIBRIUM QUALITY	PREDICTED CHF (BTU/HR-FT2) X 10-6 LOFT2	B&W-2	BARNETT	GE	MEASURED CHF (BTU/HR-FT2) X 10-6 HFLUX
183	25-1	36	2005.	0.687	0.050	0.649	0.661	0.486	0.740	0.584
190	8-3	26	2000.	0.768	-0.071	0.754	0.929	0.442	0.871	0.601
195	8-3	26	2000.	0.813	-0.128	0.795	1.064	0.486	0.928	0.626
201	8-3	26	2000.	0.792	-0.173	0.815	1.164	0.516	0.977	0.657
203	8-3	26	2005.	0.795	-0.173	0.814	1.156	0.515	0.973	0.667
204	25-1	34	2005.	0.646	0.136	0.580	0.474	0.305	0.664	0.591
226	25-1	35	2005.	0.689	0.036	0.669	0.715	0.509	0.764	0.570
235	8-1	27	2000.	1.165	-0.015	0.719	0.888	0.595	0.815	0.628
240	8-1	27	2000.	1.197	-0.062	0.777	1.013	0.661	0.862	0.683
247	8-3	26	2000.	1.273	-0.101	0.829	1.078	0.496	0.901	0.729
252	8-3	26	1995.	1.231	-0.141	0.869	1.176	0.533	0.941	0.779
257.1	8-2	27	2000.	1.119	-0.252	0.934	1.488	0.910	1.052	0.830
257.2	8-3	26	2000.	1.213	-0.194	0.914	1.301	0.580	0.994	0.830
259.1	8-2	27	2000.	1.254	-0.278	0.991	1.589	0.977	1.078	0.838
259.2	8-3	26	2000.	1.206	-0.219	0.933	1.361	0.603	1.019	0.838
321	25-1	36	2010.	0.899	0.094	0.593	0.595	0.454	0.706	0.564
334	25-1	36	2005.	0.685	0.053	0.655	0.677	0.492	0.962	0.579

LOCAL SUBCHANNEL CHF CONDITIONS (ENGLISH UNITS)
ANC3 DATA

RUN NO.	CHF ROD NO.	CHF CHANNEL	PRESSURE (PSIA)	MASS VEL. (LBM/HR-FT2) X 10-6	EQUILIBRIUM QUALITY	PREDICTED CHF (BTU/HR-FT2) X 10-6 LOFT2	BEW-2	BARNETT	GE	MEASURED CHF (BTU/HR-FT2) X 10-6 HFLUX
25	23-2	31	2000.	2.078	0.116	0.419	0.531	0.235	0.684	0.495
28	23-2	31	2005.	2.013	0.069	0.540	0.665	0.300	0.731	0.610
38	21-3	26	2005.	1.294	0.162	0.437	0.410	0.240	0.638	0.436
42.1	21-1	35	2000.	1.207	0.104	0.549	0.579	0.427	0.696	0.612
42.2	23-1	31	2000.	1.270	0.116	0.522	0.525	0.287	0.684	0.613
45.1	8-2	26	2015.	1.173	-0.019	0.719	0.851	0.413	0.819	0.782
45.2	7-2	26	2015.	1.173	-0.019	0.719	0.851	0.413	0.819	0.778
45.3	21-1	35	2015.	1.075	0.030	0.658	0.758	0.528	0.770	0.782
48	8-2	26	2000.	1.189	-0.089	0.807	1.034	0.480	0.889	0.878
51	8-2	26	2000.	1.172	-0.107	0.824	1.076	0.496	0.907	0.903
57	8-2	26	2000.	1.983	-0.030	0.764	0.950	0.430	0.830	0.853
62	8-2	26	2000.	2.014	-0.074	0.857	1.078	0.487	0.874	1.046
67	1[illegible]-2	30	2000.	1.955	-0.146	0.988	1.337	1.853	0.946	1.139
70	12-[illegible]	30	2000.	1.925	-0.182	1.046	1.354	1.919	0.982	1.165
80	12-1	30	2005.	1.384	0.062	0.599	0.696	0.478	0.738	0.586
99	21-2	35	2000.	2.412	0.073	0.500	0.691	0.400	0.727	0.563
100.1	21-2	35	2000.	2.348	0.041	0.592	0.790	0.474	0.759	0.690
100.2	21-3	26	2000.	2.471	0.048	0.567	0.740	0.314	0.752	0.690
107	14-2	31	2000.	2.503	-0.047	0.826	1.033	0.457	0.820	1.038

LOCAL SUBCHANNEL CHF CONDITIONS (ENGLISH UNITS)
ANC4 DATA

RUN NO.	CHF ROD NO.	CHF CHANNEL	PRESSURE (PSIA)	MASS VEL. (LBM/HR-FT2) X 10-6	EQUILIBRIUM QUALITY	P R E D I C T E D C H F (BTU/HR-FT2) X 10-6 LOFT2	BEW-2	BARNETT	GE	MEASURED CHF (BTU/HR-FT2) X 10-6 HFLUX
10.1	15-1	31	1005.	0.495	0.597	0.411	0.099	0.091	0.243	0.446
10.2	15-2	31	1005.	0.497	0.547	0.504	0.240	0.126	0.293	0.445
10.3	23-1	31	1005.	0.495	0.597	0.411	0.399	0.091	0.243	0.438
10.4	21-1	35	1005.	0.450	0.600	0.433	0.242	0.088	0.240	0.446
10.5	21-2	35	1005.	0.454	0.543	0.537	0.398	0.144	0.297	0.446
11.1	15-2	31	1000.	0.468	0.489	0.625	0.495	0.174	0.351	0.509
11.2	8-2	27	1000.	0.470	0.412	0.746	0.742	0.272	0.428	0.498
12.	15-2	31	1515.	0.502	0.409	0.467	0.162	0.196	0.391	0.400
13.	15-2	31	1500.	0.496	0.421	0.458	0.150	0.186	0.419	0.383
14.	15-2	31	1515.	0.477	0.335	0.582	0.363	0.239	0.505	0.474
15.	23-1	31	1500.	0.455	0.383	0.532	0.284	0.215	0.457	0.568
16.	8-2	27	1000.	0.474	0.356	0.826	0.902	0.330	0.484	0.576
21.	15-2	31	1515.	0.963	0.267	0.523	0.237	0.220	0.533	0.479
22.	15-2	31	1500.	0.953	0.245	0.570	0.313	0.244	0.555	0.521
23.	14-2	31	1000.	0.944	0.326	0.697	0.155	0.195	0.474	0.593
24.	15-2	31	1515.	0.940	0.195	0.644	0.468	0.291	0.605	0.581
25.	10-2	28	1500.	0.898	0.155	0.717	0.641	0.460	0.645	0.619
26.	14-2	31	1000.	0.841	0.313	0.755	0.339	0.232	0.487	0.684
27.	14-1	31	1500.	0.889	0.166	0.676	0.523	0.306	0.614	0.709
28.	14-2	31	1500.	1.928	0.133	0.594	0.441	0.266	0.667	0.589
29.	12-2	30	1500.	1.924	0.082	0.716	0.683	0.494	0.718	0.587
89.	15-1	31	1000.	0.882	0.233	0.870	0.596	0.307	0.567	0.844
90.	23-1	31	1500.	0.855	0.079	0.816	0.855	0.404	0.721	0.780
91.1	23-1	31	1500.	0.894	0.135	0.743	0.674	0.352	0.665	0.787
91.2	14-1	31	1500.	0.894	0.135	0.743	0.674	0.352	0.665	0.796
92.	14-1	31	1000.	0.862	0.297	0.775	0.373	0.244	0.503	0.822
93.	14-1	31	1000.	0.897	0.304	0.751	0.299	0.229	0.496	0.754
95.	15-2	31	2000.	1.263	-0.077	0.800	1.013	0.472	0.877	0.722
96.	21-2	35	1005.	1.820	0.117	0.908	0.533	0.494	0.683	0.900
97.	21-2	35	1005.	1.798	0.165	0.799	0.261	0.372	0.635	0.779
98.	15-2	31	2000.	2.005	-0.031	0.768	0.955	0.431	0.831	0.845
100.	15-2	31	2000.	1.953	-0.026	0.755	0.937	0.424	0.826	0.792
102.	21-2	35	1000.	1.823	0.174	0.777	0.198	0.346	0.626	0.730
104.	23-1	31	1500.	0.448	0.354	0.575	0.358	0.232	0.486	0.628

APPENDIX C

STEADY STATE CHF CORRELATIONS

Predicted critical heat fluxes with the following steady state correlations were compared with the measured critical heat fluxes of the LOFT data.

1. B&W-2

$$q = \frac{(a - b\,D_e)[A_1(A_2\,G)^{A_3 + A_4(P-2000)} - A_9 G X\,h_{fg}]}{A_5(A_6\,G)^{A_7 + A_8(P-2000)}}$$

where q = Critical Heat Flux (Btu/hr-ft^2)

G = Mass Velocity (Lbm/hr-ft^2)

D_e = Hydraulic Dia. (in.)

P = Pressure (psia)

h_{fg} = Latent Heat of Vaporization (Btu/lbm)

X = Equilibrium Quality

and a = 1.15509

b = 0.40703

A_1 = 0.37020×10^{8}

A_2 = 0.59137×10^{-6}

A_3 = 0.8304

A_4 = 0.68479×10^{-3}

A_5 = 12.71

A_6 = 0.30545×10^{-5}

A_7 = 0.71186

A_8 = 0.20729×10^{-3}

A_9 = 0.15208

2. BARNETT

$$q = \frac{[A\,\frac{h_{fg}}{649} - B\,h_{fg}X] \times 10^{6}}{C}$$

where

$A = 69.4\ D_h^{0.751}\ (G\times10^{-6})\ \{1.0 - 0.672\ \mathrm{EXP}\ [-6.09\ (G\times10^{-6})\ D_W]\}$

$B = 0.25\ D_h\ (G\times10^{-6})$

$C = 165.9\ D_W^{1.246}\ (G\times10^{-6})^{0.329}$

and

q = Critical Heat Flux (Btu/hr-ft^2)

D_h = Heated Equivalent Dia. (in.)

D_W = Wetted Equivalent Dia. (in.)

X = Equilibrium Quality

G = Mass Velocity (Lbm/hr-ft^2)

h_{fg} = Latent Heat of Vaporization (Btu/lbm)

3. GE

$q = 10^6\ (0.8 - X)$

FOR $G \geq 0.5\times10^6$

$q = 10^6\ (0.84 - X)$

FOR $G < 0.5\times10^6$

where

q = Critical Heat Flux (Btu/hr-ft^2)

X = Equilibrium Quality

G = Mass Velocity (Lbm/hr-ft^2)

APPENDIX D

EXPERIMENTAL FACILITY DESCRIPTION

EXPERIMENTAL FACILITY DESCRIPTION

The LOFT experiments were conducted in the Medium Pressure Heat Transfer Flow Loop of the Chemical Engineering Research Laboratories at Columbia University. The experimental facility consists of: the heat transfer loop, the associated process instrumentation and control system, the dc power supply, the Computer Controlled Data Acquisition System (CCDAS), and the test section.

Heat Transfer Loop

The heat transfer loop was constructed of 300 Series stainless steel with the main piping of diameters 3- and 4-in. nominal. The loop is shown schematically in Figure D-1, and the principal loop operational limits are given in Table D-I. Table D-II gives the loop instrumentation for experimental parameters.

The major components of the loop are a 100 hp (75 kW) Wilson-Snyder centrifugal pump, the test section housing, mixing tee, heat exchangers, makeup system, and the purification system.

Primary Loop. The 100 hp (75 kW) Wilson-Snyder centrifugal pump provides circulation of the coolant around the closed primary loop. The total flow leaving the main circulating pump splits with part going through the test section and the remainder through the heat exchangers. The flow through the test section can be varied by means of a flow-control valve which is operated manually from the loop control panel area. A second flow-control valve in the heat exchanger line provides the test section inlet temperature control. The heat exchanger secondary flow, which is controlled manually from the loop control area,

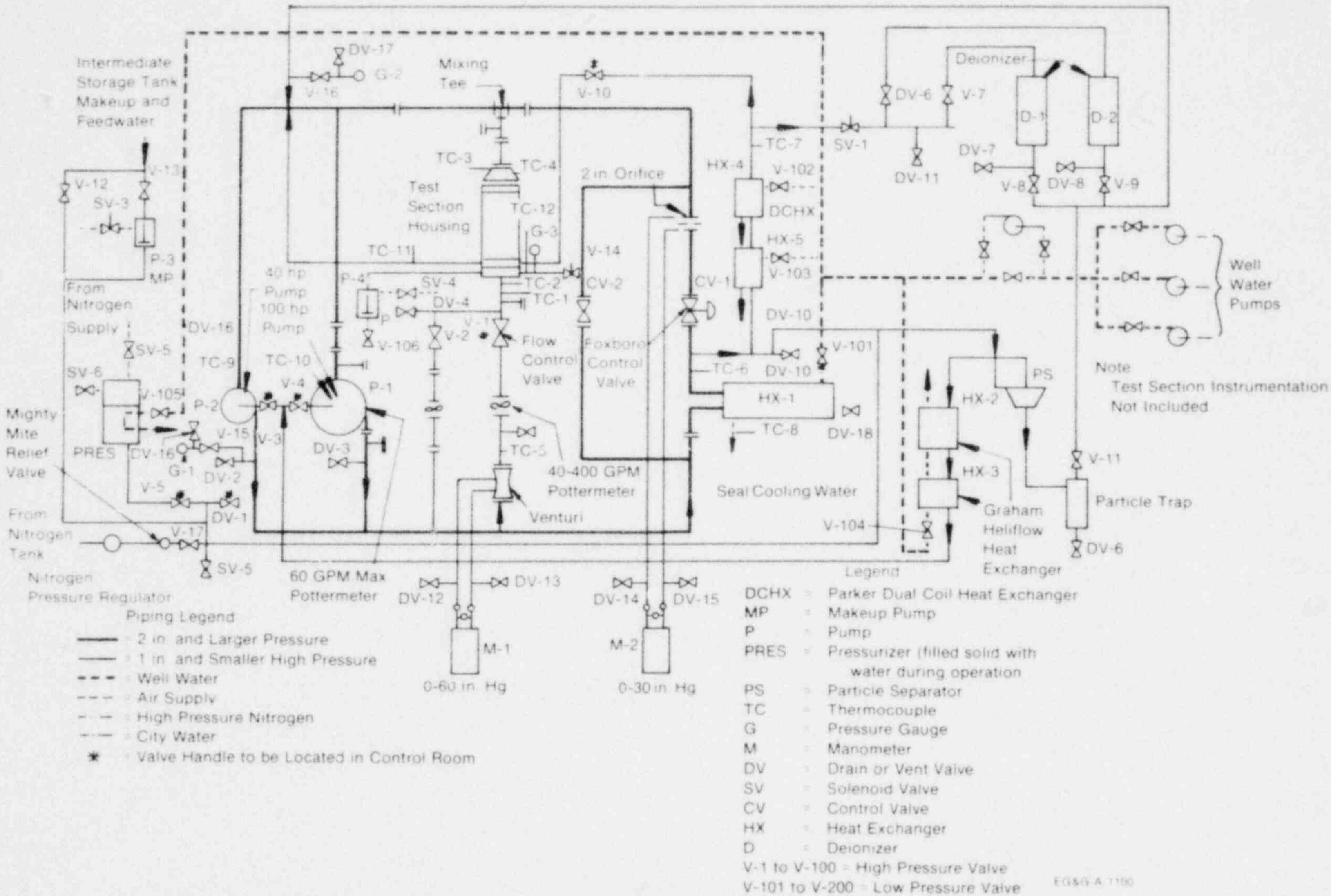

Figure D-1 Schematic of Columbia University test loop.

TABLE D-I

COLUMBIA MEDIUM PRESSURE HEAT TRANSFER LOOP OPERATIONAL LIMITS

Maximum pressure	16.5 MPa
Maximum test section flow	0.035 m^3/s
Head developed by pump	180 m of water
Test section housing length	5.09 m
Maximum heated length of bundle	3.81 m
Test section housing ID	165 mm
Heat exchanger heat transfer area	23.2 m^2
Maximum secondary (well) water flow	0.038 m^3/s
Minimum well water temperature	289 K

TABLE D-II

INSTRUMENTATION FOR THE COLUMBIA MEDIUM PRESSURE HEAT TRANSFER LOOP

Flow to test section [for flow above 0.0025 m^3/s]	(1) BIF Venturi, Serial No. 6580-1, calibrated in BIF Hydraulic Laboratory. Differential pressure visually read on a 1524-mm Meriam mercury manometer.
	(2) Potter Aeronautical Corporation turbine flowmeter, 64 mm, Serial No. 2.5-1, read-out recorded on data acquisition system described below.
Test section outlet pressure	Heise gauge, 0 to 18 MPa with 14 kPa divisions marked, calibrated with a dead weight tester, Serial No. CMM-2395, read visually.
Test section inlet temperature	(1) Calibrated iron-constantan thermocouple displayed on Foxboro Dynalog Recorder Controller, Serial No. 673818, read visually.
	(2) Calibrated platinum resistance thermometer and bridge and/or calibrated iron-constantan thermocouple, recorded on data acquisition system.

TABLE D-II (Cont'd)

Test section pressure drop	Visually read on three 1524-mm Meriam manometers, using mercury and 2.95 specific gravity nammometer fluid. Also measured using Barton differential pressure cells with electrical output recorded by data acquisition system.
Test section power	Amperage from each generator measured using calibrated manganin shunts manufactured by the Westinghouse Electric Corporation. Amperage recorded with data acquisition system. Voltage measured across the main test section power terminals and across voltage taps built into heater rods. Voltage recorded with the data acquisition system.
Subchannel coolant temperature and test section outlet temperature	Calibrated iron-constantan thermocouples, output recorded by data acquisition system.
CHF detection	Iron-constantan thermocouples inside the heater rods, continuous readout on five 8-channel Offner Dynagraph recorders manufactured by the Beckman Company, and an 80-channel

TABLE D-II (Cont'd)

	bar graph display manufactured by Metra Instruments, Inc. This instrument has an adjustable trigger mechanism which automatically shuts down the power to the test section in the event of a temperature excursion.

provides additional control capability. The test section flow is measured by a venturi and a turbine flowmeter prior to its entry into the test section housing. Within the test housing, the coolant removes heat from the heated test section and exits from the top of the test housing to unite in the mixing tee with the flow from the heat exchangers. The mixing tee provides a stable inlet temperature at the pump inlet and hence at the test section inlet. The heat exchanger branch of the primary loop consists of three heat exchangers and an air-actuated control valve. The heat exchangers have a total heat transfer area of 23.2 m^2 with 15.4 m^2 in the main heat exchanger.

The loop is constructed in such a way that the heat exchangers can be operated singly or in any combination, thus providing a wide range of achievable subcooling even for low mass flow rates. The heat exchangers are tube-in-shell type with the primary loop water on the tube side. The cooling water for the heat exchangers is obtained from onsite wells. The secondary system is a once-through open loop.

Makeup, Feedwater, and Pressure Control System. The makeup and feedwater system is used to fill the loop initially and to provide makeup water during operation to maintain loop pressure. Whenever the loop pressure decreases, a Bristol Model 1G500 FF-14 pressure recorder controller activates an air driven makeup pump (piston pump) to restore the pressure to the set value. Whenever the reference pressure exceeds the set control value, the over pressure is relieved by a "Mighty Mite" relief valve in which the reference pressure acts on one side of a diaphragm and the loop water pressure on the other side. The makeup system uses deionized water which is stored in a heated [370 K] intermediate tank. The intermediate storage tank is kept filled automatically by city water fed through the main deionizing system.

Purification System. The purification system is used to control the water chemistry in the primary loop. Part of the heat exchanger outlet flow is split into two streams. One stream is taken through the Graham Heliflow heat exchangers (Hx-2 and Hx-3 in Figure D-1) and is used to cool the pump seal, finally merging with the pump inlet flow. The second stream is taken through two Parker Dual Coil heat exchangers (Hx-4 and Hx-5) and again split into two streams. One stream passes through the deionizers and joins the pump suction stream. The second stream is used to cool one of the test section chamber seals and is returned to the pump suction stream.

Well Water System. Water from onsite wells is used as the heat sink in the loop heat exchangers and in the Parker Dual Coil heat exchangers (Hx-4 and Hx-5) and Graham Heliflow heat exchangers (Hx-2 and Hx-3) described in the purification system. The water from the wells is pumped by three centrifugal pumps, operated in parallel, to the inlet of the secondary side of the heat exchangers. The well water coming out of all the heat exchangers is discharged into the sewer.

DC Power System

The electrical power for heating of the test sections is obtained from the dc power system. The complete dc power system consists of four dc generators and the motors which drive them, motor-generator protective systems, control panels in the experimental areas for remote operation, instrumentation, and the interlocking system which controls the equipment. Power for the dc power system is supplied by two high-voltage feeders from the nearby power substation.

The principal components of the dc power system are the motor-generator sets. The two generators in the building basement have a single motor and two exciters, one supplying the fields of the two generators and the other the motor. The other two generators in the driveway area are normally operated in parallel and have independent motors. The exciter output is controlled by a semiconductor circuit, the output of which is determined by a 25-turn potentiometer in the test area, thereby allowing convenient adjustment of power to the test section. There are two potentiometers, each controlling the output of one pair of generators.

Figure D-2 shows a schematic of the dc power system for the medium and high pressure heat transfer flow loops at the laboratory. The power system specifications are summarized in Table D-III.

Computer Controlled Data Acquisition System

Hardware. The "Computer Controlled Data Acquisition System" (CCDAS) comprises:

(1) Hewlett-Packard, HP 2100 Computer 32K core, with two channel direct memory access, time base generator, and floating point hardware.

(2) A digital magnetic tape unit, 9 track, 800 bpi, 37.5 in. per second.

(3) HP 2401C digital voltmeter.

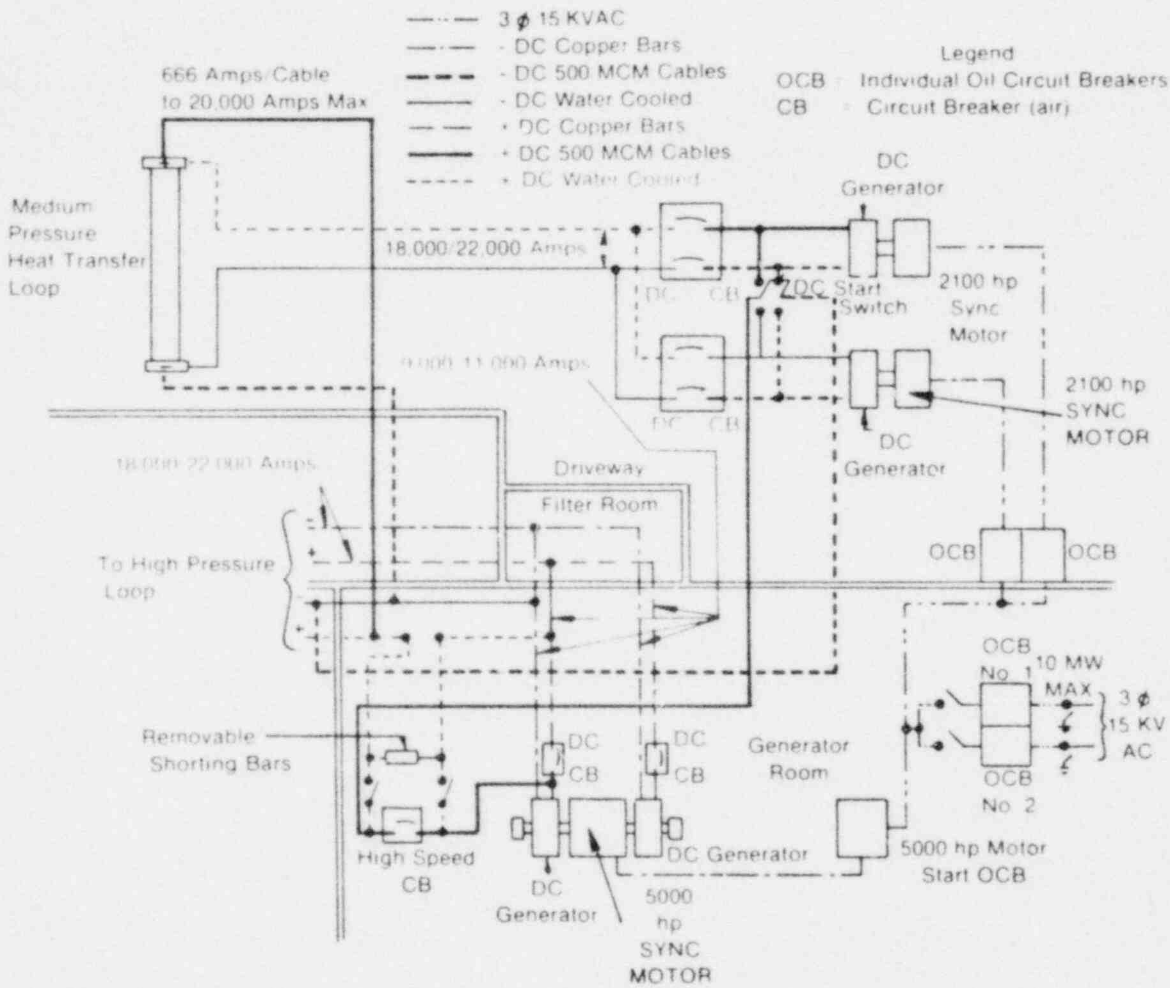

Figure D-2 DC power system.

TABLE D-III

DC POWER SYSTEM SPECIFICATIONS

	Driveway Sets	Basement Sets
	DC Continuously Variable	
Output:	-30 to 240 volts	-30 to 185 volts
Current:		
Continuous rating	6000 amps each	9000 amps each
Short time rating	8000 amps each	10,000 amps each
Type:	Separately excited	
Generator Speed:	26.9 rad/s (514 rpm)	
Ripple:	2% at 2100 Hz (2100 cps)	

(4) HP 2322 subsystem, crossbar scanner and controller (200 channel, 3-wire input).

(5) ASR 33 teleprinter.

(6) HP 2762A Terminet Printer, 30 characters per second, 118 columns.

(7) HP 2895B papertape punch unit.

(8) HP 2748B papertape reader.

(9) An HP 2313B subsystem with a programmable pacer, dual channel digital-to-analog converter and multiplexers for 112 channel differential input for high speed data acquisition (8000 samples per second for sequential channel scanning, 45 kHz single channel sampling). The computer is equipped with the necessary interfaces for the operation of the above subsystems.

The computer operates under a Magnetic Tape System (MTS). Experimental data are recorded on magnetic tape and are loaded into the core each time they are to be used.

Software. The fast data acquisition system (FDAS) software consists of a main program, LOFT3, which controls the use of a number of data reduction and acquisition subroutines. LOFT3 is in on-line contact with the test operator through the ASR 33, cathode ray tube (CRT), or the Terminet Printer and, according to the options chosen, will initiate single sequential scan, multiple-sequential scanning, scanning of a random block of channels, and either pre or posttest reduction of certain variables. The data reduction option picks the specified scan from the magnetic tape; reduces the data to engineering units (with appropriate zero corrections); makes comparison of flow from turbine flowmeter and venturi meter readings; compares temperatures from thermocouple and resistance temperature detector (RTD) (any major deviations are flagged on the output); and calculated heat balance, temperatures, pressure drops, and test section resistances. The output is returned on the teleprinter or terminet. The data acquisition and control subroutines are:

HSCAN: Performs single or multiple sampling of single channel or block or sequential channels of the multiplexer system, writes scanned data on tape, and/or prints raw data using the following HP system routines:

DATIM: HP time of day routine

SETUP: Sets up computer internal clock

STCLK: Initiates the interval timer of the computer

SCODE: An interpretation code for translating sequential channel number to a multiplexer slot and channel number address

MCODE: Interpretation program for translating multiplexer slot and channel address to octal computer address code.

The routines used in the data reduction are:

TDUMP: Controls and prints out rod thermocouple calculations using TCCA-A routine for linear interpolation in the Chromel-Alumel thermocouple conversion table

HPRT: Prints out requested channels in raw data form

HFILE: Locates a specified data file on the tape and prints its contents in volt units using an HP tape positioning routine called PTAPE

FMU: Calculates water viscosity from temperature

SAP: Calculates water saturation pressure corresponding to a specified temperature

SPVG: Calculates specific volume of the water vapor at saturation conditions

TCCC: A routine for linear interpolation in the chromel-constantan thermocouple conversion table

TCIC: A routine for linear interpolation in the iron-constantan thermocouple conversion table

SPVL: Calculates specific volume of liquid water at saturation conditions or subcooled conditions

HSL: Calculates enthalpy of liquid water at saturation conditions or subcooled conditions

SAT: Calculates water saturation temperature corresponding to a specified saturation pressure.

EXPERIMENTAL PROCEDURE

General Loop Startup and Operation Procedure

All valves in the primary loop were opened and all vent, dump, and fill valves were closed. A vacuum pump was connected to a vent line at the test section exit and the air from the primary system was evacuated until a 7 kPa pressure reading was obtained. With the vacuum pump running, the gravity fill line and the pump line to the intermediate storage tank were opened. When fill water reached the vacuum pump, the vacuum pump was stopped. When the loop pressure reached the head pressure of the storage tank the loop was vented. The loop was pressurized to 340 kPa using the makeup pump. The loop water was circulated for a period of time with part of the loop flow passing through the deionizers. When the water resistivity exceeded 10^6 ohm-cm, the deionizers were isolated, the loop pressure was raised to 3400 kPa, and the automatic controls were set. The main heat exchanger was isolated and, using power, the loop temperature was raised. The Foxboro control valve was operated manually initially to obtain the required temperature.

Critical Heat Flux (CHF)

Critical heat flux experiments were performed by maintaining the following system conditions stable: test section outlet pressure, inlet temperature, and mass flow rate. The power was then increased gradually until a temperature excursion, judged to be indicative of the CHF phenomenon, was observed with one of the rod thermocouples, at which time the power was reduced. During the approach to CHF the CCDAS was used to scan all data parameters. The set of measurements immediately prior to the rod temperature excursion were used as the CHF conditions. If for any reason a scan could not be carried out, the point was repeated. After the power was reduced, the data reduction option of the on-line computer program was exercised. The power was then reset to a level below the CHF power and inlet test conditions for the next run were set up.

Test Section Pressure Drop

Incremental and total test section pressure drops were measured in all tests. In addition, pressure drop measurements were carried out with zero power input to the test section and the loop at 300 K.

Subchannel Coolant Temperature

Subchannel coolant temperature measurements were made with the system conditions stabilized at predetermined values of power, system pressure, inlet temperature and mass flow rate. When stable operation was obtained at the desired conditions, the CCDAS was used to scan and store the output from subchannel coolant temperature sensors.

DISTRIBUTION RECORD FOR NUREG/CR-0237 (TREE-NUREG-1166)

Internal Distribution

1 - Chicago Patent Group - DOE
9800 South Cass
Argonne, IL 60439

2 - C. A. Benson
Idaho Operations Office - DOE
Idaho Falls, ID 83401

3 - R. J. Beers, ID

4 - P. E. Litteneker, ID

5 - R. E. Tiller, ID

6 - H. P. Pearson
Information Management - EG&G

7-16 - INEL Technical Library

17-86 - Author

87-116 - Special Internal

External Distribution

117-118 - Saul Levine, Director
Office of Nuclear Regulatory Research, NRC
Washington, D.C. 20555

119-120 - Special External

121-480 - Distribution under R2, Water Reactor Safety Research - Systems Engineering